Review

High-Temperature Solid Lubricants and Self-Lubricating Composites: A Critical Review

Jia-Hu Ouyang [1,*] , **Yu-Feng Li** [2], **Yun-Zhuo Zhang** [1], **Ya-Ming Wang** [1] **and Yu-Jin Wang** [1]

1   School of Materials Science and Engineering, Harbin Institute of Technology, Harbin 150001, China
2   School of Materials Science and Engineering, Harbin Institute of Technology (Shenzhen), Shenzhen 518055, China
*   Correspondence: ouyangjh@hit.edu.cn

Abstract: Solid lubricants are described as solid materials of intentionally introduced or in situ formed on contact surfaces in relative motion for the purpose of lowering friction and wear and providing protection from damage. Solid lubricants and advanced self-lubricating materials are widely used in modern industries, especially in aerospace, aviation, automotive, metallurgy, materials forming, and machining industries, and have attracted great interest in lubrication applications under very severe circumstances such as elevated temperatures, heavy loads, ultrahigh vacuum, extreme radiation, strong oxidation, and chemical reactivity environments. Many efforts have been made to develop self-lubricating composites by a variety of material preparation techniques, which include powder metallurgy, physical/chemical vapor depositions, thermal spraying, electrodeposition, laser cladding, and additive manufacturing. Although several reviews on the development of high-temperature solid lubricants have been published, most of them only focus on a type of material, a specific process, or application. In this paper, a comprehensive review is provided to present the state-of-the-art progress in solid lubricants, self-lubricating composites/coatings, and their effective functions that can be used over a wide variety of environmental conditions, especially at elevated temperatures. The solid lubricants considered include representative soft metals, layered structure materials (e.g., graphite, hexagonal boron nitride, transition metallic dichalcogenides, MAX phase), chemically stable fluorides, binary or ternary metallic oxides, especially alkaline earth chromates, and sulfates, and synergistic effects from these solid lubricants. This paper also provides new insights into design considerations of environmental adaptive solid lubrication, and the challenges and potential breakthroughs are further highlighted for high-temperature solid lubrication applications.

Keywords: solid lubricants; self-lubricating composites; friction; wear; extreme environments

1. Introduction

Solid lubricants are described as solid materials of intentionally introduced or in situ formed on contact surfaces in relative motion for the purpose of lowering friction and wear and providing protection from damage. Solid-lubricating materials for modern machinery, which uses rolling and sliding contact surfaces, mainly serve in extremely harsh conditions, such as elevated temperature, alternation of moist air atmosphere and vacuum, heavy load, high speed, strong oxidation and chemical reactivity, and severe thermal shock environments [1–5]. High friction, excessive wear, severe oxidation, and premature failure will inevitably occur if no lubrication mechanism is provided associated with the above-mentioned operation conditions. Nowadays, humanity is facing new challenges in the field of advanced solid lubrication, and novel self-lubricating components are required to operate durably and reliably in different industries such as aerospace, aviation, power generation, automotive, metallurgy, hot metal processing, and cutting tools.

Research in solid lubrication is understandably the minimization and elimination of materials and energy losses where sliding and rolling contact surfaces in relative motion are

involved. Effective solid lubrication will bring greater materials and energy savings, higher efficiency, better comprehensive performance, and fewer machinery failures toward more reliable operations when exposed to extreme environments. Nowadays, there is a great need for lubricating polymeric, metallic, or ceramic components in sliding and rolling contacts, such as bearings and bushings for space satellites, gas turbine seals, bearings and variable stator vane bushings, and cylinder wall/piston ring lubrication for specific engine types from cryogenic temperatures to high operating temperatures [1,2,6–8]. For next-generation propulsion systems, a significant goal in the tribological design of advanced engines, bearings, and seals is to reduce undesirable friction and wear and attain a friction coefficient lower than 0.2 and a wear rate smaller than 10^{-6} mm^3/(Nm), which is expected to be independent of sliding velocity, applied load and ambient temperature for further increasing the efficiency of engines and reducing the emission of NO$_x$ and CO$_2$ [9]. However, developing new tribo-materials with a low friction coefficient and a small wear rate over a broad temperature range (i.e., room temperature to 1000 °C or even higher) has always been considered to be quite difficult and extremely challenging [10]. Higher operating temperatures in advanced power generating systems will provide improved efficiency, increased effectiveness, and reduced environmental impact where severe challenges are put forward to the existing solid lubricants, particularly from the point of view of high-temperature structural and chemical stability or surface lubricity intermittently but reliably [11]. Different motion mechanisms in nuclear power, hypersonic vehicles, and ballistic missiles also involve a very high operating temperature environment [12].

In the literature survey of solid lubricants and self-lubricating materials/coatings, the following classes of compounds are generally considered: polymer composites, soft metals, layered materials (graphite, hexagonal boron nitride, and transition metal dichalcogenides), alkaline earth fluorides, binary oxides (PbO, B$_2$O$_3$, Magneli phases TiO$_2$, V$_2$O$_5$, and MoO$_3$), and multi-component oxides (molybdates, tungstates, vanadates, tantalates, chromates, sulfates, silicates), oxythiomolybdates, MAX phases (Ti$_3$SiC$_2$, Ti$_2$AlC, etc.) [1,2,6–8,13,14].

High-temperature solid lubricants can be directly applied to the surfaces of machinery components by simple methods, such as painting and burnishing. A variety of fabrication methods of high-temperature self-lubricating materials or coatings include powder metallurgy processes such as pressureless sintering, hot pressing (HP), hot isostatic pressing (HIP), and spark plasma sintering (SPS), and coating processes such as electrodeposition, thermal/plasma spraying, magnetron sputtering, pulsed laser deposition, chemical vapor deposition, laser cladding, and additive manufacturing [2,8,15–18].

There have already been some reviews of various solid lubricants and preparation methods. However, few reviews deal with tribological design, diverse industrial applications of self-lubricating materials/coatings, and their underlying mechanisms, especially under extreme environmental applications [1–5]. The solid lubricants in this review concentrate on soft metals (Ag, Au), layered graphite and boron nitride (*h*-BN), transition metallic sulfides (MoS$_2$, WS$_2$), chemically stable fluorides (CaF$_2$, BaF$_2$), binary and multi-component oxides including silver-containing oxides, chromates and sulfates, and combinations of various solid lubricants. As it is difficult to investigate all compounds in these classes, this review proposes general design considerations relevant to environmental adaptive solid lubrication and provides a comprehensive understanding of self-lubricating materials and their effective function involved in challenging high-temperature environments.

2. Mechanisms of Solid Lubrication

In the case of no liquid/gas/grease lubrication, considerable adhesion exists between the rubbing surfaces of solid contact if two solid surfaces are clean (fresh metallic surface or in ultra-high vacuum) and all of the chemical films and adsorbates are removed. Generally, adhesion is regarded as either a physical or chemical interaction in nature [19]. In sliding and rotating machinery applications, adhesion usually results in friction and wear. Strong adhesion at tribo-stressing surfaces always leads to serious friction damage, cold welding, scuffing, or even breakdown, such as gears and bearings when subjected

to heavy loads, high velocities, and elevated temperatures. Adhesion depends mainly upon material pairs such as crystal structure, crystallographic orientation, mutual solubility, chemical activity, and separation of charges, as well as interface conditions such as surface cleanliness, normal load, temperature, atmosphere, duration of contact, and velocity [19]. In a hot metal forming process [4], components are subjected to extremely high thermal and mechanical dynamic loads and high velocity, which results in severe plastic deformation wear, and fatigue. Clearly, proper lubrication at elevated temperatures is needed to lower the friction stresses during forming and to avoid direct metallic contact, seizure, and galling. In a high-speed dry machining process, tool wear results from various wear mechanisms including adhesive, abrasive, chemical (by thermal diffusion), and electrochemical wear [4,5,19]. In the case of pantograph contact strips for electric railways [4], wear is derived from high-temperature mechanical impact, adhesion, and particle transfer due to arc discharge attack. For the thin-strip steel casting process, refractory side dams operate under severe environments of mechanical load, corrosion, wear, and thermal shock at elevated temperatures. Abradable seals used in the high-temperature compressor and turbine sections of gas turbine engines have to struggle against the degradation from adhesive, abrasive, thermal/corrosive, fatigue wear, and blistering. The failure modes of rolling-contact bearings, which contain substantial sliding for operating in a vacuum and high temperatures, are fatigue spalling under cyclic contact stressing and severe adhesive wear, commonly called scuffing or smearing [20].

Lamellar solids with weak interplanar cohesive bonds have a strong anisotropy of mechanical properties. Therefore, cleavage occurs generally at low shear stresses in some materials with anisotropy of mechanical properties and finally results in a distinctly reduced friction at the interface during sliding. These lamellae become self-lubricating due to the crystallographic slip mechanism at low shear stresses [21]. Similarly, conventional solid lubricants (such as MoS_2, graphite, etc.) have an easy-to-shear layered structure to provide self-lubricity; however, they generally become ineffective mainly due to oxidation-induced structural degradations in an oxidizing atmosphere (oxidation onset temperatures of 350 °C for MoS_2 and 450 °C for graphite) at elevated temperatures [11].

Non-lamellar soft solids, such as In, Pb, Sn, Ag, Au, and other soft compounds such as chemical stable fluorides, can lower friction and wear effectively when used as a strongly adherent thin film to the rubbing surfaces. Thus, the second solid lubrication mechanism is related to the formation of continuous and adherent soft solid films on a hard substrate during sliding. In this case, the shear strength of contacting asperities is determined by the softer thin solid film; however, the contact area is determined by the hard substrate. Clearly, the frictional force determined by the asperity shear strength and contact area becomes quite low under such conditions. The actual contact is between effective soft solid lubricants themselves due to the formation of a strongly adherent transfer film on the contact surface after a short running-in period. For example, a thin transfer film of lead is formed to provide self-lubricity for the lead-based alloys during sliding, while a low shear strength film is provided by the silver and fluoride eutectic constituents for the plasma-sprayed $Ni80Cr20$-Cr_2O_3-Ag-CaF_2/BaF_2 composite coatings (PS304). They exhibit low coefficients of friction in dry sliding and are commonly used as bearing and seal materials [1,7,19].

The above-mentioned two fundamental modes of solid lubrication based on lamellar solids and soft films have been widely used for various sliding and rolling contact components. In addition, a variety of metals, intermetallic compounds, or ceramics react in air or water vapor atmospheres to some extent to form lubricious tribo-chemically reacted films. These tribo-chemically reacted films act as a low-shear-strength film and lead to low friction, which effectively separates the two metallic or ceramic surfaces from direct contact. Examples of vanadium or chromium as alloying elements in metals or nitride coatings form tenacious and lubricious oxide films, which are also responsible for low friction at elevated temperatures [2,22].

Although most oxides generally have poor lubrication properties due to their strong chemical bonds and brittle features, microstructurally designed thermally stable oxides may provide extreme high-temperature lubrication applications, especially in the oxidizing atmosphere. The lubrication mechanisms associated with lubricious oxides include the following seven aspects: (1) easy-shearing ability due to screening of cations by surrounding anions based on the crystal-chemical model [10,23]; (2) oxides are known to soften above the ductile-to-brittle transition temperature, which is typically 0.4–0.7 T_m where T_m is the melting point (in K). Material softening and plastic smearing contribute to the lubricious behavior observed for typical soft oxides once the operating temperature is attained to such a critical temperature [24]; (3) Low friction characteristic of melting wear for the oxides by exceeding T_m has scarcely been examined, which is similar to the mechanism of viscous flow occurring from very thin liquid film, such as glass lubrication in hot metal forming process [21,22,25,26]; (4) creation and transfer of a reacted layer with lamellar structure and weak interplanar cohesive bonds (similar to the easy-shearing mechanism occurring in graphite and MoS_2) by oxidation or tribo-chemical reaction [27]; (5) intracrystalline slip deformation mechanism in textured nanocrystalline grains due to dislocation glide [28,29]; (6) The strain hardening at room temperature generally increase the friction stress during sliding, however, grain boundary sliding and grain rotation occurring in the microstructurally-refined surficial layer reduce the resistance to slide between the rubbing surfaces at elevated temperatures, and also contribute to the self-lubricity [26]; (7) in situ formation of glazed film with ultrafine nanograins by thermo-mechanically deformation-induced dynamic recrystallization and tribo-chemical reaction of surficial layer, which contributes to low friction at elevated temperatures [26]. Voevodin et al. [30] concluded that the primary adaptive lubrication mechanisms over a wide environmental range are associated with environmental-assisted oxidation to form easy-to-shear and low-melting-point binary TiO_2, V_2O_5, MoO_3 Magneli phases and ternary oxides including silver molybdates, vanadates, tungstates, niobates and tantalates, temperature-activated diffusion or melting of soft metals, and thermo-mechanically-induced phase transitions to reorient hexagonal solids and promote surface self-hardening. Franz et al. [31] also summarized that the addition of V to nitride hard coatings enables a self-adaption mechanism via the formation of lubricious oxides at elevated temperatures, which improves the overall wear resistance and applicability of these coatings in metal cutting, in particular under dry-cutting conditions. A new approach is proposed to overcome brittleness in ceramic materials at relatively low temperatures [32,33]. Polycrystalline oxide lubricants with a reduced grain size of only a few nanometers may become more ductile during sliding and rolling contact. In this case, nano-sized oxides produce plastic deformation under tribo-stressing, in large part, due to grain boundary sliding or grain rotating at relatively low temperatures [34]. Thus, adaptive and lubricious oxide nanofilms introduced or generated on the rubbing surfaces may exhibit large plastic deformation and viscous flow to expand their lubricity over a broader operating temperature range.

3. Characteristics of Solid Lubricant Materials

As the primary function of solid lubricants and self-lubricating materials/coatings is to reduce friction and wear in sliding and rotating machinery, they must have the basic properties for effective lubrication and provide protection from damage over a wide variety of environmental conditions. In addition to superior lubricity, a suitable solid lubricant material should possess certain specialized properties such as high oxidation resistance, excellent thermal and chemical stability, high thermal conductivity, and low shear strength, particularly for specific engineering applications. Solid lubricant materials can be used in the form of bulks or coatings/films as well as dry powders, dispersions in lubricating oils or greases, and self-lubricating composites/coatings impregnated with solid lubricants.

The properties of an environmentally adaptive solid lubricant material include the following [1,11,26]: (1) Solid lubricants have low friction and moderately small wear rate in sliding or rolling contact without external lubrication from liquids or greases, and they must

possess low shear strength either by easy-to-shear lamellar microstructure such as graphite, MoS_2, and *h*-BN or by increased ductility at elevated temperatures such as Ag, Au, and CaF_2/BaF_2 eutectic. (2) Easy-to-shear alone does not ensure sufficient lubricity if the film does not strongly adhere to the contact surface. The solid films formed on the tribo-stressing surfaces must have a strong physical or chemical bond with the surface, which must remain continuous and intact during sliding or rotating processes such as physical vapor deposit MoS_2 films in non-oxidizing environments. (3) As surface heating caused by heavy loads or high sliding velocities results in the generation of easy-to-shear film and even localized melting, effective solid lubricants must remain thermally stable up to elevated temperatures such as thermally stable alkaline earth fluorides or sulfates. (4) The self-lubricating film must have good thermal conductivity to dissipate frictional heating from the contact region such as carbon-graphite parts impregnated with metallic fillers. (5) The self-lubricating film should function effectively between surfaces when subjected to high unit pressures and high velocities such as self-adaptive ultrahard multilayered or nanocomposite coatings. (6) Solid lubricants must be inert chemically to environments containing reactive vapors or fluids such as BN-based side-dam materials incorporated with *m*-ZrO_2 and SiC used for twin roll strip steel casting, and structural stability when subjected to radiation from radioactive sources such as high irradiation tolerant self-adaptive YSZ-doped MoS_2 nanocomposite films. (7) The self-lubricating film must have excellent oxidation/corrosion resistance at elevated temperatures such as plasma-sprayed Ag-CaF_2/BaF_2–containing composite coatings at elevated temperatures. (8) The self-lubricating film must have good electrical conductivity for the lubrication of sliding electrical contacts or brushes at elevated temperatures such as noble metal-, graphite- or MAX phase-based electrical contact materials. (9) Solid lubricants are able to provide safe operation, non-toxicity, and environmental compatibility, such as avoiding the usage of toxic PbO lubricant.

4. Classification of Solid Lubricants

Solid lubricants and self-lubricating solids are solid materials introduced or in situ generated between two rubbing surfaces, which exhibit low friction and wear in sliding or rotating machinery without external lubrication from liquids or greases. The most commonly used solid lubricants are polytetrafluoroethylene (PTFE), soft metals, graphite, and molybdenum disulfide [1–5,11,19]. Although these lubricants have been widely used singly or in various combinations, each of them has certain limitations. These limitations of common lubricating solids have stimulated the synthesis of novel lubricious compounds and composites/coatings with self-lubricating properties.

4.1. Polytetrafluoroethylene (PTFE) and Polyimides

Many polymers have low densities, low friction coefficients, high chemical stability, and excellent machinability, and they are generally used under the conditions of cryogenic temperatures and vacuum [11]. Polytetrafluoroethylene (PTFE) and polyimides are the currently widely used solid lubricants in the family of polymers due to their good thermal stability and excellent tribological properties under different environmental conditions. However, these polymers exhibit poor thermal conductivity, high thermal expansion, and low radiation stability, and they are usually subjected to excessive cold flow under load (particularly at elevated temperatures), which leads to a lack of both strength and dimensional stability due to relatively poor heat dissipation efficiency [11]. PTFE, a fluorocarbon $(C_2F_4)_n$, is a crystalline polymer with a melting point of 325 °C. The simple zigzag backbone of –CF_2-CF_2- groups has a gentle twist of 180° over a distance of 13 CF_2 groups. The lateral packing of these rodlike molecules is hexagonal with a lattice constant of a = 0.562 nm [19]. The easy slippage of these rodlike molecules parallel to the c axis and their easy transfer onto the sliding partner account for the low friction characteristic of PTFE.

PTFE in the unfilled or filled forms retains good mechanical properties and lubricity up to 260 °C and can be used as a bearing material, which has the lowest coefficient of friction among any known solid lubricants, including graphite or MoS_2 [11]. A commonly adopted

value is 0.04 for the friction coefficient of PTFE against steel, while it can be as low as 0.016 at very high loads [11]. The PTFE coating on finger seals exhibits excellent wear resistance for reducing wear rates by 39%, which provides a valuable reference for the design of finger seals [35]. PTFE is usually reinforced with additives or filler reinforcements such as powdered graphite, MoS_2, or graphite fluoride (CF_x) in order to reduce the cold flow under severe load and speed conditions. Although these powdered additives can enhance tribological properties, they generally reduce their load-carrying capability. In this case, fiber reinforcement is used to meet the needs of maximum load capacity [36]. The fibers in the form of woven fabric are usually used to improve the creep resistance of bonded PTFE liners in airframe bearings and some heavily loaded bearings. From tests of nonmetallic plain cylindrical bearings, which were made of aramid (Kevlar) fiber-reinforced shell with a bonded, self-lubricating woven liner of polyester fiber-reinforced PTFE, low friction and wear were achieved up to 121 °C with a load capacity in excess of 207 MPa. However, the bearings are limited by creep deformation at higher temperatures [1].

Polyimide, used especially as coatings and films, are a class of imide-group-containing polymeric synthetic resins resistant to wear, corrosion, and high temperatures. The additions of CF_x or MoS_2 solid lubricants to the polyimide varnish not only reduce the friction and wear of the coatings at room temperature but also eliminate completely the influence of molecular relaxation transition on tribological properties up to 500 °C. The polyimide-bonded CF_x films are found to be excellent backup lubricants for foil gas bearings up to about 350 °C. Interestingly, polyimides are resistant to most common chemicals and solvents, but they easily suffer from the attack of alkalies.

Polyimides were widely used in bearings, bushings, gears, seals, and mechanical parts operating below 300 °C, at GE Aircraft Engine, Pratt & Whitney, Rolls & Royce, for example, the Vespel CP-8000 from DoPont^{TM} for stator bushings of compressor in BR710 engine. Graphite fiber-reinforced polyimide (GFRPI) has attracted great attention for aviation applications and is being widely investigated for airframe and gas turbine engine applications due to the high strength, high thermal conductivity, and lubricity of graphite fibers. The Fibercomp, a chopped fiber/graphite-reinforced polyimide, from Foundry Service & Supplies, Inc., Ontario, CA, USA, has a friction coefficient of 0.1 to 0.2 and compressive strength of 172 MPa at 260 °C. The upper limit temperature for lubricious polyimides in the air is 350 °C, depending upon the type of polyimide. Polyimides are prone to becoming brittle and finally lead to wear damage by surface brittle fracture [11,37].

Interestingly, three-dimensional (3D) polyimide architectures with low volume shrinkage of only about 6% are fabricated by the UV-assisted direct ink writing (DIW) method, which provides the potential for three-dimensional printing of polyimides in the fields of aerospace, aviation, automobiles, and microelectronics [38]. The 3D target-region-lubrication printing of PTFE-filled photosensitive polyimide (PSPI) with excellent tribological properties for self-lubricating devices was realized by digital light processing and post-heat treatment. The PSPI-7wt.%PTFE composites fabricated by 3D printing exhibit a sharp reduction in friction coefficients by 88% and wear rates by 98%, respectively, and excellent mechanical properties with tensile strengths higher than 90 MPa, thermal stability up to 384 °C, and interlayer bonding as well [39]. For example, the friction coefficients are reduced to 0.09 for surface-lubricating and 0.04 for alternate-lubricating at 20 N. Importantly, a 3D-printed target-region-lubricating bearing was demonstrated effectively [39].

4.2. Soft Metals

There are some pure metals such as In, Sn, Pb, Zn, Ag, Au, and Pt, which are soft enough to be considered solid lubricants with their main lubrication mechanisms of enhanced ductility and the formation of an easy-to-shear tribolayer. The melting points and Mohs hardness values of these typical metals are shown in Table 1 [26]. In, Sn, Pb, and Zn have low melting points and Mohs hardness. Soft metal films of In, Sn, Pb, Zn, and their alloys with low melting points contain multi-slip systems and are able to compensate for microstructural defects effectively by frictional heat, which contributes to their

self-repairing ability as solid lubrication coatings under lightly loaded conditions and at relatively low temperatures. However, Ag, Au, and Pt have high melting points and low Mohs hardness [26]. Ag, Au, and Pt films with high melting points are easy-to-shear with a relatively inert nature to ambient vapor and temperatures, for a wide range of tribological applications such as long-term effective lubrication in X-ray tubes and satellites. Table 2 represents the fabrication methods and tribological behavior of self-lubricating materials containing soft metals [40–44].

Sn-Co binary alloy coatings are widely used for the substitution of hard chromium coatings in engineering applications. Ion-plated Pb coatings are especially designed for slow-rotating rolling element bearings in space mechanisms and have a higher cycle life than sputtered MoS_2 coatings in rolling contact bearing applications due to the unavoidable presence of lubricious PbO formed within the coatings. Pb-Sn-Cu in the form of plating on steel has been used as a lubricant for many years. The lubricious Pb-Sn-Ag and Ag-Cu-Pb-Sn additives were well distributed into the TiC-reinforced high-speed steel pre-forms to form an interpenetrating network microstructure for reducing friction and wear at elevated temperatures, and the wear rate can even be reduced by two orders of magnitude at 300–700 °C [45].

Table 1. Melting points and Mohs hardness values of typical soft metals [26].

Material	Melting Point	Mohs Hardness
In	155 °C	1.0
Sn	232 °C	1.8
Pb	328 °C	1.5
Zn	419 °C	2.5
Ag	961 °C	2.5
Au	1063 °C	2.5
Pt	1755 °C	4.3

Table 2. Fabrication methods and tribological behavior of self-lubricating materials containing soft metals [40–44].

Materials	Fabrication Method	Tested Conditions	Results/Observations
TiN-In [40]	Sputtering deposition	Pin-on-disk; Al_2O_3 ball; load 1 N; 0.1 m/s; 150–1200 °C	• μ: 0.5–0.6 • TiN-In coating has high sustainability of lower friction coefficient for more than 1500 cycles. • TiN-In coating exhibited four times longer wear life than TiN coating in wet machining. • Friction coefficient significantly increased due to the indium oxidization above 450 °C.
NiMoAl-Ag [41]	High-velocity oxy-fuel spraying	Ball-on-disk Si_3N_4 ball; load 5 N; 0.1 m/s; 20–800 °C	• μ: ~0.3 (20–600 °C), 0.09 (800 °C) • W: 1.4×10^{-5}, 7.7×10^{-4}, 6.0×10^{-5} mm^3/(Nm) (20, 600, 800 °C) • Enriched silver on sliding surface form a lubrication film below 400 °C. • A synergistic effect of molten Ag and Ag_2MoO_4 by tribochemical reactions gives a high lubricating property at high temperature.

Table 2. *Cont.*

Materials	Fabrication Method	Tested Conditions	Results/Observations
NiMoAl-Al$_2$O$_3$-Ag [42]	Plasma spraying	Ball-on-disk Al$_2$O$_3$ ball; load 12 N; 0.1 m/s; RT-900 °C	• μ: 0.53, 0.36, 0.17 (RT, 500, 900 °C) • W: 1.47 × 10^{-5}, 8.84 × 10^{-5}, 3.35 × 10^{-5} mm^3/(Nm) (RT, 500, 900 °C) • Continuous lubricating film mainly consisted of NiO and Ag$_2$MoO$_4$ formed at 900 °C. • Continuous lubricating film forming at high temperature improved subsequent friction performance during multitemperature cyclic tests.
Al$_2$O$_3$-DLC-Au-MoS$_2$ [43]	Magnetron-assisted pulsed laser deposition	Ball-on-disk; M50 steel ball (RT); Si$_3$N$_4$ ball (500 °C); load 100 g; 0.2 m/s; air at 40% RH and N$_2$ at <1% RH	• μ: 0.13–0.14 (air at 40% RH), 0.02–0.03 (N$_2$ at <1% RH), 0.1 (air at 500 °C) • Cycles to failure 500 °C: >10,000 • The higher ratio of hard phase contributes to extend coating wear life at 500 °C.
Ta-Ag [44]	Magnetron sputtering deposition	Ball-on-disk; Si$_3$N$_4$ ball; load 2 N; 0.128 m/s; 25–600 °C	• μ: 0.2 (6% textured dimple density, between 25 and 600 °C) • W: 5.2 × 10^{-5} mm^3/(Nm) (at 600 °C) • Ta$_2$O$_5$ and silver lead to low friction coefficient at high temperature. • Textured dimples store lubricants to extend the wear life.

Electrodeposition and physical vapor deposition processes have been applied to fabricate soft metallic coatings such as Ag, Au, and Pt, which are particularly valuable at very high temperatures and under severe conditions, such as in spacecraft. Ag and Au lubricating films deposited by oxygen-ion assisted screen cage ion plating can avoid undesirable subsurface cracking and reduce friction and severe wear. Herein, achieving low and steady friction coefficients and low wear is mainly attributed to the strong adhesion of lubricious Ag and Au films to alumina [46]. Self-lubricating Au and Ag films can be used in space capsules, advanced jet engines, and high-speed lightly loaded machines. An Au-Co alloy coating was designed for effectively lubricating ring tracks and rolling flexures in the roll ring assembly on space station freedom.

Composite brushes used in the solid lubricated slip ring assemblies on spacecraft consist mainly of a conductive metal such as Ag, Au, and/or Cu, incorporated MoS$_2$ and/or a small amount of graphite, which contributes to a balance of low friction and wear and low electrical contact resistance. The graphite was originally added into the conductive metallic matrix to generate self-lubricity for military aircraft, where both MoS$_2$ lubrication in low humidity at high altitude and graphite lubrication in humid air at low altitude are needed. Clearly, incorporating multiple solid lubricants such as soft metals, graphite, and MoS$_2$ can achieve reversible surface chemistry and morphology during sliding that is well-suited for lubrication over a broad range of ambient environments.

Au and Ag lubricants can be incorporated into high-temperature intermetallic or ceramic matrix composites/coatings for providing lubrication from room temperature to 600 °C [3]. They have high diffusion coefficients, which help the easy formation of lubrication films onto the surfaces of intermetallic or ceramic matrix composites, which are used to lubricate bearings, seals, and fasteners in sliding or rolling contact, and exhibit good thermochemical stability up to elevated temperatures [5]. Figure 1 shows the worn surfaces of the cermets infiltrated with and without Ag lubricant. The Ag-infiltrated cermet exhibited a thin lubricating film on the surface; however, obvious furrow marks were observed on the unmodified cermet. Friction heat and surrounding temperature induce the formation of a melting film, which can effectively reduce the friction coefficient [47]. Typical examples of Au- and Ag-containing coatings for tribological applications under the harshest conditions are YSZ/Au/MoS_2/DLC, YSZ/Ag/Mo, and Al_2O_3/DLC/Au/MoS_2 nanocomposite films fabricated by hybrid magnetron sputtering and pulsed laser deposition processes. All these films have friction coefficients of 0.1–0.4 for from 5000 to 10,000 cycles at 500 °C due to the migration of easy-to-shear noble metals to the surface to provide a lubricious layer [3,43,48,49].
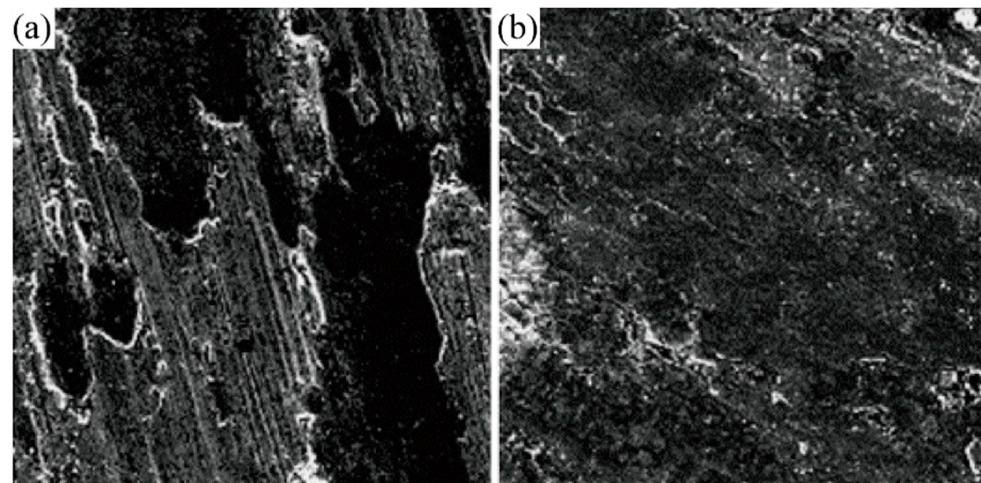

Figure 1. Morphologies of worn surface of the cermets infiltrated with and without Ag lubricant at p = 50 N and T = 800 °C. (**a**) without Ag lubricant added; (**b**) Ag-infiltrated. Reproduced with permission from Reference [47], Copyright © Elsevier B.V. 2006.

Since the lubrication films of soft metals are easily removed by shear, they generally have poor wear resistance and a short useful lifetime under severe tribo-stressing, particularly after becoming softened at elevated temperatures. This challenge can be partially overcome by intentionally designing the reservoirs of soft metals in hard textured surfaces and gradually releasing these softer materials during sliding to generate an easy-to-shear transfer film when needed [50]. Examples are the incorporation of silver [44] or in combination with MoS_2 [51] as solid lubricants applied to a textured hard surface to reduce friction and wear.

In addition, some metals such as Fe, Cu, Ni, Mo, and Cr exhibit high coefficients of friction at room temperatures, but considerable improvements in friction reduction to only half of their original values are noted during sliding above their oxidational temperatures [26]. This improvement in friction during sliding is associated with the formation of oxidized products in the wear track for these metals. Therefore, these soft oxides formed on the surfaces of metals and alloys provide the most effective friction-reducing characteristics and separate the rubbing surfaces from direct metallic contact. In recent years, pulsed laser deposition, plasma spraying, magnetron sputtering, and ion bombardment assisted deposition (IBAD) have been employed to produce Au/Cr, Zn/W, Ni/Ti, Cu/Mo, W/MoS_2, and AlCuFeCr multilayered films for tribological applications, such as turbomachinery components of bearings, seals, and fretting interfaces up to 580 °C.

4.3. Layer Lattice Solid Lubricants

4.3.1. Graphite

Graphite is hexagonal in orientation and is composed of planes of polycyclic carbon atoms. The bonding between the basal planes is weaker due to the presence of a longer distance between carbon atoms along the *c* axis, and the parallel layers of hexagons stack 0.34 nm apart. Close examination of a metallic mating surface in sliding against graphite reveals coefficients of friction ranging from 0.05 to 0.15 in an ambient environment. However, the coefficient of friction when sliding on a face perpendicular to the basal planes compared to sliding parallel to the basal planes is three times or even higher [19]. Therefore, if tested parallel to the basal planes, graphite is soft and lubricates in normal air; however, it fails to lubricate in a vacuum or at high altitudes and wears rapidly. In fact, its coefficient of friction in vacuum or dry nitrogen is typically ten times greater than in air. Both natural and synthetic graphite must adsorb moisture or other condensable vapor such as hydrocarbons in order to be slippery and lubricious. The bonding energy between the hexagonal planes of graphite is reduced to a lower level by the adsorption of water under high-humidity environments. In fact, graphite exhibits excellent lubrication in boundary lubrication conditions due to its good affinity for hydrocarbon lubricants. In an oxidizing atmosphere, graphite lubricates effectively up to 450 °C and then fails due to structural degradation by oxidation [26]. Powdered graphite lubricants entrained in a gaseous carrier were used for rolling-contact bearings and high-speed spur gears for operation at temperatures over 650 °C in military aircraft. Impregnated graphite parts are not suited for applications in which mechanical shock or loading is relatively high and are often used in high-temperature structural applications such as missile-nozzle inserts, heat shields, and fuel-chamber liners. Under some circumstances, graphite additives are able to provide very short-term lubrication up to 1000 °C or even 1200 °C in the hot metal forming process. Graphite is widely used as the rubbing element in mechanical seals and as electrically conducting brushes for motors and generators. Generators used in airplanes flying at high altitudes worsen the performance of graphite brushes due to the lack of moisture in the air and water vapor. In this case, the brushes wear out rapidly at high altitudes, and thus, oxygen and water vapor are considered to be the most important gases for the brushes.

For applications where only a minor lubricity is needed and a more thermally insulating coating is required, amorphous carbon is predominant. In this case, amorphous carbon and graphite can be combined to take full advantage of the strengths and weaknesses of each. Parts made from carbon-graphite are strong and hard and exhibit low friction. Some carbon-graphite bearings are capable of extended service at temperatures above 580 °C, which is ideal for chemically aggressive applications. Carbon-bonded graphite with high thermal conductivity is desirable for high-temperature applications with high sliding speeds up to 150 m/s (e.g., encountered in aircraft jet engine seals) in order to dissipate the frictional heat. Many carbon-graphite parts impregnated with fillers such as various metals (e.g., Ag, Cu-Pb alloys) and high-temperature chemical salts provide lower permeability, higher strength and hardness, low friction, wear and oxidation resistance in dry air at temperatures up to 750 °C. In a hot metal forming process, a high-temperature graphite-based solid lubricant consisting of amorphous silica, aluminum dihydrogen phosphate, and graphite exhibits strong adhesion to the substrate and excellent tribological properties with a low friction coefficient of about 0.05 and good wear protection for the workpiece at elevated temperatures in the air [52].

Graphite fluoride $(CF_x)_n$, also referred to as carbon monofluoride (when $x = 1$), is a solid lubricant that can be described as a layer lattice intercalation compound of graphite [1]. It is an electrical insulator, unlike graphite, and is non-wettable by water. Graphite fluoride is generally synthesized by the direct reaction of graphite with fluorine gas at controlled pressure and temperature. However, the frictional properties of graphite fluoride are less influenced by humidity than either MoS_2 or graphite. Graphite fluoride synthesized by the above-mentioned method exhibits grey to pure white depending upon

its composition parameter, where x can vary from about 0.3 to 1.1. The fluorine to carbon bonds are covalent with the fluorine atoms located between the distorted basal planes. The spacing between the basal planes is expanded from 0.34 nm in graphite to 0.75 ± 0.15 nm in $(CF_x)_n$, which leads to a further decrease in shear and cleavage strength parallel to the basal planes [11]. $(CF_x)_n$ is not known to oxidize in air, but it decomposes thermally above about 450 °C to form carbon tetrafluoromethane, other low molecular weight fluorocarbons, and carbon. $(CF_x)_n$ exhibits extreme plasticity within lubricated contact.

4.3.2. Hexagonal Boron Nitride (h-BN)

h-BN, either in its pure form or as a composite, is an extremely suitable material for a variety of high-temperature applications, such as solid lubrication material, gas seals for oxygen sensors, high-temperature furnace parts, crucibles for molten glass and metals, as well as evaporation boats for aluminum and side dams for thin-strip casting [53]. h-BN, referred to as "white graphite", is composed of a layered structure containing a network of $(BN)_3$ rings. It has very anisotropic shear properties with preferred shear parallel to the basal planes or perpendicular to the c-axis [11]. Lamellar slip along the basal plane is regarded as the prominent lubrication mechanism at high temperatures. However, h-BN has significant drawbacks such as weak adhesion to most metals and ceramics and the ability of difficult-to-sinter, which generally leads to low strength and low quality of composite materials [1,11]. The h-BN layers show a down-graded tribological performance due to relatively stronger van der Waals interlayer forces than graphite or MoS_2. However, it works better under humid and high-temperature conditions due to its stronger oxidation resistance and higher thermal stability, making it suitable for sintering processes. Especially h-BN is currently used as an additive to improve the tribological performance of ceramics and composites [54]. h-BN exhibits friction coefficients of 0.2–0.25 in a normal atmosphere, below 0.1 in humid air, and even smaller in water and Vaseline [55–57]. In order to improve the lubricity under different environmental conditions, h-BN as lubricating micro-particles are also impregnated into a porous surface [58,59] or added to lubricating oil [60] or even water [61]. The thermal stability of h-BN is better than that of MoS_2 or graphite, but its friction coefficient at room temperature is relatively high; however, it drops to about 0.15 at 600 °C. Interestingly, h-BN exhibits a good lubrication feature even at a service temperature of 1200 °C in an oxidizing atmosphere. Friction and wear tests of pure h-BN and h-BN-10 wt.% CaB_2O_4 was performed in sliding against Si_3N_4 counterpart on a ball-on-disk tribometer in atmospheric and water vapor environments from room temperature to 800 °C [56]. Both pure h-BN and h-BN-10 wt.% CaB_2O_4 have a similar friction coefficient of less than 0.2 in atmospheric conditions at room temperature. At 400 °C, both of them exhibit high friction coefficients of 0.58 and 0.51 due to the adhesion of h-BN on the coupled Si_3N_4 ball, respectively. On further increasing the test temperature to 800 °C, the coefficients of friction for pure h-BN and h-BN-10 wt.% CaB_2O_4 decreased to 0.38 and 0.35, respectively, which is attributed to the formation of molten B_2O_3. Interestingly, the friction and wear tests performed in the water vapor environment showed prominently reduced friction coefficients of 0.08 and 0.07 for pure h-BN and h-BN-10 wt.% CaB_2O_4 at room temperature, respectively. However, increasing the test temperature to 400 °C leads to an increase of the friction coefficient to between 0.25 and 0.23, which is distinctly lower than those tested under atmospheric conditions, due to the reaction of h-BN with water vapor to form B_2O_3 and finally H_3BO_3. The formed H_3BO_3 has a lamellar structure that can shear very easily under tribo-stressing to reduce friction and wear. At 800 °C, the friction coefficients for pure h-BN and h-BN-10 wt.% CaB_2O_4 are 0.22 and 0.21, respectively, which are also lower than those obtained under atmospheric conditions. Table 3 summarizes the fabrication methods and tribological behavior of self-lubricating materials containing h-BN [56,59,62–65].

Table 3. Fabrication methods and tribological behavior of self-lubricating materials containing *h*-BN [56,59,62–65].

Materials	Fabrication Method	Tested Conditions	Results/Observations
h-BN *h*-BN-10 wt.% CaB$_2$O$_4$ [56]	Hot pressing	Ball-on-disk; Si$_3$N$_4$ ball; load 1.5 N; 0.188 m/s; RT-800 °C	• μ: 0.18, 0.58, 0.38 (*h*-BN, atmosphere ambience, at RT, 400, 800 °C) • μ: 0.08, 0.25, 0.22 (*h*-BN, water vapor ambience, at RT, 400, 800 °C) • CaB$_2$O$_4$ as the sintering additive promoted crystallization of *h*-BN and decreased the friction coefficient. • H$_3$BO$_3$ formed by the reaction of water vapor with *h*-BN has a lamellar structure to reduce friction and wear.
Cu-based composites (Cu-Sn-Al-Fe-*h*-BN-Graphite-SiC) [59]	Hot pressing	Block-on-ring; AISI52100 bearing steel; load 50–125 N; 1.04–2.6 m/s; RT	• μ: ~0.5 • W: 1.3×10^{-5}–4.3×10^{-5} mm^3/(Nm) • (Varying with the content of *h*-BN and graphite) • The higher ratio of graphite to *h*-BN contributed to form relatively continuous and compact tribo-films.
B$_4$C-*h*-BN [62]	Hot pressing	Pin-on-disk B$_4$C pin; load 10 N; 0.656 m/s; 25 °C	• μ: 0.591–0.321 (content of *h*-BN rising from 0 to 30 wt.%) • W: 2.07×10^{-5}–1.94×10^{-4} mm^3/(Nm) (content of *h*-BN from 0 to 30 wt.%) • The transfer film formed on the wearing surface is considered as the main cause of tribological properties improvement.
NiCr/Cr$_3$C$_2$-NiCr/*h*-BN [63]	Plasma spraying	Ball-on-disk; Si$_3$N$_4$ ball; load 9.8 N; 0.188 m/s; 20–800 °C	• μ: 0.65–0.55 (20–800 °C) • W: 5.3×10^{-5}–1.15×10^{-4} mm^3/(Nm) (20–800 °C) • *h*-BN reduces the friction coefficient but weaken the wear resista nce due to the poor cohesive strength.
Ni-P-*h*-BN [64]	Electroless plating	Pin-on-disk; AISI52100 steel ball; load 2 N; 0.1 m/s; RT	• μ: 0.2 • W: 1.24×10^{-6} mm^3/(Nm) • Stable sliding distance > 1000 m
NiCrWMoAlTi-*h*-BN-Ag [65]	Hot pressing	Ring-on-disk; AISI52100 steel ball; load 20 N; 1 m/s; RT-600 °C	• μ: 0.54–0.37 (RT-600 °C) • W: 7×10^{-5}, 7×10^{-4}, 2×10^{-4} mm^3/(Nm) (RT, 200, 600 °C) • Stable sliding distance > 600 m

The addition of BN or TiN into the Si$_3$N$_4$ matrix can reduce the friction and wear in the sliding of self-mated couples below 100 °C, especially at room temperature in humid air, where the friction coefficient is reduced to 0.1 and the wear rate is one-fifth that of monolithic Si$_3$N$_4$. Besides the optimized mechanical properties of Si$_3$N$_4$-BN and Si$_3$N$_4$-TiN composites without any glass phase, the distinct improvement in tribological behavior was attributed to the tribo-chemical reaction to form relatively soft lubricious oxide layers such as H$_3$BO$_3$ and TiO$_{2-x}$ or an intrinsic solid lubricant of BN·H$_2$O [9,66]. For Si$_3$N$_4$-based cutting tools, chipping and subsequent fracture lead to unavoidable failure when subjected to fatigue loading and high temperatures, particularly during high-speed machining of hard-to-cut materials [67]. However, when *h*-BN is added to Si$_3$N$_4$, a significant tribological improvement is achieved with austenitic stainless steel as tribo-pair due to the formation of a tribo-film comprising Fe$_2$O$_3$, SiO$_2$, and B$_2$O$_3$. *h*-BN is used as a high-temperature solid

lubricant in the ceramic matrix such as Al_2O_3, TiB_2, and B_4C [62] due to its high chemical stability and resistance to oxidation. However, one challenge of using *h*-BN as the additive in the cutting tool is the difficulty to sinter of fully densification and poor adhesion with ceramics due to its flaky structure and low diffusion coefficient [68].

h-BN, as a clean solid lubricant, is able to replace dirty graphite or MoS_2 in Al-forming processes without staining. The tribological performance, including the lubrication-film stability and the surface quality, depends mainly upon the particle size and concentration of *h*-BN powders [69]. *h*-BN is chemically inert and difficult to wet with most molten metals. Therefore, *h*-BN is an important solid lubricant for various industrial applications, especially in aircraft turbo engines [56] and in metalworking processes where high-temperature lubrication and/or environmental cleanliness are preferentially required [60].

Layered-structure *h*-BN is incorporated with monoclinic zirconia or ZrO_2-SiC or SiAlON as a composite material for side dams in twin roll strip steel casting due to its unique combination of properties such as excellent release and lubrication properties, high-temperature thermal shock resistance, chemical inertness, and easy machinability to produce complex shapes from the as-sintered billets [53,70,71]. One of the main products of ESK ceramics GmbH & Co. KG, a subsidiary of Ceradyne Inc., is hexagonal boron nitride, which can be used as powders, coatings, or in its sintered form either as pure BN or as a composite at a maximum operating temperature of up to 1100/1500 °C in an oxidizing/inert atmosphere, respectively [53].

BN-based materials incorporated with monoclinic ZrO_2 and SiC are used in steel production as the best side-dam material for twin roll strip steel casting as well as a broken ring for horizontal continuous casting [53,72–74]. Wear tests were carried out from room temperature to 400 °C using a pin-on-disc high-temperature tribometer with BN-based composite pins sliding against a rotating disc of nickel [70]. Control of the wear process requires a better understanding of the mechanisms of third body formation and the velocity accommodation mechanisms. The wear surface of BN-based composites shows textured grooves, brittle fracture, and microplastic deformation [53].

C/C-*h*-BN-SiC composites were prepared by molding, carbonization, and liquid silicon infiltration processes, which exhibited excellent oxidation resistance, self-healing function, and self-lubrication properties for high-temperature applications. Herein, *h*-BN addition promotes the formation of a lubricious tribofilm and distinctly reduces the friction and wear of C/C-*h*-BN-SiC composites without any clamping stagnation phenomenon in high braking speed conditions [75].

h-BN is used as a solid lubricant or release agent either as a sintered body (e.g., side dams) or applied as suspensions or powders or coatings (e.g., aluminum extrusion or titanium shaping, aluminum casting, superior lubricity). A 15 μm thick *h*-BN coating prepared from a polyborazylene polymeric precursor was deposited on titanium alloys and annealed via infra-red irradiation in a rapid thermal annealing furnace for high-temperature tribological applications. The friction coefficient tested at 360 °C was reduced from 0.72 for Ti-alloys to 0.35 for the Ti@*h*-BN coating when sliding against the coupled 15-5PH stainless steel cylinders using a cylinder/disk configuration [76,77]. The Ni-P-35 vol.% *h*-BN autocatalytic composite coating has a wear rate in the order of 10^{-6} mm^3/(Nm) and a friction coefficient of 0.2 against the tribopair of AISI52100 steel ball at ambient temperature [64]. The addition of silver and *h*-BN nanopowders into nickel-based composites exhibits a self-lubricity from room temperature to 600 °C [75]. The mechanical strength and tribological behavior of ion-beam-deposited *h*-BN films on non-metallic substrates were also investigated with diamond pin sliding experiments. BN films on Si and SiO_2 exhibited low friction coefficients of less than 0.1; however, BN films on nonmetallic substrates could fracture at a critical load [78].

4.3.3. Transition Metal Dichalcogenides

Transition metal dichalcogenides (TMD) solid lubricants include a wide range of hexagonal layered compounds formed by the bonding between chalcogenides such as sulfur, selenium, and tellurium, as well as transition metals such as molybdenum, tungsten, and niobium [79,80]. The lubrication mechanism for this class of solid lubricants is closely related to their microstructure, and the weak van der Waals adhesion forces between sulfur-like atoms lead to the formation of easy-to-shear lamellas [54]. Some compounds, such as Mo- and W-disulfides and Nb-diselenide, have a closely packed lamellar structure with strong bonding between the transition metal and chalcogenide ligands. MoS_2 and WS_2 are typical representatives of intrinsic solid lubricants and are the best lubricants of choice, especially for vacuum applications. They do not require adsorbed materials or additives to develop lubricating capability. However, when subjected to the adsorption of chemical compounds like H_2O from the environment, the lubricity worsens rapidly, which significantly influences the ability of the lamellas to slide against each other. It must be noted that a layered microstructure is not sufficient to achieve self-lubrication, and the strength of the interlayer bonding is a decisive factor, as observed for similarly layered TMDs like NbS_2, TiS_2, etc. One of the main prerequisites to achieving ultralow friction for MoS_2 lubricants is the absence of contaminants, such as oxygen, water, and hydrocarbons [81]. The susceptibility of MoS_2 films to moisture is reduced by adding different dopants, including Pb, Au, and polytetrafluoroethlene (PTFE). It is noted that the addition of carbon to burnished and bonded MoS_2 improves the performance of MoS_2 in humid air [3].

MoS_2 is thermally stable in non-oxidizing environments up to 1100 °C, but in the air, the onset oxidation temperature of MoS_2 is at around 350 °C. The oxidized product MoO_3 is believed to be abrasive, which limits the maximum-use temperature, although now it may be virtually innocuous. Friction coefficients for sputtered MoS_2 in a vacuum were reported to be as low as 0.01, however, oxygen and especially water vapor in the ambient atmosphere causes a slow oxidative degradation of MoS_2, which leads to early failure. The oxidation rate also depends strongly on the airflow rate through the reaction chamber. MoS_2 was oxidized to molybdic oxide (MoO_3) in 1 h at 400 °C at a low flow rate of 5.5×10^{-6} mm^3/s and lost the lubricating ability in the air. Therefore, MoS_2 is a poor lubricant when used in humid air, and it is also corrosive to the mating metallic surface due to the formation of a surface layer comprising oxysulfide ($MoOS_2$) and sulfuric acid of H_2SO_4. WS_2 is a better lubricant than MoS_2 at high temperatures in both air and non-oxidizing atmospheres. Similarly, WS_2 starts to oxidize appreciably above 425 °C, which also limits distinctly its usefulness in air. The XPS analysis on the wear scar of WS_2 coatings in Figure 2 shows a significant difference in elemental distribution and oxidation state at temperatures of 100 °C and 500 °C. A very low W^{6+} content from WO_3 peaks indicates slight oxidization of the surface on the wear scar at 100 °C. However, sulfur almost disappears at 500 °C, and WS_2 is completely oxidized to form WO_3 [82]. WS_2 nanoparticles with a closed-cage structure have already been investigated for superior lubrication applications under harsh circumstances, which provide excellent performance for the tribological contact between silicon nitride ball and alumina ceramic block due to gradual exfoliation of the fullerene-like WS_2 onions followed by transfer of monomolecular WS_2 sheets to the coupled surface [83].
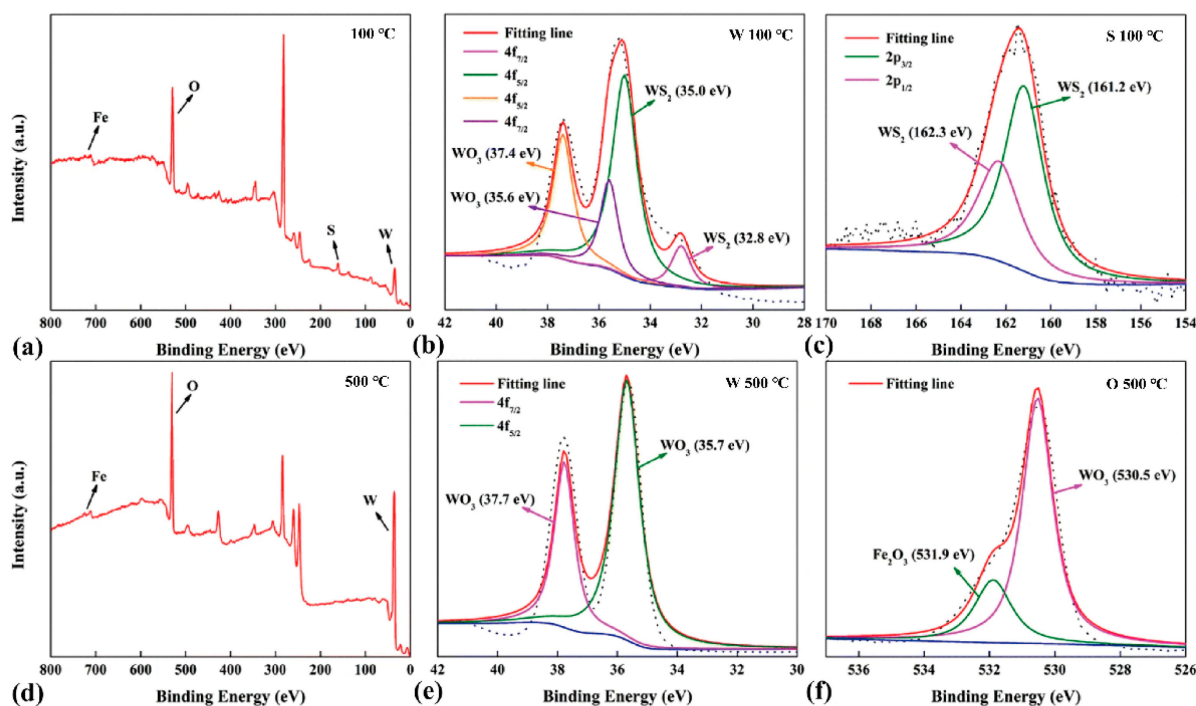
Figure 2. Elemental distribution at (**a**) 100 °C and (**d**) 500 °C. XPS spectra of W 4f at (**b**) 100 °C and (**e**) 500 °C, S 2p at (**c**) 100 °C, and O 1s at (**f**) 500 °C. Reproduced with permission from Reference [82], Copyright © Springer Science Business Media, LLC, part of Springer Nature 2020.

TMD compounds can be used as lubricants themselves or as lubricant additives to reduce both friction and wear. TMD powders are frequently used in such applications as metal-forming dies, threaded parts, sleeve bearings, and electrical contacts in relays and switches. The applications of TMD-containing materials include bulk composites sintered by powder metallurgy, thin films deposited by PVD or burnishing, and thick coatings either by laser cladding or thermal spraying [54]. No matter what techniques are adopted for material fabrication, superior low friction and small wear rate must be provided in a wide operating temperature range to achieve the desired lubricity [2]. Refractory metal-based composites containing MoS_2 or WS_2 can be used at loads up to 70 GPa at 500 °C and 7 GPa at 800 °C in a vacuum, such as applications for bushings, seals, gears, clutch facings, and electric motor brushes. Applying MoS_2 as a solid lubricant onto solid surfaces includes burnishing, spray bonding, physical vapor deposition, and, in particular, sputtering, such as for applications of bearings employed in spacecraft, which contributes to maintaining essential lubrication properties, thus reducing friction and/or wear as well as enhancing their service life and energy efficiency by avoiding premature failures.

In the case of burnished MoS_2 or WS_2 coatings, the preferential orientation of MoS_2 or WS_2 crystallites can be introduced within the coating where the basal planes are mostly parallel to the sliding direction to achieve low friction, which is commonly used in bearings and other sliding/rolling applications. Bonded coatings can be applied by spraying to produce a more uniform coating with careful process control, such as the superior lubrication of gears for the space station remote manipulator system (SSRMS) without apparent wear over several million cycles. Solid lubrication techniques of MoS_2 films have been successfully adopted in representative ball bearings, pointing mechanisms, slip rings, gears, and release mechanisms in space applications [84]. The increasing solid lubrication of MoS_2 needs to operate in a wide range of temperature conditions for longer durations in a robust and reliable fashion for planned space missions, such as the ESA's BepiColombo mission to Mercury, where long-term exposure to temperatures on the order of 250 °C is involved [85]. Herein, a particularly important example associated with the failure of the MoS_2-based solid lubricant during space operation is the catastrophic high-gain antenna

deployment failure associated with the Galileo spacecraft [86], although the reliability of lubrication provided by MoS_2 was successfully tested before deployment on Earth under ambient conditions. MoS_2 was also determined as the solid lubricant of choice for precision instruments on the Hubble Space Telescope and its successor of the James Webb Space Telescope (JWST) [80].

Sputtered and resin-bonded MoS_2 coatings are used in numerous applications of satellites and the space shuttle. Resin-bonded spray coatings followed by the heat-curing process are typically from 5 to 15 μm thick with friction coefficients of only from 0.06 to 0.15 and superior wear life, depending on humidity and sliding conditions. However, the main inorganic binders in inorganic-bonded MoS_2 coatings used for space applications are generally silicates (e.g., Na_2SiO_3) and phosphates (e.g., $AlPO_4$), which can tolerate moderately elevated temperatures up to 650–750 °C for various types of gears and low-cycle bearings on launch vehicles. However, one challenge is associated with softening or degradation in the presence of water/humidity. A phosphate-bonded MoS_2 coating is used for the lubrication of the Mars Science Laboratory (MSL) Curiosity Rover Main Differential Pivot to deliver the frictional torque. Sputter-deposited MoS_2 coatings incorporated with or without soft metals and other compounds exhibit considerably low friction for the lubrication of components in space programs. However, a main technical obstacle associated with these sputtered coatings is the difficulty of deposition on large parts in a vacuum [87].

4.3.4. Layered MAX Phase Materials

MAX phase materials include ternary MAX phases ($M_{n+1}AX_n$), MAX phase-like compounds ($M_{n+2}A_2X_n$ and $M_mA_nX_p$, m ≠ n + p), quaternary MAX phases (M',M'')$_{n+1}AX_n$ and high-entropy MAX phases such as M_2AlC (M = Ti, Zr, Hf, Nb, Ta) or V_2AC (A = Sn, Fe, Co, Ni, Mn). Layered ternary MAX phase materials have the general formula $M_{n+1}AX_n$, where M represents a transition metal element, A is a group III or IV element of the periodic table, X is either C or N, and *n* ranges from 1 to 3. It is noted that the MAX phase exhibits the properties of both metals and ceramics. MAX phase compounds such as Ti_3SiC_2, $Ti_3Au_2C_2$, Ti_3SnC_2, Cr_2AlC, Ta_2AlC, and Ti_2Au_2C were reported to show good tribological properties, high-temperature self-healing ability, and electric conductivity, depending upon the nanolaminated structure of MX slabs with an interlayer of pure A element. Examples of the remarkable tribological performance of MAX phase materials were verified by sliding against the tribopair of Ni-based superalloys at an ambient temperature of 550 °C. The Cr_2AlC MAX phase exhibits excellent wear- and corrosion-resistant properties when used for automotive applications. Further, the incorporation of silver improves the tribological properties significantly and reduces the friction coefficient at room temperature. For example, hot-pressed NiMoAl-Cr_2AlC-Ag composites exhibited a low friction coefficient of 0.27 and a small wear rate, which is attributed to the tribochemical-reacted films of mixed oxides such as Ag_2MoO_4 and Al_2O_3 formed on the worn surface [88–91]. Ti_3SiC_2-PbO-Ag composites fabricated by spark plasma sintering exhibited a friction coefficient of 0.3 and a small wear rate in sliding against Inconel 718 alloy at 800 °C [92]. Ternary MAX phase materials have also attracted considerable interest as pantograph contact strips for electric railways.

4.4. Chemically Stable Fluorides

Chemically stable fluorides, such as CaF_2, BaF_2, and their binary eutectic combinations, are lubricious to reduce friction and wear from about 400 to 900 °C; however, they exhibit poor tribological behavior at low to moderate temperatures [1,11]. CaF_2, BaF_2, and BaF_2-CaF_2 eutectics have melting points of 1418 °C, 1353 °C, and 1022 °C, respectively. The lubrication mechanism of alkaline earth fluorides and eutectics depends upon a marked softening effect occurring at temperatures close to 500 °C due to a brittle-to-ductile transition [1]. Alkaline earth fluorides and eutectics are widely used as solid lubricants in metallic and ceramic matrix composites in industrial applications such as advanced engines due to their high chemical and thermal stability.

CaF_2 is a non-layered structure, however, it exists a slip plane of Ca atomic compact plane in its phase structure. Under high-temperature conditions, the slip plane is easy to shear off due to the decrease in atomic force. LiF, MgF_2, and some rare-earth fluorides, particularly LaF_3 and CeF_3, show some lubricating capability in the air at high temperatures up to at least 1000 °C [11]. Most fluorides are able to operate under heavy loads or in chemically reactive environments [1,11]. These solid lubricants can be applied in the form of either coatings or bulk composites, such as fused fluoride coatings or as fluoride/metal or fluoride/ceramic self-lubricating composites or composite coatings. Their coefficients of thermal expansion are matched well with many alloys to which they can be bonded, such as nickel-base superalloys. The tribological properties of rare-earth fluorides and BaF_2-CaF_2 eutectics at elevated temperatures were investigated [1]. Friction coefficients of nickel-base composite coatings containing CeF_3 and LaF_3 were from 0.3 to 0.4 with increasing test temperature to about 500 °C. The average coefficient of friction was 0.2 from 500 °C to 1000 °C, which verified the good potential of these fluorides as high-temperature lubricants in oxidizing environments [1]. Interestingly, the relatively high friction of fluoride eutectics at low temperatures and sliding velocities stimulated the synergistic lubrication of combining silver with the BaF_2-CaF_2 eutectic coatings, which finally led to low and stable friction from room temperature to 900 °C. Sliney pioneered the combination of silver and fluoride eutectics in plasma sprayed composite coatings as a way to reduce friction and wear over a wide temperature range over repeated temperature cycling, especially the development of plasma spray coatings incorporated with silver and BaF_2-CaF_2 eutectics such as PS212 and PS304 for aerospace applications [7,93]. A particularly important example associated with successful applications of these plasma sprayed coatings is a high-temperature cylinder wall coating for a Stirling engine and a backup lubricant coating for gas bearings [94,95]. Rare-earth fluorides of CeF_3, LaF_3, and NdF_3 were also found to be used as anti-wear, friction-reduction, and extreme pressure additives in lubricating greases and oils [96].

A series of self-lubricating composites based on BaF_2-CaF_2 eutectic and silver solid lubricants were also developed by powder metallurgy methods [1,94,95]. These composites were designed to consist of a wear-resistant, metal-bonded matrix and solid lubricants of silver and BaF_2-CaF_2 eutectic. Typical examples of powder metallurgy parts include process valve stem bushings, control surface bearings, and turbine engine bushings [94]. The PM212 composite, which was designed to consist of a metal-bonded Cr_3C_2 matrix and solid lubricants of Ag and BaF_2-CaF_2 eutectic, exhibited a friction coefficient of 0.29–0.38 from 25 to 850 °C in the air [95]. Similarly, the PM304 composite, which was comprised of a hardener Cr_2O_3 within a Ni80Cr20 matrix and Ag and BaF_2-CaF_2 eutectic solid lubricants, was developed with good tribological performance from room temperature to 650 °C. The friction coefficient of PM304 showed an almost the stable value of 0.33 at temperatures of 200–800 °C [97]. Several Ni_3Al matrix composites of Ni_3Al-Cr-Ag-BaF_2/CaF_2 and Ni_3Al-Mo-Ag-BaF_2/CaF_2 were developed based on lubrication characteristics of Ag below 400 °C and fluoride eutectics at elevated temperatures and barium salts formed in situ on the worn surface [98–100].

$ZrO_2(Y_2O_3)$ matrix composites incorporated with BaF_2-CaF_2 eutectic exhibited good friction and wear properties only above 400 °C when tested in dry sliding against alumina ball in a test temperature range from 25 to 800 °C [101]. In order to generate good self-lubricity from room temperature to about 400 °C, soft noble metals of Au or Ag were added into $ZrO_2(Y_2O_3)$-CaF_2 composites, which finally exhibited low friction coefficients and small wear rates in the order of 10^{-6} mm^3/(Nm) from room temperature to 800 °C [102,103].

4.5. Binary Metallic Oxides

Commonly used hard oxides such as alumina, zirconia, and mullite exhibit good wear resistance but generally have high friction coefficients in dry air, which generate high tensile stresses and lead to surface cracks and debris particles [101]. Some oxides have good potential for solid lubrication due to their high thermal stability in the air, even at quite high temperatures. However, they have not been extensively investigated for room temperature solid lubrication due to their typical brittle nature. Their inability to deform plastically or shear easily at room temperature hinders them from forming smooth and lubricious transfer films on worn surfaces. In addition, the wear debris from oxide surfaces is generally abrasive. Oxide surfaces are usually inert in dry air and do not form strong adhesive bonds, such as metals in tribological contact.

In a search for high-temperature solid lubrication, many efforts have been made on various soft oxides. For example, lead monoxide (PbO) has low friction coefficients, especially at elevated temperatures due to its viscous flow, with a friction coefficient of 0.07 at 675 °C. Small amounts of SiO_2, B_2O_3, and Fe_2O_3 are added into PbO to form a sintered ceramic coating that is able to protect against oxidation of PbO and improve adhesion to substrates. Lubricious binary (e.g., PbO, Bi_2O_3, B_2O_3, V_2O_5) and ternary oxides (e.g., Ag_3VO_4, Ag_2MoO_4) are thermally stable and effective lubricants at high temperatures. However, they are generally not capable of providing lubrication at room temperature. These changes in friction and wear properties are closely related to the softening effect after the brittle to ductile transition above a critical temperature. Oxides are known to soften above their ductile-to-brittle transition temperature, which is typically 0.4–0.7 T_m where T_m, is the melting point (in K).

A crystal-chemical model was proposed to establish the relationship between friction coefficient and ionic potentials of lubricious oxides at sliding interfaces [10]. Re_2O_7, B_2O_3, and V_2O_5 have high ionic potentials and relatively low melting points of 301.5 °C, 450 °C, and 680 °C, respectively. In this case, the higher the ionic potential of oxides, the lower the friction coefficient of binary oxides. Herein, cations are screened more effectively by oxygen anions and thus less likely to interact with other cations at the contact surface, which can be used to explain the decrease in the overall shear strength and the observed lubricious behavior of vanadium or molybdenum oxides. However, some oxides, such as PbO and Bi_2O_3, have very low ionic potentials and exhibit exceptionally low friction, which does not coincide with the above-mentioned model [104].

A polarizability approach was proposed to classify oxides into acidic, basic, and very basic oxides according to the average ionic polarizability, binding energy, optical basicity, and interaction parameter [105]. A relatively low interaction parameter in basic or very basic oxides with large polarizability and low binding energy is closely related to a high unshared electron density and the increased ionicity of chemical bonds [104]. In this case, a high lubricity at elevated temperatures is achieved for an oxide with a low interaction parameter, which has generally a high surface free energy and a low bond strength [106]. Friction for doped oxides or mixtures at the sliding contact is normally reduced by decreasing the interaction parameter. The formation of vacancies and the hopping of ions at the surface of oxides determine to a large extent the frictional behavior at elevated temperatures, which may be valuable to explain the complicated friction behavior of a variety of binary/mixed oxides, based on the polarizability [105].

Computational modeling and simulations are also used to investigate the relationship between crystal structure and frictional behavior of oxides to obtain a better fundamental understanding of experimental observations and make predictions. As is well known, the most widely used atomic-scale modeling approaches are based on density-functional theory (DFT) and molecular dynamics (MD) simulations. DFT-calculations are used to investigate the relationship between layer distance and interlayer bond strength in binary Magneli phases (e.g., V_2O_5, TiO_2, MoO_2, WO_3, and ReO_3), which explains their as-observed low shear behavior by tailoring the chemical composition [107]. However, DFT calculations are generally limited to relatively small systems (on the order of a nanometer) and static

properties, which is quite time-consuming and inefficient. Molecular dynamics simulation deals with the dynamic behavior of moving atoms in successive configurations of a system, which helps to understand friction and wear properties on length scales accessible to experimental methods.

Substoichiometric compounds of certain transition metallic oxides (e.g., Me_nO_{2n-1}, Me_nO_{3n-1}, or Me_nO_{3n-2}) contain planar lattice faults, which may result in crystallographic shear planes with reduced binding strength. Interestingly, Magneli phases such as TiO_x, VO_x, MoO_x, and WO_x deform by plastic flow rather than by brittle fracture at elevated temperatures [108]. Vanadium-based Magneli phases were verified to possess good self-lubricity in the industrial applications of high-temperature hard nitride coatings up to 700 °C [31]. The friction coefficients are reduced distinctly when these hard coatings were tested from 100 °C to 700 °C until the melting of the V_2O_5 phase at about 690 °C [109,110]. Hard nitrides or carbides containing W or Mo elements exhibit improved high-temperature tribological properties due to the formation of lubricious Magneli phases such as binary WO_x and MoO_x or multi-component oxides in the sliding contact [111,112]. A variety of binary metallic oxide coatings and their combinations provide solid lubrication at elevated temperatures, but the repeatability and sustainability of solid lubrication are still unknown under long-term thermal cycling conditions. Atomic layer deposited zinc titanate ($ZnTiO_3$) coatings after annealing exhibited a friction coefficient of only 0.12 and a small wear rate of 1×10^{-7} $mm^3/(Nm)$ in unidirectional sliding against stationary Si_3N_4 ball, which is potential candidates for high-temperature solid lubrication in moving mechanical assembles up to 550 °C [28].

In addition, binary or multi-component eutectic oxide systems are of considerable interest for lubricity. As the eutectic points in these systems are normally reduced, they are possible to have lower shear strength than individual oxides. The frictional characteristics of $CuO-Re_2O_7$, Cs_2O-MoO_3, $CuO-MoO_3$, Ag_2O-MoO_3, $PbO-B_2O_3$, $PbO-MoO_3$, $CoO-MoO_3$, Cs_2O-SiO_2, $CuO-V_2O_5$, and $NiO-MoO_3$ systems were studied at different test temperatures to evaluate the effectiveness of two oxide systems [10]. Similarly, the ability to form an easy-to-shear compound or a low-melting-point system can be improved by increasing the difference in ionic potential; therefore, they tend to exhibit lower shear strength and hardness at elevated temperatures [10]. The complex superconductor oxide of $YBa_2Cu_3O_y$ exhibits a friction coefficient of from 0.20 to 0.50 from room temperature to 1000 °C, which may be considered a potential candidate for high-temperature solid lubricant. $YBa_2Cu_3O_{7-delta}/Ag$ composites were prepared to evaluate the mechanical and tribological properties from cryogenic to high temperature to identify the contribution of the phonon and electron to friction behavior [113].

Strongly adherent and lubricious thin oxide films can be either directly fabricated by coating technologies, such as reactive magnetron sputtering under an oxygen-containing atmosphere, or by in situ formation by tribo-chemical reaction at elevated temperatures during the wear process. Nowadays, hard coating advancements have evolved from mainly high hardness coatings to current coatings with multifaceted functionalities of high hardness, toughness, temperature stability, oxidation resistance, low friction, and wear [114]. Nitride coatings have generally high hardness and wear resistance, and the vanadium incorporation into the nitride coating contributes to the reduction in the friction coefficient, especially at elevated temperatures via self-adaptation of the hard coating during sliding [31]. Vanadium-containing nitride coatings begin to form lubricious V_2O_5 on the worn surfaces when the test temperature is increased above 400 °C, and correspondingly, the friction coefficient decreases from 0.45 at room temperature to 0.25 at 700 °C [115]. Similarly, reciprocating wear tests of reactive cathodic arc ion-plated (V,Ti)N coatings were carried out using a ball-on-disc configuration from room temperature to 700 °C. The friction coefficient of (V,Ti)N coatings exhibited a distinct decrease at 500 °C, corresponding to the formation of a reacted layer containing TiO_2 and V_2O_5 oxides. With further increasing the wear test temperature to 700 °C, a melting phenomenon of Magneli phase V_2O_5 oxides was observed on the worn surface during sliding, which led to a further decrease in friction

coefficient [22]. Likewise, hard nitride coatings form lubricious metallic oxides adaptively on the contact surfaces in high-temperature oxidizing environments [114]. From these studies, V_2O_5 and related Magneli phases are closely related to the reduction in friction from 450 °C to 650 °C, just below the melting point of V_2O_5, which is well consistent with the adaptive lubrication mechanisms summarized by Voevodin et al. [30,31]. Some alloys of Ni-Cu-Re, Fe-Re, and Cu-Re exhibit friction coefficients from 0.2 to 0.3 due to the in situ formation of lubricious oxides at elevated temperatures [116]. Considerable progress has been made in identifying and exploring adaptive mechanisms to enable broad-temperature solid lubrication of hard coatings.

Although most binary oxides maintain low shear strengths only in a very narrow temperature range, mainly at elevated temperatures, it is definitely believed that binary oxides have the potential to lubricate in selected environments through suitable surface design and composition tailoring and will become the focus of future studies. The material selected from the oxide family can be operated adaptively at elevated temperatures, in moist air, or in a vacuum.

4.6. Ternary Metallic Oxides

4.6.1. Molybdates

Some metallic molybdates, such as $PbMoO_4$ [117], $ZnMoO_4$, $CoMoO_4$, K_2MoO_4, $BaMoO_4$ [118], $CaMoO_4$, $SrMoO_4$, Ag_2MoO_4 and $Ag_2Mo_2O_7$ [119], are found to be lubricious at elevated temperatures. $PbMoO_4$ and $CaMoO_4$ have melting points of 1070 °C and 1065 °C, and relatively low Mohs hardness of 3.0 and 3.5 at room temperature, respectively. $BaMO_4$ is one of the most important molybdates with a scheelite-type tetragonal structure and has potential applications in solid lubrication, photoluminescence, solid-state lasers, and photocatalysts. Currently, $BaMoO_4$ and $SrMoO_4$ powders have been prepared by microwave-assisted synthesis, hydrothermal route, micro-emulsion route, complex polymerization method, and electrochemical method [120]. $SrMoO_4$ has a tetragonal structure with the lattice parameters of a = b = 0.539 nm and c = 1.202 nm.

Silver molybdates such as Ag_2MoO_4 and $Ag_2Mo_2O_7$ have layered microstructures similar to WS_2, which may lead to low friction at high temperatures [27,121]. B-Ag_2MoO_4 has a typical AB_2O_4 cubic spinel structure with excellent high-temperature stability, and its related lattice parameters are a = b = c = 0.9318 nm. The unit cell of β-Ag_2MoO_4 is composed of two basic structural units, with [AgO_6] octahedral clusters and [MoO_4] tetrahedral clusters. Under the action of external forces, the Ag-O bond is more likely to break and cause interlayer sliding for high-temperature lubrication performance [122]. Table 4 represents the fabrication methods and tribological behavior of self-lubricating materials containing molybdates [117–119,122–124].

From wear tests of $Mo_2N/MoS_2/Ag$ coatings, the corresponding lubrication mechanism is considered to be associated with the formation of molybdates such as Ag_2MoO_4 and $Ag_2Mo_2O_7$ layer sliding during relative motion due to weak bonding [119]. Herein, the combination of silver and molybdenum compounds can provide effective lubrication at low temperatures, while the presence of tribochemical reaction on the worn surface generates lubricious silver molybdates at elevated temperatures. The in situ formation of silver molybdates in plasma sprayed coatings containing silver and pure molybdenum was also studied [123]. As compared with unmodified Ni-based alloy, plasma sprayed coatings exhibited a distinct decrease in both friction and wear at 600 °C and even up to 800 °C. A tribochemically reacted layer was formed on worn surfaces at high temperatures, such as $Ag_2Mo_4O_{13}$ at 600 °C and $Ag_2Mo_2O_7$ and Ag_2MoO_4 at 800 °C, respectively. Especially theeutectic molybdates of $Ag_2Mo_2O_7$ and Ag_2MoO_4, which were melted below 500 °C, were reported [125].

Table 4. Fabrication methods and tribological behavior of self-lubricating materials containing molybdates [117–119,122–124].

Materials	Fabrication Method	Tested Conditions	Results/Observations
$PbMoO_4$ [117]	Pulsed laser deposition	Ball-on-flat (RT); Pin-on-disc (700 °C) 440C steel ball; 1 N; 0.6 m/s; RT, 700 °C	• μ: 0.6, poor lubricant and failed immediately (RT) • μ: 0.3–0.4, well lubricated and lasted for over 2 h (700 °C)
$NiCr$-$BaMoO_4$ [118]	Hot pressing	Ball-on-disk; Si_3N_4 ball; load 5 N; 0.126 m/s; RT–600 °C	• μ: 0.6, poor lubricant (RT) • μ: 0.26, 0.31 (400, 600 °C) • W: 8×10^{-6}, 2.15×10^{-5}, 4.25×10^{-6} mm^3/(Nm) (RT, 400, 600 °C) • The addition of $BaMoO_4$ reduces the friction and wear at high temperature.
Mo_2N-MoS_2-Ag [119]	Magnetron sputtering deposition	Ball-on-disk; Si_3N_4 ball; load 1 N; 0.11 m/s; RT–600 °C	• μ: 0.4, 0.3, 0.1 (RT, 350, 600 °C) • W: 2×10^{-5}, 6×10^{-6}, 8×10^{-7} mm^3/(Nm) (RT, 350, 600 °C) • 600 °C test cycles > 30,000 • Silver molybdates contribute to good lubrication at high temperature. • Types of silver molybdate phases depended on the ratio of MoS_2 to Ag.
$NiCoCrAlYTa$-Ag-Mo [122]	High-velocity oxy-fuel spraying	Ball-on-disk; Al_2O_3 ball; load 5 N; 0.1 m/s; 25–1000 °C	• μ: maximum of 0.48 at 400 °C, minimum of 0.22 at 800 °C • W: maximum of 3.2×10^{-4} mm^3/(Nm) at 400 °C, minimum of 1.1×10^{-5} mm^3/(Nm) at 800 °C • At 1000 °C, abrasive particles affect the formation of Ag_2MoO_4 lubricant film.
$NiCrAlY$-Ag-Mo [123]	Atmospheric plasma spraying	Ball-on-disk; Si_3N_4 ball; load 5 N; 0.3 m/s; 20–800 °C	• μ: maximum of 0.4 at 400 °C, minimum of 0.28 at 800 °C • W: 1×10^{-4} mm^3/(Nm) at 400 °C. • • Silver molybdate phases formed at high temperature.
Ni_3Al-Ag-$BaMoO_4$ [124]	Hot pressing	Ball-on-disk; Si_3N_4 ball; 20 N; 0.19 m/s; 20–800 °C	• μ: 0.33, 0.28, 0.28, 0.35 (20, 400, 600, 800 °C) • W: 1.1×10^{-4}, 2.6×10^{-4}, 4.1×10^{-5}, 1.5×10^{-4} mm^3/(Nm) (20, 400, 600, 800 °C)

High-velocity oxy-fuel spraying was used to deposit NiCoCrAlYTa/Ag/Mo composite coatings. A continuous lubricious film comprising layer-like Ag_2MoO_4 was formed at 800 °C on composite coatings with a friction coefficient of 0.22 and wear rate of 1.1×10^{-5} mm^3/(Nm) in sliding against sintered Al_2O_3 ball [122]. The addition of CaF_2 to the Fe-Mo alloys leads to the formation of a surface glaze consisting of $CaMoO_4$, CaF_2, Fe_2O_3, and MoO_3 after sliding wear tests at 600 °C. Ternary metal oxides such as Ag-V(Mo,Nb)-O formed on the worn surface are efficient high-temperature solid lubricants due to their structural and chemical inertness, as well as their excellent plasticity and low shear properties. Pulsed laser-deposited $PbMoO_4$ films were lubricious with a friction coefficient of 0.35 and good wear resistance at 700 °C; however, they exhibited a high friction coefficient and failed quickly at room temperature [117].

Nickel-chromium matrix composites incorporated with different amounts of $BaMoO_4$ were hot-pressed to evaluate the tribological properties using a ball-on-disc tribometer up to 600 °C. It is noted that the NiCr-20 wt.% $BaMoO_4$ composite possesses the best tribological performance, with a lower friction coefficient and almost an order of magnitude lower wear rate than the unmodified Ni-Cr composite at 600 °C, which is closely related to the lubricity of a smooth and dense oxide layer formed on worn surfaces, with strong Raman peaks corresponding to $BaMoO_4$ [118]. The self-lubricity of Ni_3Al matrix composites in a temperature range of room temperature to 800 °C is attributed to the synergistic lubrication of Ag and $BaCrO_4$ and $BaMoO_4$ barium salts in sliding against coupled Si_3N_4 ball [124]. However, the formation of non-lubricious $BaAl_2O_4$ in the composite must be avoided during the fabrication process.

4.6.2. Tungstates

Some metallic tungstates such as Ag_2WO_4 [27], $ZnWO_4$ [126,127], $CoWO_4$, $CaWO_4$, $BaWO_4$, and $SrWO_4$ [128] are found to be lubricious at elevated temperatures. $CoWO_4$ has a friction coefficient from 0.2 to 0.25 at temperatures from 600 °C to 800 °C. AWO_4 (A = Ca, Ba, and Sr) with a tetragonal scheelite structure is an important material for solid lubrication and electro-optical properties. $BaWO_4$ can be prepared by high-temperature flux crystallization, solid-state reaction, and hydrothermal-electrochemical methods. $BaWO_4$ powders with different morphology, such as olive-like, flake-like, and whisker-like structures, have been successfully prepared through a hydro-thermal process in the presence of different surfactants [129]. Dendrite-like, hollow, and various ordered structures of $BaWO_4$ were prepared by the solution methods, applying organic template and soft hydrothermal conditions, use of polymer or micro-emulsions [130,131]. $SrWO_4$ exhibits a tetragonal structure and has lattice parameters of a = b = 0.542 nm and c = 1.195 nm. In addition, the tribological performance of Ag_2WO_4 at elevated temperatures was investigated by means of ab initio calculations through MD simulations [27].

Ni_3Al-based composites incorporated with silver, BaF_2-CaF_2, and W were produced using powder metallurgy to evaluate tribological performance up to 800 °C on a ball-on-disc high-temperature tribometer. Stable friction and low wear rates are attributed to the formation of $CaWO_4$ and $BaWO_4$ during sliding at elevated temperatures [128].

Thin WS_2-ZnO composite films are deposited to produce lubrication over a wide temperature range. The tungsten disulfide reacted with the zinc oxide to form a lubricious $ZnWO_4$ phase at elevated temperatures [126]. Similarly, tribological properties of burnished films comprising WS_2 and ZnO are tested at high temperatures using a unidirectional ball-on-disc friction and wear tester [127]. The lubricious ternary $ZnWO_4$ oxide layer formed at 500 °C leads to low and stable friction during wear tests. These composite coatings were adaptively lubricious where WS_2 provided the low-temperature lubrication and then reacted with zinc oxide to form an effective high-temperature lubricant. However, the drawback associated with this synergistic lubrication is that the low-temperature lubrication of WS_2 will lose inevitably due to an irreversible reaction once returning to room temperature during the long-term thermal cycling process.

4.6.3. Vanadates

Lubricious binary V_2O_5 and ternary oxides of $AgVO_3$ [132,133], Ag_3VO_4 [27,121], $BiVO_4$, $Bi_4V_2O_{11}$, and $Bi_2V_3O_9$ are thermally stable and effective lubricants at high temperatures, although they are generally ineffective at providing self-lubricity at room temperature. Vanadate is a pentavalent monomer of vanadium oxide that can exist either as the meta- or ortho- form depending on the number of oxygen ligands around the vanadium atom. Vanadate powders with different particle size distributions and morphologies have been synthesized by simple and facile approaches such as hydrothermal and wet precipitation routes at room temperature. $BiVO_4$ powders with a monoclinic structure were also synthesized by a high-temperature solid-state reaction at 700 °C. Many efforts have been made on the synthesis and characterization of monoclinic phase β-$AgVO_3$ and

nanostructured $Ag@Ag_3VO_4$ [134,135]. Silver vanadates such as Ag_3VO_4 have layered microstructures, which may lead to low friction at high temperatures [27,121]. Table 5 shows the fabrication methods and tribological behavior of self-lubricating materials containing vanadates [121,132,133].

Table 5. Fabrication methods and tribological behavior of self-lubricating materials containing vanadates [121,132,133].

Materials	Fabrication Method	Tested Conditions	Results/Observation
VN-Ag [121]	Magnetron sputtering deposition	Ball-on-disk; Si_3N_4 ball; load 2 N; 0.11 m/s; RT-1000 °C	• μ: 0.37, 0.3, 0.12, 0.2 (RT, 350, 700, 1000 °C) • Silver, vanadium oxide and silver vanadate formed on the surface. • Ag_3VO_4 with layered atomic structure is presumed to improve the lubricant performance.
VN-Ag [132]	Pulsed laser deposition	Ball-on-disk; Al_2O_3 ball; load 10 N; 0.063 m/s; RT-900 °C	• μ: 0.3, 0.2, 0.18, 0.1, 0.08 (RT, 200, 400, 600, 800 °C) • The synergy of silver vanadate and molten lubricant vanadium oxides generates a low friction coefficient at high temperature.
NiCrAlY-Cr_3C_2(NiCr)-V_2O_5-Ag_2O [133]	Laser cladding	Ball-on-disk; Si_3N_4 ball; load 3 N; 0.188 m/s; 25–800 °C	• μ: 0.52, 0.49, 0.35, 0.25, 0.15 (25, 350, 600 °C) • W: maximum of 6.9×10^{-5} mm^3/(Nm) at 400 °C, minimum of 2.9×10^{-5} mm^3/(Nm) at 800 °C

Silver-based vanadate ($Ag_{0.33}V_2O_5$) thin films deposited by PVD have a higher friction coefficient at moderate temperatures but exhibit a lower friction coefficient up to 500 °C and even to about 0.25 at 600 °C than V_2O_5 coatings [109]. VN thin films incorporated with different silver contents deposited by unbalanced reactive magnetron sputtering exhibit good frictional behavior within the temperature ranges up to 1000 °C using a ball-on-disc friction and wear tester, with a minimum friction coefficient of 0.2 at 700 °C, which is attributed to the in situ formation of lubricious silver vanadate an Ag_3VO_4 during sliding [121]. Similarly, Ag/VN thin films by pulsed-laser deposition also exhibited reduced friction and wear at 700 °C and 900 °C when sliding against an Al_2O_3 ball, due to the formation of V_2O_5, $AgVO_3$, and Ag_3VO_4 [132]. Laser-clad NiCrAlY-based coatings incorporated with V_2O_5 and Ag_2O solid lubricants have low friction and wear from 600 °C to 800 °C, due to the formation of $AgVO_3$ and Ag_3VO_4 [133]. In addition, soft metal-containing inorganic compounds such as Ag_3VO_4 were also embedded into textured hard surfaces to produce continuous self-lubricity over a wide temperature range up to 800 °C [136].

4.6.4. Tantalates

Ternary metal oxides of (Ag, Cu)-Ta(V,Mo)-O such as $AgTaO_3$, $CuTaO_3$, and $CuTa_2O_6$ have recently been explored as promising lubricants for high-temperature applications due to their structural and chemical inertness and low friction at elevated temperatures. A soft metallic silver-containing phase is generated when silver tantalate ($AgTaO_3$) with a layer-like structure is highly resistant to oxidation and is subjected to sliding at elevated temperatures [137]. Layered $AgTaO_3$ has a relatively high melting temperature of 1172 °C and undergoes a series of structural phase transitions with temperature until it reaches its melting point [138]. The temperature dependence of mechanical and tribological responses to sliding is closely linked with the above-mentioned structural changes of $AgTaO_3$.

Several processing approaches were explored to fabricate lubricious silver tantalate films on Inconel substrates for extreme temperature applications as follows: (1) burnished powder films on the substrate; (2) magnetron sputtered monolithic silver tantalate films; (3) sputter-deposited adaptive tantalum nitride/silver nanocomposite coatings, which forms a lubricious silver tantalate layer on its surface by high-temperature tribochemical reaction during sliding. For example, this coating has friction coefficients in the range from 0.06 to 0.15 at 750 °C in dry sliding against Si_3N_4 counterfaces [137,139]. A mechanically mixed layer comprising nanocrystalline Ag, Ta_2O_5, and $AgTaO_3$ phases was generated due to surface reconstruction induced by friction heat and shear stress. The aggregated silver clusters on the sliding surface are beneficial for low friction [139]. However, the silver diffuses rapidly on the surface, and its high mobility leads to a relatively low wear resistance for $AgTaO_3$. It is more noteworthy that silver particle clusters were observed to migrate randomly and finally led to system failure in various sliding components at elevated temperatures [139–141].

Recently, density-functional theory (DFT) and molecular dynamics (MD) simulations have been used to reveal the friction and wear processes of three ternary oxides—$AgTaO_3$, $CuTaO_3$, and $CuTa_2O_6$—through newly developed empirical potential parameters and experimental measurements. The sliding mechanisms are verified through both experimental characterization of the film composition before and after sliding, and quantification of Ag or Cu cluster formation during the evolution of the film in MD, and DFT energy barriers for atomic migration on the surface. All the experimental observations and theoretical calculations supported the hypothesis that metal (or metal oxide) clusters generated on the sliding surface exert a strong influence on friction and wear behavior [140]. The friction and wear performance of $AgTaO_3$ at elevated temperatures were investigated through ab initio MD simulations [141], which also quantified the presence and migration of silver clusters by contact sliding simulations [139].

4.6.5. Alkaline Earth Metallic Chromates

In recent years, ternary chromate compounds of $MCrO_4$, MCr_2O_4, and $MCrO_3$ (M = Ba, Sr, and Ca) between chromium sesquioxide and alkaline earth metallic oxides have been investigated as potential solid lubricants for self-lubricating metallic or ceramic matrix composites [15,142–144]. In the $MCrO_4$ class of oxometallates, M represents different alkaline earth metals with oxidation states of +2. $BaCrO_4$ consists of $[CrO_4]^{2-}$ tetrahedra and the coordinated Ba^{2+} cations, and each Ba^{2+} cation connects with 7 tetrahedra of $[CrO_4]^{2-}$ with a coordination number of 12. Figure 3 shows the schematic diagram of the crystal structure of $BaCrO_4$. $BaCrO_4$ has an orthorhombic structure with lattice parameters of a = 0.9113 nm, b = 0.5528 nm, and c = 0.7336 nm. The first principle calculations and the Castep modules are used to calculate the bulk modulus and compression coefficient of $BaCrO_4$, which are 28.1GPa and 0.0357 GPa^{-1}, respectively. $BaCrO_4$ has been widely used as a model system for the study of morphological control of inorganic minerals, as well as an oxidizing agent, a catalyst for enhancing vapor-phase oxidation reactions, and high-temperature solid lubricants [15,145].

Oxides of some bivalent metallic elements and trivalent chromium form a group of oxometallates, which have the general formula of $M^{2+}Cr_2^{3+}O_4^{2-}$ and exhibit two different crystal structures depending upon the ionic radius ratio of M^{2+}/Cr^{3+}. Most MCr_2O_4-type (M = Fe, Mn, Cu, Mg, Zn, Ni, and Co) compounds with a spinel structure have good thermal stability. However, alkaline earth metallic oxometallates such as $BaCr_2O_4$, $SrCr_2O_4$, and $CaCr_2O_4$ are another part of the family of $M^{2+}Cr_2^{3+}O_4^{2-}$ compounds [146]. These chromates have a layered structure with triangular sheets of formula CrO_2 separated by M^{2+} in trigonal prismatic coordination [142]. Figure 4 shows the schematic diagram of the crystal structure of MCr_2O_4 (M = Ca, Ba, Sr) [142]. $BaCr_2O_4$ is an orthorhombic phase with lattice parameters of a = 1.2286 nm, b = 0.5921 nm, and c = 0.5146 nm, and is thermally stable in the non-oxidizing atmosphere of argon It does not decompose up to 1400 °C.

The calculated bulk modulus and compression coefficient of $BaCr_2O_4$ are 71.6 GPa and $0.014\ GPa^{-1}$, respectively.
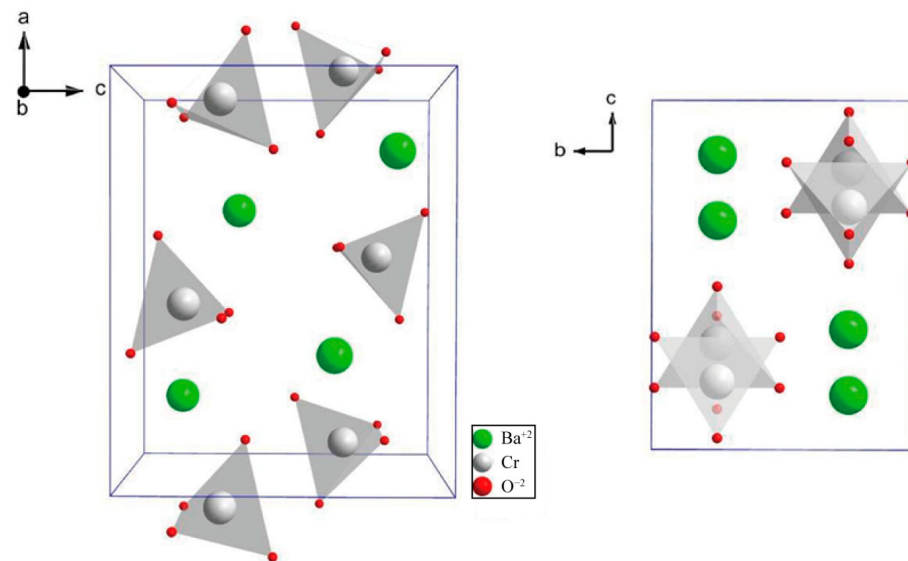

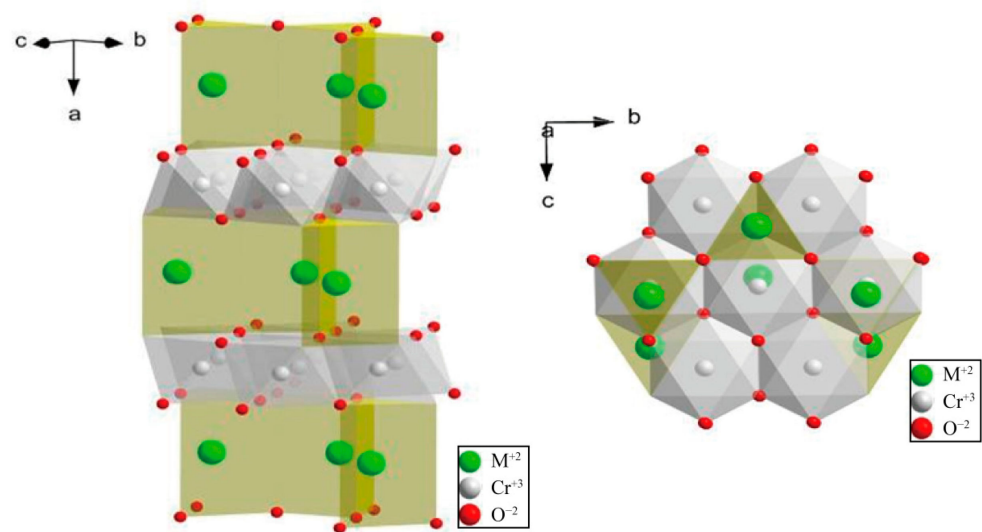**Figure 3.** Schematic diagram of crystal structure of $BaCrO_4$.

Figure 4. Schematic diagram of crystal structure of MCr_2O_4 (M = Ca, Ba, Sr). Reproduced with permission from Reference [142], Copyright © Springer 2012.

$BaCrO_3$ exhibits a variety of layered structures with 4, 6, 12, 14, and 27 layers, which correspond to various c/a values of 1.654, 2.433, 4.901, 5.752, and 11.101, respectively. The local density approximation (LDA) method is used to calculate the properties of three kinds of hexagonal $BaCrO_3$ structures (e.g., P63/mmc (194, Z = 4, 6, and 14)), which have bulk moduli of 94.7 GPa, 100 GPa, and 85.5 GPa, and compression coefficients of $0.0106\ GPa^{-1}$, $0.01\ GPa^{-1}$ and $0.0117\ GPa^{-1}$, respectively.

$BaCrO_4$ particles with various size distributions and morphologies have been synthesized in different synthesis routes in the open literature. For example, $BaCrO_4$ powders with different crystallographic morphologies and sizes were prepared by the chemical co-precipitation method, which is important for large-scale production when considered as a high-temperature solid lubricant [145]. The influences of temperature and atmosphere on the thermal stability of $BaCrO_4$ powders synthesized by a facile aqueous solution route were evaluated. Differential thermal analysis-thermogravimetry (DTA-TG) and X-ray

diffraction verify that thermally stable $BaCrO_4$ does not decompose in the air up to 1400 °C. However, the decomposition of $BaCrO_4$ in a vacuum depends mainly upon a two-stage chemical reaction. It is noteworthy that $BaCrO_4$ is finally decomposed into $BaCr_2O_4$ with trivalent Cr^{3+} cations and $Ba_3(Cr^{6+}Cr^{5+})_2O_{9-x}$ with both pentavalent Cr^{5+} and hexavalent Cr^{6+} cations after heat treatments in a vacuum [147]. In a previous study, $BaCrO_4$ is not thermally stable during vacuum sintering because the sample containing $BaCrO_4$ changes its color from yellow to green on polished surfaces after vacuum sintering at 1050 °C [143]. Generally, thermal stability must be taken into account if the lubricant is designed to operate at elevated temperatures and different atmospheres. Gontarz [148] claimed that $BaCrO_4$ is decomposed to a mixture of $Ba_3(CrO_4)_2$ and $BaCr_2O_4$ with the release of oxygen. Similarly, Azad et al. [149] also reported that $BaCrO_4$ is decomposed into $BaCr_2O_4$ and $BaO \cdot Cr_2O_3 \cdot CrO_3$ beyond 900 °C in the non-oxidizing atmosphere according to the Ba-Cr-O phase diagram.

Microsized $BaCr_2O_4$ powders were synthesized by a solid-state reaction method using stoichiometric amounts of $BaCO_3$ and Cr_2O_3 powders calcined at 1250 °C for 3 h in a vacuum [150]. In a previous study, $BaCr_2O_4$ was found to be thermally unstable in an air atmosphere at elevated temperatures. An oxidation reaction of $BaCr_2O_4$ occurs at 790.2 °C, which leads to the oxidized products of $BaCrO_4$ and Cr_2O_3. It is supposed that such an oxidation reaction contributes to the self-lubricity at elevated temperatures during wear tests. The formed $BaCrO_4$ lubrication layer is easy-to-shear and is prone to spread out in the wear track at elevated temperatures [142].

A ball-on-disc high-temperature friction and wear tester was used to investigate the friction and wear characteristics of pure $BaCr_2O_4$ ceramics. They were investigated up to 800 °C in dry sliding against an alumina ball. $BaCr_2O_4$ crystallizes with connections between the layers of edge-shared CrO_6-octahedra and the $[BaO_4]$-chains, which is also beneficial for reducing friction and wear. $BaCr_2O_4$ ceramics have low friction coefficients and small wear rates at temperatures increasing up to 400–600 °C. Interestingly, $BaCr_2O_4$ is oxidized in air to form a smooth self-lubricating film comprising $BaCrO_4$ and Cr_2O_3 on the worn surface to effectively reduce friction and wear. However, if severe oxidation leads to a decrease in the relative density of pure $BaCr_2O_4$ ceramics, it further expedites the wear process [142].

Table 6 shows the fabrication methods and tribological behavior of self-lubricating materials containing alkaline earth metallic chromates [15,142–144,150,151]. Both $BaCrO_4$ and $BaCr_2O_4$ can be added into a metallic or ceramic matrix to fabricate self-lubricating composites or coatings by a variety of fabrication technologies such as powder metallurgy [143,151], low-pressure plasma spraying [15], and electrodeposition methods [150]. For example, the spark-plasma-sintered $ZrO_2(Y_2O_3)$ matrix composites containing $BaCrO_4$ exhibited friction coefficients of 0.29–0.32 and wear rates in the order of 10^{-6} mm^3/Nm in the air from room temperature to 800 °C [143]. The worn surface of $ZrO_2(Y_2O_3)$-50$BaCrO_4$ composite after 800 °C wear test in sliding against alumina ball is shown in Figure 5. Clearly, the barium chromate becomes softening at 800 °C, which spreads out on the sliding surfaces under tribo-stressing and creates a self-lubricating fine grain layer. The lubrication mechanism is associated with the in situ formation of surface glaze with ultrafine nanograins due to thermo-mechanical induced recrystallization/deformation at elevated temperatures. In this case, grain boundary sliding and grain rotation of $BaCrO_4$ nanograins in the glaze layer also promote plastic smearing and self-lubricity at elevated temperatures. Low-pressure plasma sprayed ZrO_2-$BaCrO_4$ coating also showed good lubricity at elevated temperatures [15].

Table 6. Fabrication methods and tribological behavior of self-lubricating materials containing alkaline earth metallic chromates [15,142–144,150,151].

Materials	Fabrication Method	Tested Conditions	Results/Observations
$ZrO_2(Y_2O_3)$-$BaCrO_4$ [15]	Low-pressure plasma spraying	Ball-on-block; Al_2O_3 ball; load 50 N; frequency of 10 Hz with stroke of 1 mm; RT-800 °C	• μ: 0.81, 1, 0.92, 0.58, 0.57, 0.5 (RT, 100, 200, 400, 600, 800 °C); • Wear depth: 42% reduction from 100 °C to 800 °C; • Lubrication resulting from the formation of transfer $BaCrO_4$ films at high temperatures.
$BaCr_2O_4$ [142]	Hot pressing	Ball-on-disk Al_2O_3 ball; load 5 N; 0.126 m/s; RT-800 °C	• μ: 0.7, 0.38, 0.35, 0.4 (RT, 400, 600, 800 °C) • W: 9.7×10^{-5}, 1.56×10^{-5}, 1.43×10^{-5}, 4.9×10^{-5} mm^3/(Nm) (RT, 400, 600, 800 °C) • Friction heat at the surface contributes to the oxidization of $BaCr_2O_4$ at between 400 and 600 °C. • $BaCrO_4$ as oxidized product dominates the formation of lubricating films. • Severe oxidation at 800 °C degenerates the wear resistance.
$ZrO_2(Y_2O_3)$-$BaCrO_4$ [143]	Spark plasma sintering	Ball-on-block; Al_2O_3 ball; load 30 N; frequency of 10 Hz with stroke of 1 mm; RT-800 °C	• μ: 0.55, 0.45, 0.46, 0.38, 0.41 (RT, 200, 400, 700, 800 °C) • W: 5.35×10^{-5}–1.44×10^{-5} mm^3/(Nm) (RT-800 °C) • • Addition of 50 wt.% $BaCrO_4$ significantly improves tribological properties at high temperatures.
Al_2O_3-$BaCrO_4$ [144]	Spark plasma sintering		• μ: 0.65, 0.81, 0.6, 0.7, 0.55 (RT, 200, 400, 600, 800 °C) • W: 6.5×10^{-5}, 1.5×10^{-4}, 1.6×10^{-5}, 3×10^{-5}, 1.6×10^{-5} mm^3/(Nm) (RT, 200, 400, 600, 800 °C) • Sintered samples contain a lot of pores.
Al_2O_3-$BaCrO_4$-SiO_2 [144]	Spark plasma sintering	Ball-on-block; Al_2O_3 ball; load 10 N; frequency of 10 Hz with stroke of 1 mm; RT-800 °C	• μ: 0.6, 0.7, 0.8, 0.7, 0.6 (RT, 200, 400, 600, 800 °C) • W: 3.1×10^{-5}, 2.2×10^{-5}, 3×10^{-6}, 4×10^{-6}, 4×10^{-6} mm^3/(Nm) (RT, 200, 400, 600, 800 °C) • SiO_2 doping as sintering additive improves the density of composites, resulting in notably lower wear rate, especially at high temperatures.
Al_2O_3-$BaCrO_4$-Ag [144]	Spark plasma sintering		• μ: 0.7, 1.2, 0.44, 0.46, 0.5 (RT, 200, 400, 600, 800 °C) • W: 5×10^{-5}, 6×10^{-5}, 2×10^{-6}, 2×10^{-6}, 1.2×10^{-5} mm^3/(Nm) (RT, 200, 400, 600, 800 °C) • Silver instead of $BaCrO_4$, works as lubricant at 600 °C.

Table 6. *Cont.*

| Materials	Fabrication Method	Tested Conditions	Results/Observations
NiCr-BaCr$_2$O$_4$ [151]	Hot pressing	Ball-on-disk Al$_2$O$_3$ ball; load 5 N; 0.126 m/s; RT-800 °C	• μ: 0.72, 0.27, 0.25, 0.27 (RT, 400, 600, 800 °C) • W: 2.29 × 10^{-5}, 9 × 10^{-6}, 2.6 × 10^{-6}, 4.5 × 10^{-6} mm^3/(Nm) (RT, 400, 600, 800 °C) • Addition of BaCr$_2$O$_4$ significantly reduces friction and wear of NiCr alloy at 400–800 °C.
Ni-16.6 vol.% BaCr$_2$O$_4$ [150]	Electrodeposition	Ball-on-disk Al$_2$O$_3$ ball; load 2 N; rotating speed 400 rpm; rotating radius 3 mm; RT	• μ: 0.31 • W: 2.79 ×10^{-6} mm^3/(Nm) (RT) • Enhanced microhardness 745Hv • BaCr$_2$O$_4$ particles enhance the hardness and the resistance to scuffing wear of composite coating.
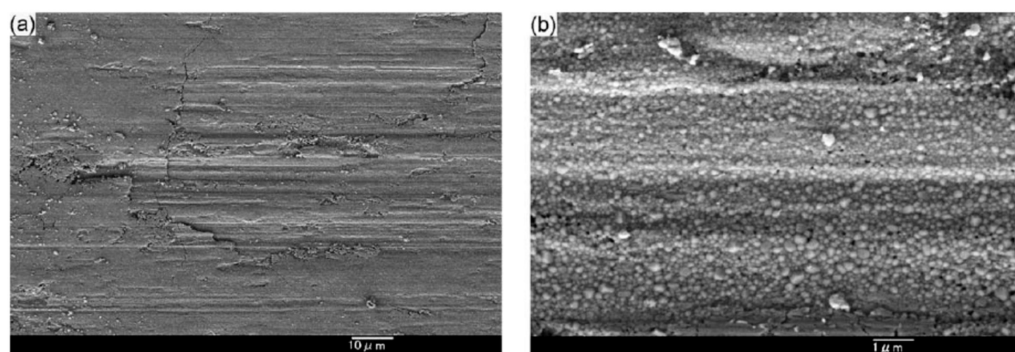
Figure 5. Worn surface of ZrO$_2$(Y$_2$O$_3$)-50BaCrO$_4$ composite after 800 °C wear test: (**a**) morphology, (**b**) enlarged view of (**a**). Reproduced with permission from Reference [143], Copyright © Elsevier B.V. 2005.

4.7. Alkaline Earth Metallic Sulfates

Alkaline earth metallic sulfates, such as BaSO$_4$ (barite), SrSO$_4$ (celestite), and CaSO$_4$ (anhydrite), have been widely used as important inorganic chemical products in ceramics, pigments, electronics, cosmetics, papermaking, and high-temperature solid lubricants [152,153]. Especially the excellent lubricating properties of barite and celestite as well as their sulfate solid solutions are closely related to their structures and morphologies. The lubrication mechanisms are associated with the slippage along the basic plane of (001) at room temperature and the in situ formation of surface glaze with ultrafine nanograins due to thermo-mechanical induced recrystallization/deformation at elevated temperatures. Similar to the BaCrO$_4$ crystal, SrSO$_4$ consists of [SO$_4$]$^{2-}$ tetrahedra and the coordinated Sr^{2+} cations, and each Sr^{2+} cation connects with 7 tetrahedra of [SO$_4$]$^{2-}$ with a coordination number of 12. Figure 6 shows the schematic diagram of atomic arrangements at planes of (002) and (210) in the SrSO$_4$ crystal. Alkaline earth sulfate particles with a variety of unusual and well-defined crystallographic morphologies were obtained via controlled nucleation and growth by using various additives as crystal modifiers from an aqueous solution [154]. SrSO$_4$ has an orthorhombic structure with lattice parameters of a = 0.8359 nm, b = 0.5352 nm, and c = 0.6866 nm, while BaSO$_4$ has the same structure with lattice parameters of a = 0.8881 nm, b = 0.5454 nm, and c = 0.7157 nm at room temperature. TG/DTA thermal analysis indicates that barite and celestite as well as their sulfate solid solutions are thermally stable, and have almost no weight loss up to 1300 °C and only a structural transition of orthorhombic to monoclinic phase at about 1100 °C. The formation process of

sulfate hierarchical architectures is quite complicated and is affected by crystal structure and crystal growth environments, such as surface energy, the degree of supersaturation, and diffusion of the reaction [152–155].

A facile aqueous solution route was employed to prepare $SrSO_4$ nanocrystals from a needle-like to a tablet-like feature by increasing the molar ratio (R) of Sr^{2+} cations to SO_4^{2-} anions from R = 1:2 to R = 2:1 at room temperature without using any surfactants or templates [152]. The crystallographic morphology of $SrSO_4$ depends mainly upon the preferential absorption of excessive strontium cations on the (020) and (210) planes. Monodispersed peanut-type $SrSO_4$ particles with an average length of 1.7 µm and an aspect ratio of 1.4 were synthesized using a facile precipitation reaction of Sr-EDTA chelating precursors at ambient temperature. These peanut-type $SrSO_4$ particles have a relatively large Brunauer–Emmett–Teller (BET) surface area of about 20.9 $m^2\,g^{-1}$ and contain mesopores with a mean pore size of about 34.3 nm [153]. The $Ba_xSr_{1-x}SO_4$ solid solution nanocrystals synthesized by the chemical precipitation method have an orthorhombic structure, an average size of 80–100 nm, and an ellipsoidal-shaped morphology. These $Ba_xSr_{1-x}SO_4$ solid solutions with different composition parameters are perfectly indexed as a single phase of orthorhombic with a space group, Pbnm (62) of $Ba_{0.25}Sr_{0.75}SO_4$, $Ba_{0.5}Sr_{0.5}SO_4$, and $Ba_{0.75}Sr_{0.25}SO_4$, respectively [155].
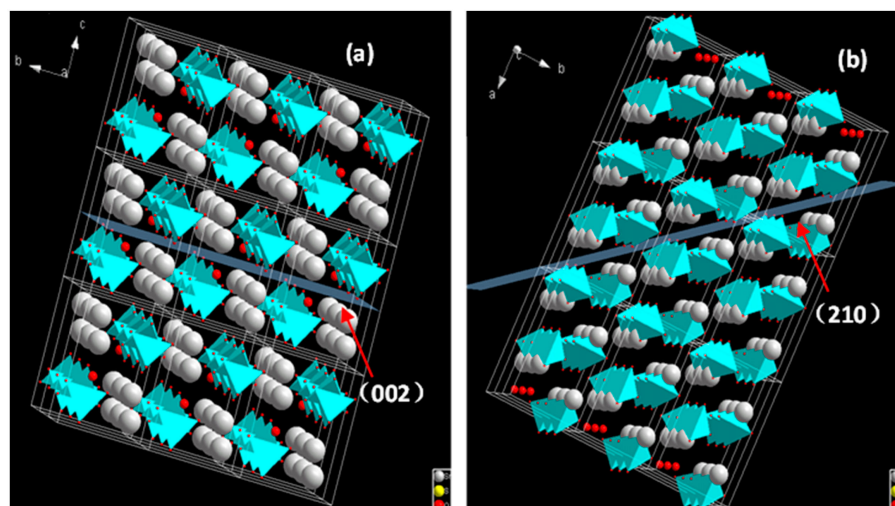

Figure 6. Schematic diagram of atomic arrangements at planes of (002) and (210) in $SrSO_4$ crystal (white-strontium, yellow-sulfur, red-oxygen): (**a**) (002) plane by arrow, (**b**) (210) plane by arrow.

Fabrication methods and tribological behavior of self-lubricating materials containing alkaline earth sulfates are summarized in Table 7 [101,136,156–160]. In our previous work, the alkaline earth sulfates with a barite-type structure such as $BaSO_4$, $SrSO_4$, and $Ba_xSr_{1-x}SO_4$ possessed excellent self-lubricity, thermo-chemistry stability, and innocuity. These sulfates are also verified to possess lubrication ability, especially at elevated temperatures. Textured hard surfaces embedded with $BaSO_4$ additives are able to provide sustainable self-lubricity [136]. In fact, barite exhibits good tribological properties, which only change slightly with the increase in temperature, and the wide availability of the barite mineral greatly reduces the cost. Barite can be used as the lubricant filler for brake pads. Both the coefficient of friction and wear rates are reduced by increasing the barite ratio in a brake pad. Interestingly, the variations in sliding velocity and rubbing pressure have little effect on the friction coefficient of the barite-containing brake pad materials. High stability of the friction coefficient and excellent fade resistance are guaranteed by increasing the $BaSO_4$ content in the friction material. Particularly, barite is resistant to high temperatures and has no significant change in its properties at temperatures above 300 °C [161,162].

Table 7. Fabrication methods and tribological behavior of self-lubricating materials containing alkaline earth sulfates [101,136,156–160].

Materials	Fabrication Method	Tested Conditions	Results/Observations
Al_2O_3-Mo-$BaSO_4$ [136]	$BaSO_4$ was burnished onto textured surface of hot pressed Al_2O_3-Mo.	Pin-on-disk; Al_2O_3 pin; load 70 N; frequency of 10 Hz with stroke of 1 mm; RT-800 °C	• μ: 0.45, 0.57, 0.44, 0.3, 0.3 (RT, 200, 400, 600, 800 °C) • $BaSO_4$ effectively improves the wear resistance and could remain a lot in micro-dimples.
$ZrO_2(Y_2O_3)$-$BaSO_4$ [101]	Spark plasma sintering	Ball-on-block; Al_2O_3 ball; load 5 N; frequency of 1 Hz with stroke of 10 mm; RT-800 °C	• μ: 0.36, 0.3, 0.33 (RT, 400, 800 °C) • W: 4.72×10^{-6} mm³/(Nm) (800 °C) • Softened $BaSO_4$ fine-grain layer forms on the worn surfaces at high temperature.
Al_2O_3-$SrSO_4$ [156]	Spark plasma sintering		• μ: 0.38, 0.44, 0.42, 0.35, 0.29 (RT, 200, 400, 600, 800 °C) • W: maximum of 8×10^{-4} mm³/(Nm) at 200 °C, minimum of 1×10^{-4} mm³/Nm at 600 °C
Al_2O_3-$PbSO_4$-SiO_2 [156]	Spark plasma sintering	Ball-on-block; Al_2O_3 ball; load 5 N; frequency of 1 Hz with stroke of 10 mm; RT-800 °C	• μ: 0.32, 0.36, 0.26, 0.26, 0.31 (RT, 200, 400, 600, 800 °C) • W: maximum of 1×10^{-4} mm³/(Nm) at 800 °C, minimum of 1×10^{-5} mm³/(Nm) at 200 °C
Al_2O_3-$BaSO_4$-Ag [156]	Spark plasma sintering		• μ: 0.38, 0.3, 0.21, 0.21, 0.22 (RT, 200, 400, 600, 800 °C) • W: maximum of 4×10^{-4} mm³/(Nm) at 800 °C, minimum of 5×10^{-6} mm³/(Nm) at 200 °C
$ZrO_2(Y_2O_3)$-Al_2O_3-$Ba_{0.5}Sr_{0.5}SO_4$ [157]	Spark plasma sintering	Ball-on-block; Al_2O_3 ball; load 5 N; frequency of 1 Hz with stroke of 10 mm; RT, 760 °C	• μ: 0.21, 0.11 (RT, 760 °C) • W: 5×10^{-5}, 3.6×10^{-6} mm³/(Nm) (RT, 760 °C) • Friction coefficient at 760 °C is much more stable than that of unmodified $ZrO_2(Y_2O_3)$-Al_2O_3 composites due to the formation and effective spreading of $Ba_{0.5}Sr_{0.5}SO_4$ lubricating film.
Fe_3Al–$Ba_{0.25}Sr_{0.75}SO_4$ [158]	Hot pressing	Ball-on-disk; Si_3N_4 ball; load 10 N; 0.01 m/s; RT-800 °C	• μ: 0.3, 0.6, 0.54, 0.19, 0.29 (RT, 200, 400, 600, 800 °C) • W: maximum of 4×10^{-5} mm³/(Nm) at 400 °C • The main wear mechanism is abrasion wear at high temperature.
Ni-6.83 vol.% $SrSO_4$ [159]	Electrodeposition	Ball-on-disk; SAE52100 bearing ball; load 0.5 N; rotating speed 50 rpm; rotating radius 5mm; RT	• μ: 0.31 • W: 5.3×10^{-4} mm³/(Nm) (RT) • Enhanced microhardness 450 Hv • $SrSO_4$ particles enhance the hardness and the resistance to scuffing wear of coating.
$SrSO_4$-Ag [160]	Chemical precipitation	Ball-on-block; Al_2O_3 ball; load 5 N; frequency of 1 Hz with stroke of 10 mm; RT-800 °C	• μ: 0.18, 0.2, 0.22, 0.26, 0.27 (RT, 200, 400, 600, 800 °C) • W < 2×10^{-6} mm³/(Nm)

Various approaches were developed to fabricate the self-lubricating sulfate-containing composites, such as plasma spraying, physical vapor deposition, electrodeposition, hot pressing, spark plasma sintering, and so forth. $BaSO_4$, $SrSO_4$, and $(Ba,Sr)SO_4$ can be added or in situ formed into a metallic or ceramic matrix to synthesize self-lubricating composites or coatings by powder metallurgy [101,156–158,163], Pulsed laser deposition [126], electrodeposition [159], and burnishing methods [160,164]. For example, the friction and wear properties of $ZrO_2(Y_2O_3)$-Al_2O_3-$50BaSO_4$ composites are distinctly improved at elevated temperatures, as contrasted with unmodified $ZrO_2(Y_2O_3)$-Al_2O_3 ceramics. Figure 7 shows the frictional behavior of the $ZrO_2(Y_2O_3)$-Al_2O_3-$50BaSO_4$ composite as a function of the wear cycle at different temperatures when sliding against an alumina ball. $BaSO_4$-containing composite has a friction coefficient of 0.33 and a wear rate of 4.72×10^{-6} $mm^3/(Nm)$ at 800 °C. Figure 8 shows the worn surface of the $ZrO_2(Y_2O_3)$-Al_2O_3-$50BaSO_4$ composite after the 800 °C wear test. Clearly, a self-lubricating $BaSO_4$ fine-grain layer is observed on the sliding surfaces at elevated temperatures, which avoids the direct tribo-contact between the oxide ceramics and the coupled ball. The lubrication mechanisms at elevated temperatures are associated with the formation of surface glaze with ultrafine nanograins due to thermo-mechanical induced recrystallization/deformation. Similarly, grain boundary sliding and grain rotation of $BaSO_4$ nanograins in the glaze layer also promote plastic smearing and self-lubricity at elevated temperatures [101].
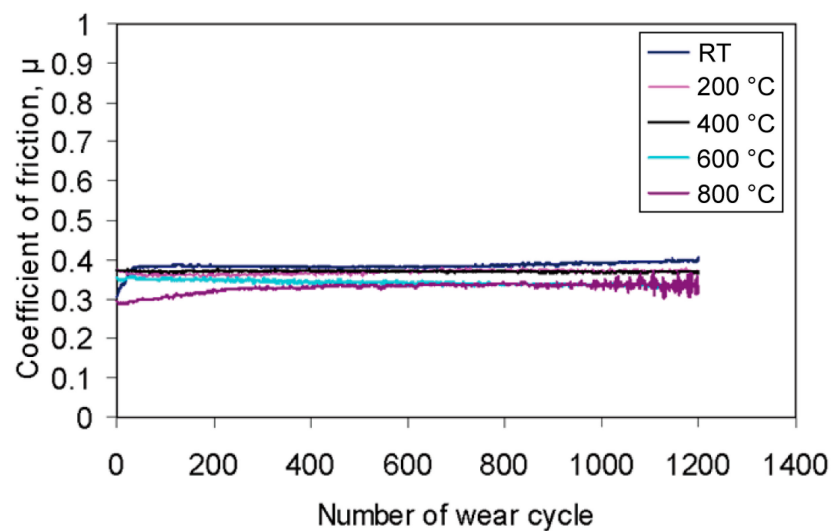

Figure 7. Friction coefficients of $ZrO_2(Y_2O_3)$-Al_2O_3-$50BaSO_4$ composite as a function of wear cycle at different temperatures.
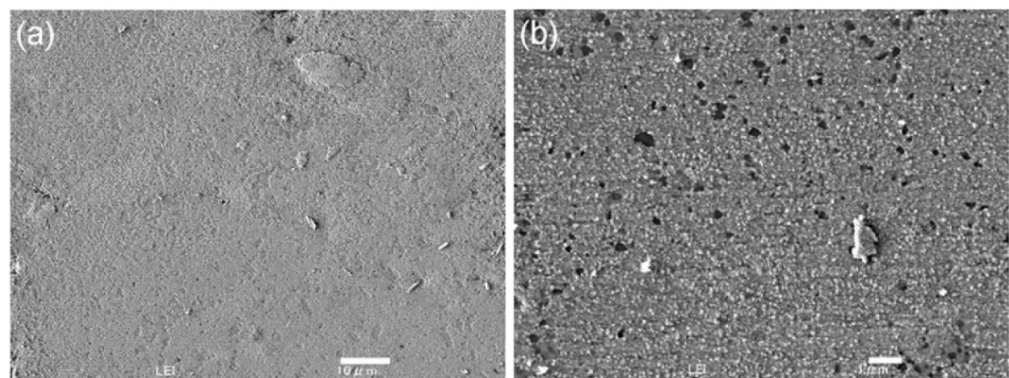
Figure 8. Worn surface of $ZrO_2(Y_2O_3)$-Al_2O_3-$50BaSO_4$ composite after 800 °C wear test: (**a**) morphology, (**b**) enlarged view of (**a**). Reproduced with permission from Reference [101], Copyright © Elsevier B.V. 2009.

Alkaline earth sulfate-containing coatings also contribute to good tribological properties. Low friction coefficients and small wear rates are validated for $SrSO_4$, or $SrSO_4$-Ag films coated on $ZrO_2(Y_2O_3)$-Al_2O_3 and Si_3N_4 ceramics by the chemical precipitation method over a wide temperature range [160,164]. Pulsed laser-deposited $CaSO_4$-containing films tend to be fairly soft and to be easily deformed, which lubricates better at elevated temperatures than CaF_2 when incorporated into a layered structure with silver [126]. The friction and wear properties of $BaSO_4$ and $SrSO_4$ powder films coated on different substrates of Al_2O_3 and SUS316 stainless steel are investigated by using a reciprocating ball-on-block high-frequency induction-heated tribometer to slide against Al_2O_3 or SUS316 steel balls, respectively. Both the $BaSO_4$ and $SrSO_4$ powder films coated on Al_2O_3 substrate by chemical precipitation have average friction coefficients of less than 0.4 up to 800 °C in air. In particular, the friction coefficients of flake-shaped $BaSO_4$ powder films coated on an Al_2O_3 substrate are lower than those of lump-shaped $BaSO_4$ powder films. The $BaSO_4$-10mass% Ag films formed on the SUS316 substrate have average friction coefficients from 0.2 to 0.4 from room temperature to 800 °C in the air [164].

4.8. Silicates

The silicates generally have the building blocks of $(SiO_4)^{4-}$ units, where each O^{2-} ion is coordinated with two Si^{4+} ions, so the tetrahedral join at corners. The SiO_4 tetrahedra can be either kept separated or linked to one another to form chains or rings, which can be made into sheets or double chains. A special feature of silicates is that the cations that are outside the SiO_4 tetrahedra are quite easy to be replaced, e.g., the replacement of Si^{4+} with other similar-sized ions such as Al^{3+} without changing the nature of oxygen coordination. Layered micas are very rigid but cleave very easily along a plane. The bonds within the layers are very strong, but the van der Waals bonds between the layers are weak. Therefore, micas and other minerals such as serpentine and attapulgite are designed to supply easy paths for crack propagation and improve the machinability of some commercial ceramics [165].

Inorganic silicate polymers are salts of the oxyacids of silicon. The silicate anion structure is formed by repeated condensation of tetrahedral SiO_4^{4-} groups, by linking through the covalent bridging oxygen atoms to form chains, cyclic and larger polymeric structures [166]. Silicate-based additives have been used in the lubrication of bearings or gearboxes under heavy loads or high-temperature circumstances. The sodium or potassium silicate reacts with metallic rubbing surfaces to form a lubricating film of metallic silicate on the sliding interface. Silicate-based compounds such as $Al_4[Si_4O_{10}](OH)_4$ [167], and aluminum–magnesium silicate [168] are designed to protect the surfaces of engines and reduce effectively friction and wear as lubricious additives. The silicates have self-restoration capability at the sliding contacts [169]. These additives can self-repair the mechanical damage at the sliding surfaces, as evidenced by the mineral elements within the tribofilm, which are different from the base materials. However, the silicates generally lubricate the rubbing contacts only at high temperatures due to the formation of a viscous silicate melt layer. However, silicates behave such as rigid solid at low temperatures, where the friction is almost unaffected by the deformation strain rate. Lubrication is quite essential to improve the energy efficiency and durability of tools. The presence of inorganic sodium metasilicate at 920 °C for high-temperature friction tests of steel-to-steel contacts can reduce the friction coefficient to half and minimize one order of magnitude of wear rate [170].

Wang et al. [171] developed a magnesium silicate hydroxide-MoS_2-Sb_2O_3 nanocomposite coating for the high-temperature super-lubricity application. This composite coating with a thickness of 150–250 nm is accomplished by uniformly burnishing hydrothermally synthesized lamellate magnesium silicate hydroxide, molybdenum disulfite, and antimony trioxide powders onto a copper substrate. With increasing the temperature up to 400 °C, the friction coefficient of the composite coating rapidly decreases to below 0.01 within 100 revolutions and finally reaches a super-lubricity state, which is attributed to the synergistic characteristics of lubricating antimony trioxide, molybdenum disulfide,

and magnesium silicate hydroxide phases, and enables easy shearing. Magnesium silicate hydroxide is a type of layered silicate that releases unsaturated Si-O-Si, O-Si-O, OH-Mg-OH, OH-, and O-H-O groups, thus forming a tribofilm during sliding [171]. The magnesium silicate hydroxide-C-Sb_2O_3 coating burnished on a nickel superalloy substrate also exhibits high-temperature super-lubricity due to the formation of an easy-to-shear silicate-containing carbon film tribochemically-activated during sliding [172].

4.9. Cesium Oxythiomolybdate Cs_2MoOS_3

Research on cesium oxytrithiomolybdate (Cs_2MoOS_3), zinc oxytrithiomolybdate ($ZnMoOS_3$), and cesium oxytrithiotungstate (Cs_2WOS_3) was initiated as a response to the requirement for a high-temperature solid lubricant for ceramic bearings in lightweight single-use engines. The US Air Force Research Laboratory at Wright-Patterson Air Force Base (WPAFB) developed a thin bonded lubricious coating of the complex chalcogenide, Cs_2MoOS_3, which could adequately lubricate silicon nitride bearings in the air at temperatures up to 760 °C, speeds up to 1.2 million DN (DN = bearing bore size in mm × shaft rpm) and thrust loads of 890 N for periods of five to six hours in 1987.

Cesium oxytrithiomolybdate-based lubricants have been applied by burnishing; however, the burnished powders need to often be replenished to prevent failure and ensure a long wear life. Pulsed laser deposition is an excellent method for highly adherent Cs_2MoOS_3 films due to its characteristic of replicating the target chemistry in the film. Therefore, Cs_2MoOS_3 films were developed to react with the environment to form new lubricious phases at elevated temperatures for the lubrication of silicon nitride bearings by pulsed laser deposition [173,174]. Figure 9 shows the friction behavior of Cs_2MoOS_3 films pulsed laser deposited on Si_3N_4 in sliding against Si_3N_4 ball [174]. This adaptive lubricant provides a low-friction surface with an average friction coefficient value of 0.03 at 600 °C. Not only that, room temperature and 700 °C are suitable as well; however, it does not work at temperatures of 300 °C and especially 800 °C. A high-temperature lubricious phase is formed based on the reaction of the components with each other and O_2 with the increase in test temperature. Cesium oxytrithiomolybdate (Cs_2MoOS_3) used in a coating with a sodium silicate binder exhibited a friction coefficient of below 0.2 at 650 °C [174]. However, one challenge in using Cs_2MoOS_3 as a lubricant is its thermal instability above 200 °C. Oxidation products of Cs_2MoOS_3 powders at 600–800 °C consist of Cs_2SO_4, cesium oxides, Cs_2MoO_4, and other molybdenum oxides. Oxidation of Cs_2MoOS_3 to form lubricious Cs_2MoO_4, MoO_3, and other oxides on the sliding surface provides good lubrication on ceramics at temperatures between 300 and 600 °C. Cs_2MoOS_3 films on the substrates of alumina and zirconia have friction coefficients of below 0.2 when sliding against an alumina ball. However, Cs_2MoOS_3 films lubricate well on Si_3N_4 substrates between 600 and 750 °C, and on SiC substrates between 500° and 600 °C, with a friction coefficient of below 0.1 in sliding against silicon nitride ball. The lubrication mechanisms depend mainly on the oxide softening and the formation of cesium silicate glass on the sliding surface [174].

Cesium oxytrithiotungstate (Cs_2WOS_3) and zinc oxytrithiomolybdate ($ZnMoOS_3$) are also thermodynamically stable and have exceptional potential for lubrication of silicon nitride bearings at elevated temperatures [6,174]. The formation of a low shear strength glass was previously postulated as the lubrication mechanism for cesium tungsten (Cs_2WOS_3) bonded coatings (containing lubricious cesium silicate glass) on silicon nitride bearings by Rosado et al. [175]. The high-temperature rolling contact endurance and tribological properties of lubricious cesium-based compounds were investigated on silicon nitride balls at 650 °C when applied as either a bonded or fused coating [6]. The best comprehensive performance was achieved with a cesium silicate reaction film formed in situ by $Cs_2O \bullet SiO_2$ and a hydrated cesium silicate bonded coating of $Cs_2O \bullet 3SiO_2 \cdot nH_2O$, which provided rolling friction coefficients less than 10^{-3} and small wear coefficients to obtain very long endurance lives at high contact stresses. In fact, alkali ions are known to reduce the viscosity of silicate glasses, which have been used as lubricants for steel working for over 70 years. Generally, glass lubricants with desirable properties above 600 °C can lubricate

the hot extruded steel surfaces at large area reductions and in longer lengths [176]. Since thin PLD films are not suited to long-term use, they are most advantageously employed for short-duration and one-time applications. Experimental prototypes of other engine parts (e.g., piston pins, intake and exhaust valves, camshafts, cam lobes, roller followers, high-temperature seals, etc.) made from Si_3N_4 must be considered to further evaluate their tribological performance and reliability.
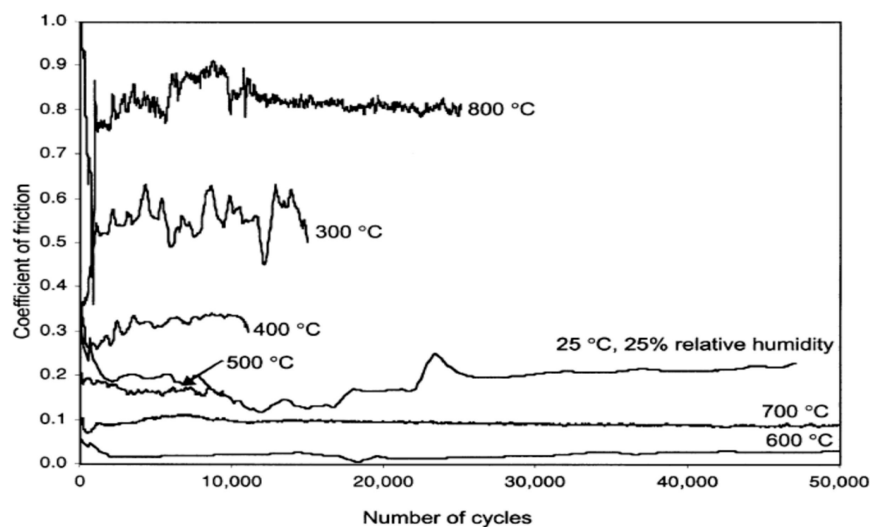

Figure 9. Friction behavior of Cs_2MoOS_3 films pulsed laser deposited on Si_3N_4 in sliding against Si_3N_4 ball. Reproduced with permission from Reference [174], Copyright © Elsevier Science B.V. 2002.

4.10. Synergistic Effects of Various Solid Lubricants

Lubrication problems are particularly challenging in the aerospace industry since aerospace components experience high and low temperatures, alternative moist air and vacuum, heavy load, high speed, and strong radiation conditions [177]. For example, lubricants that are effective over an extreme temperature range are necessary for new-generation advanced engines with increased propulsion. Lubricants for space vehicles must be able to function in moist air through a vacuum, such as on reusable launch vehicles. The coated satellite components designed for long lifetimes may be tested and stored in a terrestrial environment before they are operated in the vacuum of space. Unfortunately, it is particularly difficult to find a single solid lubricant that can provide the best lubrication performance over all conditions. As no individual solid lubricant material can provide adequate lubrication properties under environmental conditions of low/high temperature, high radiation, high pressure, high chemical reactivity, and ultrahigh vacuum, a microstructurally engineered combination of various solid lubricants will become necessary for advanced lubrication systems [177].

Before an optimized solid lubricant combination is microstructurally designed, it is of great importance to understand the fundamental characteristics and fabricating methods of different constituents. Soft metals of Ag and Au contain multiple slip planes and produce enhanced ductility and easy-to-shear tribolayer. Graphite, *h*-BN, and MoS_2 are typical layered materials with easy-to-shear interlayers. Nb(S, Se, Te)$_2$ is used in applications requiring good electrical conductivity. CaF_2 or BaF_2/CaF_2 are common high-temperature lubricants (i.e., >500 °C), while PbO has good lubricating properties from about 450 to 700 °C, although it is still limited by its low temperature shear strength and by phase transition, reactivity, and melting at high temperatures. Figure 10 shows effective operating temperature ranges for a variety of solid-lubricating materials [20]. The synergistic effects of different solid lubricants have been widely explored for humidity-, temperature-, vacuum-, or load-adaptive tribological applications.
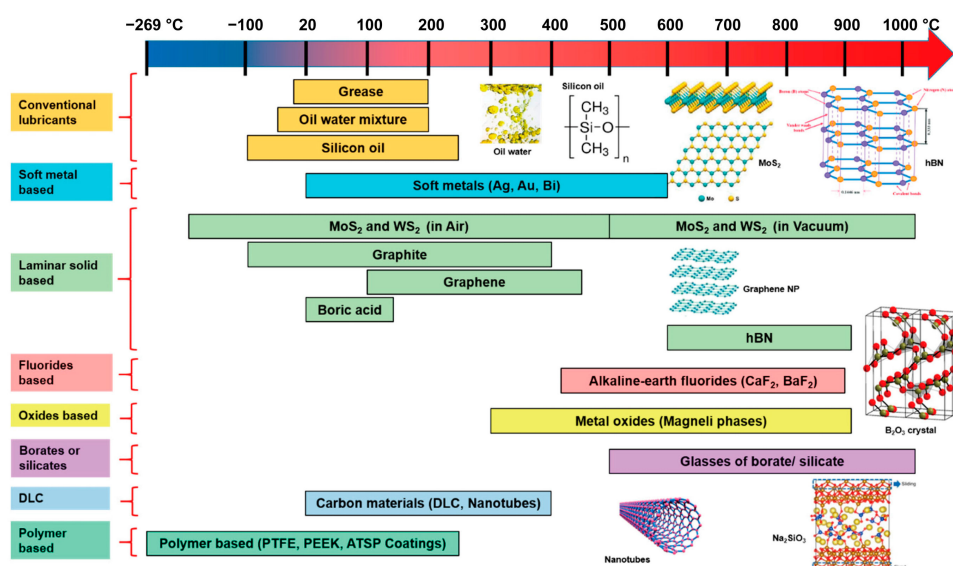
Figure 10. Effective operating temperature ranges for a variety of solid-lubricating materials. Reproduced from [20].

Typical examples associated with these combinations of various solid lubricants are quite inspiring for specific engineering applications such as aircraft and satellites, where continuous variations from humid air to vacuum during launch and flight or return periods over a broad vacuum range. Graphite, DLC, and MoS_2/WS_2 powders are combined to lubricate across humid air (graphite, DLC) and vacuum (MoS_2/WS_2). Multiple mechanisms for air-space humidity-adaptive response of W-C-S, W-C-Se, YSZ-Au-MoS_2-DLC, and Al_2O_3-Au-MoS_2-DLC nanocomposite coatings are designed for lubrication subjected to environmental cycling [3]. Interestingly, the 500 nm thick W-C-S coating exhibited a friction coefficient comparable to that of pure graphite in humid air and simultaneously attained the equivalent friction coefficient of pure WS_2 in vacuum for more than 2×10^6 cycles with a wear rate less than 10^{-7} $mm^3/(Nm)$. The sensitivity of MoS_2 and WS_2 coatings to relative humidity can be reduced through the use of dopants, additives, or interlayers such as W-C-S and W-C-Se coatings. A novel scheme to operate across a range of climatic conditions was described whereby a circular groove was laser milled into a TiC/DLC composite coating and filled with MoS_2 additives. MoS_2 additives form a transfer film and generate lubrication in a vacuum and dry N_2, while a graphite-like transfer film provides lubrication in moist air. A promising path of incorporating multiple lubricants in a composite coating to reduce friction and wear will emerge for a useful number of cycles through a broad range of ambient humidity and temperatures on a reusable air-space vehicle capable of multiple atmospheric reentries.

Sliney and Dellacorte pioneered self-lubricating composites or coatings comprising silver for low-temperature lubrication, BaF_2-CaF_2 eutectic for high temperatures, and Cr_3C_2 or Cr_2O_3 for enhanced wear resistance in tribological applications such as foil air bearings and mechanical seals of advanced propulsion systems. This lubrication combination of silver-BaF_2/CaF_2 eutectic is quite thermally stable over a wide temperature range, which can be cycled to provide self-lubricity between low and high temperatures for long-term service [1,7,93,94]. Similarly, the addition of both gold and CaF_2 into $ZrO_2(Y_2O_3)$ ceramics significantly reduces the friction and wear up to 800 °C tested with a ball-on-disc configuration. Interestingly, gold was not able to entirely cover the contact region at room temperature by diffusion, but it does reduce friction and wear significantly [102]. The enhanced wear resistance is attributed to the lubrication of discontinuous protective layers at moderate temperatures or nano-scale gold particles on CaF_2 layers at high temperatures.

The use of gold as an effective solid lubricant is specialized for lubrication applications in aerospace tribology or the protection of electronic connectors [2].

Typical examples of synergistic lubrication in MoS_2-containing composite coatings include PbO-MoS_2 [117,178], MoS_2-Sb_2O_3, YSZ-Ag-Mo-MoS_2 [179], YSZ-MoS_2-DLC-Au [3], Mo_2N-MoS_2-Ag [119], Ni-Al-Ag-MoS_2 and Ni-Al-Ag-MoS_2-hBN [180]. These coatings provide effective lubrication protection over a broad temperature range in a combination of the lubricity of MoS_2 at lower temperatures and vacuum with the in situ formation of easy-to-shear lubricious oxides at elevated temperatures [30,181,182]. However, adaptive lubrication surfaces by Au or Ag may have some challenges, including the random migration of soft metal clusters, poor adhesion in the presence of oxygen, and excessive deformation at elevated temperatures on the sliding surface. It is particularly important to note that, the tribo-chemical reactions to the lubricious film are not reversible, and the tribo-chemical induced oxides do not provide lubrication at low temperatures for repeated thermal cycling [8]. The primary adaptive mechanisms are associated with environmental-assisted oxidation to form easy-to-shear and low-melting-point binary TiO_2, V_2O_5, MoO_3 Magneli phases and ternary oxides including silver molybdates, vanadates, tungstates, niobates, and tantalates, etc., temperature-activated diffusion of soft metals, and thermo-mechanically induced phase transitions to reorient hexagonal solids and promote surface-hardening [30,31]. Adaptive lubricants must be engineered due to the irreversible tribo-chemical reactions so that they can be cycled between low and high temperatures [177].

The challenge associated with this issue was the reversibility of the thermally adaptive tribological surfaces over multiple thermal cycles, analogous to their humidity- or vacuum-adaptive counterparts occurring in various engineering applications. Several approaches are postulated for adaptive multilayered coatings and surface multifunctional design, such as bionic compositing, tunable surface texturing, and tribo-reaction of oriented lubricants. For example, temperature-adaptive composites exhibiting diffusion-, melting-, or oxidation-limiting lubrication are developed over multiple thermal cycling through microlaminate architectures in engineered designs to activate the functionality of various solid lubricants [30,177]. A microlaminate coating comprising alternative adaptive coating layers and diffusion barrier layers would inhibit the diffusion and migration of Ag or Au clusters from the underlying layers and restrict the diffusion of oxygen into the coating to generate tribo-oxidation until needed [3]. Thus, both the diffusion and migration of soft metallic clusters and the formation of lubricious oxide would occur on demand in such a microlaminate coating.

5. Production Technologies of Self-Lubricating Composites and Coatings

There are different approaches for applying high-temperature solid lubricants for a variety of engineering applications [21]. (1) Powdered solid lubricants have obvious shortcomings, in spite of powder lubrication as the oldest and simplest method. Two factors impeding the development of powder lubrication are associated with the difficulty of forming a continuous solid lubricating film and the need to constantly replenish the lubricant during the wear process. (2) Bonded coatings supply a larger film thickness and an enhanced wear lifetime, which improves the reliability and durability of traditional solid lubrication. However, most resin- or inorganic-bonded coatings lubricate only at low temperatures and are not suitable for high-temperature conditions. (3) Surface texturing of sliding metallic [183,184] or ceramic components/coatings [185] by laser [186], pulsed electric arc [187], ion etching, and electron beam followed by filling of various solid lubricants such as graphite, MoS_2/WS_2 [188], Mo/MoS_2/Ag [51], CaF_2, etc. (4) Self-lubricating composites or coatings are the most widely used and most promising solid lubrication technologies. A variety of processing approaches of large-scale two-dimensional layered films from graphene, *h*-BN, and TMD, to black phosphorous nanosheets and MXenes for solid lubrication as shearing films and nano-roller bearings, have been developed rapidly with the advent of graphene, which includes mechanical or chemical exfoliation, atomic/molecular

layer deposition, chemical vapor deposition, magnetron sputtering, pulsed laser deposition, electrophoretic deposition, ink-jet printing, spray/spin coating, or directly burnishing onto the substrate. Preparation techniques of self-lubricating composites or coatings include physical/chemical vapor deposition, thermal/plasma spraying, electrodeposition, laser cladding, powder metallurgy processes such as pressureless sintering, hot pressing, hot isostatic pressing and spark plasma sintering, and hot rolling.

5.1. Self-Lubricating Coatings by Physical Vapor Deposition

Physical vapor deposition processes are versatile in the composition of coating materials. They have the ability to produce very thin coatings as low as several nanometers with high purity, high adhesion, and unusual microstructures at high deposition rates. Physical vapor-deposited coatings for friction and wear applications include the following two different types: soft solid-lubricant coatings and hard wear-resistant coatings. Applying PVD coatings includes simple vapor deposition, sputtering, ion plating, and pulsed laser deposition.

Recently, various ion beam-assisted deposition methods, referred to as modifications of the more basic process, have been used to deposit very adherent tribological coatings at relatively low deposition temperatures. Strongly adherent MoS_2-Au(Ag)-Re composite films deposited by PVD combined with ion bombardment exhibit columnar structure and five times higher wear resistance than conventional sputtered MoS_2 film. Besides the sputtered MoS_2 films, two other categories of PVD coatings that are tribologically significant are sputtered hard coatings for wear control, such as diamond-like carbon coatings doped with or without additives, and ion-plated soft metals (Au, Ag, or composites) for lubrication, such as magnetron sputtering assisted pulsed laser deposition (MSPLD). Adaptive WC-WS_2-DLC, YSZ-Au-DLC-MoS_2 coatings are designed to provide graphite-like lubrication in humid air and molybdenum and tungsten sulfite lubrication in dry sliding and vacuum [3]. Gradient multilayered soft metal films of Ni-Cu-Ag-In significantly improve the load capacity and mechanical properties of films on space harmonic gears and rocket turbo-pump bearings. Sputtering is probably the most widely used vapor deposition technique. Nano-crystallization drove high-temperature self-lubricating WS_2 coatings deposited by magnetron sputtering, which have a low friction coefficient of 0.07–0.2 at temperatures of 100–400 °C. At 500 °C, the oxidation-induced formation of WO_3 with a relatively low hardness reduces the friction and improves wear resistance [82]. A self-lubricating Al_2Au-containing Al-Au coating was deposited onto cemented carbide substrates using unbalanced magnetron sputtering, which exhibits a fine-grained structure and a hardness value of 4 GPa. The coatings are thermally stable up to about 850 °C, and then the onset of oxidation occurs, and tribo-oxidation contributes to a low friction coefficient when testing against alumina tribopairs at temperatures of 500 °C to 700 °C [189]. RF magnetron sputtering was used to deposit periodic CrAlN/VN multilayer coatings with various bilayer periods, which provide preferable anti-wear performance due to interfacial coherent strengthening and lubricious vanadium oxide layers formed on the sliding surface [190]. In reactive sputtering, a reactive gas is introduced to produce compound coatings. Silver tantalate coatings of the Ag-Ta-O system produced by unbalanced magnetron sputtering exhibit excellent tribological properties at high temperatures [191]. Self-lubricating ceramic-Ag coatings were investigated due to the large variety of functionalities (e.g., lubricity, surface plasmon resonance, and antibacterial effect) that silver possesses and the possibility of selecting the proper matrix to support the metallic lubricant [192].

Researchers at the USA Air Force Research Laboratory, Wright-Patterson Air Force Base (WPAFB), developed PVD deposition methods for lubricous adaptive coatings, where initial multiphase adaptive oxide and fluoride coatings for high-temperature lubrication were progressively evolved to hard oxide matrices with additions of easy-to-shear gold and silver for moderate temperatures and dichalcogenide and graphite for near room temperature lubrication [3,30]. Thin composite films of MoS_2 with PbO, WS_2 with ZnO, MoS_2 with Sb_2O_3, and later WS_2 with CaF_2 are deposited to produce lubrication over

a wide temperature range. In this case, the metal dichalcogenides reacted with the oxides to form lubricious $PbMoO_4$, $ZnWO_4$, and $CaSO_4$ phases at elevated temperatures [126,127]. However, the drawback to this concept is that the reaction is irreversible, and the low-temperature lubrication will lose inevitably once returning to room temperature during the thermal cycling process.

5.2. Self-Lubricating Coatings by Thermal Spraying

The thermal spraying process has nowadays become a cost-efficient and reliable method to deposit thick coatings with a wide variety of feedstock materials and substrates, which has been successfully applied in aerospace, aviation, and power generation, becoming an essential component of modern industry [193]. The thermal energy necessary to melt the spraying material in the form of powder, wire, or even liquid suspension can be produced by a flame created by combustion gases, the electric plasma produced by an electric discharge, the detonation of the combustion gas by a spark plug, or an electric arc. Generally, only those thermally stable feedstock materials without the occurrence of oxidation or decomposition can be sprayed. In a plasma spraying process, the spraying feedstocks are fed into the plasma flame by a carrier gas, where they become melted or semi-melted and are then propelled to the substrate at high velocity due to high plasma enthalpies.

Plasma-sprayed ceramic and cermet coatings, especially those based on oxides (Al_2O_3, Cr_2O_3, etc.) and carbides (WC, Cr_3C_2, etc.), are widely used for wear and corrosion protection. Solid lubricants of graphite, MoS_2, fluorides, and lubricious binary or ternary oxides embedded in plasma sprayed coatings have been employed in different industries, especially in those applications under severe operation conditions [194,195]. The status-of-the-art developments involve reactive plasma spraying and plasma-sprayed oxide ceramic coatings containing nanophases either from nanostructured precursors or post-precipitated by purposely designed thermal treatments [180].

Composite Magneli phases of $Ti_6Cr_2O_7$ and $CrTi_2O_5$ from the system $Ti_{n-2}Cr_2O_{2n-1}$ formed on the plasma-sprayed TiO_2-Cr_2O_3 coating provide solid lubrication to 800 °C during wear tests [108]. Ni-Al-Cr_2O_3-Mo-Ag coatings were plasma sprayed on the surfaces of Inconel 718 alloy. The sliding process at elevated temperatures could promote the formation of lubricious silver molybdate films to reduce friction and wear [196]. Plasma sprayed WC-Co-Cu-BaF_2/CaF_2 self-lubricating coatings not only offer effective solid lubrication but also self-heal the surface defects and protect WC from decarburization [195]. The optimized composite coating consists of 70 wt.% WC-$(W,Cr)_2$C-Ni, 15 wt.% Ag, and 15 wt.% BaF_2-CaF_2 exhibits excellent friction and wear performance over a wide range of temperature up to 600 °C [197]. The synergistic effects of Ag, MoS_2, and hBN help to improve the tribological performance of Ni-Al-Ag-MoS_2 and Ni-Al-Ag-MoS_2-hBN on the surface of titanium- and nickel-matrix alloys [180].

Researchers from the NASA Glenn research center developed different self-lubricating plasma-sprayed coatings, such as PS100, PS200, PS300, PS304, and PS400, for extreme temperature applications. The objective of these composite coatings is to incorporate these fluorides and soft metals (i.e., Ag and Au) into matrix materials to reduce friction and wear at elevated temperatures. PS100 was a plasma sprayed nickel-chromium-based coating containing glass as a binder and silver and fluorides as the solid lubricants for applications of low speed, oscillating, plain spherical bearings. PS100 exhibited a very low friction coefficient and relatively low wear resistance over a broad range of temperatures, which was designed for high-temperature applications involving moderately loaded, up to at least 34 MPa, sliding contact bearings and for shaft seals requiring a degree of conformability [1]. PS200 was a plasma-sprayed nickel-cobalt-based chromium carbide coating, with silver and BaF_2-CaF_2 eutectic fluorides as the solid lubricants. This provides better tribological performance at temperatures as high as 900 °C for applications in the cylinder walls of Stirling engines. A linear alternator is a reciprocating device that is driven by a solar or nuclear-powered Stirling engine to generate electrical power. The power piston and cylinder were made of Ti-6Al-4V alloy and were designed to be lubricated by

a hydrodynamically-generated gas film, where rubbing was generated during starts and stops and there was the possibility of an occasional high-speed rub to lead to a severe galling tendency in sliding contacts, and thus a back-up self-lubricating coating on the cylinder and/or piston was needed [93,95,198]. PS212 coatings could be used for foil gas bearing applications [194]. PS300 was a plasma sprayed nickel-chromium bonded chromium oxide coating with 60 wt.% Cr_2O_3, 20 wt.% Ni80Cr20, 10 wt.% silver, and 10 wt.% BaF_2-CaF_2 eutectic solid lubricant additions, which provided good friction and wear properties in a partial-arc foil bearing at 500 °C. The PS300 coating was successful in lubricating a foil gas bearing at 500 °C for over 15,000 start-stop cycles. However, excessive foil wear was still observed at room temperature, and journal coating adhesion was poor, especially during repeated thermal cycles, which led to the spalling of PS300 coating (delamination) directly from the journal surface due to a mismatch in thermal expansion coefficients. Subsequent research resulting in a modification to the PS304 coating could achieve low friction and a small wear rate at elevated temperatures up to 650 °C [94]. PS304 is a 60 wt.% Ni80Cr20 matrix that contains solid lubricants, 10 wt.% Ag and 10 wt.% BaF_2-CaF_2 in eutectic composition. In total, 20 wt.% chromium oxide particles were used for strength enhancement, while Ag and BaF_2-CaF_2 were used to provide lubrication properties at different temperatures [199]. PS304 was found to be a suitable coating for many applications of foil air bearings and seals, exhaust gas recirculation (EGR) and turbocharger waste gate valve stems, steam turbine control valve components and bushings and shafting in heat treatment furnaces [200]. PS304 coating exhibits an increase in adhesive strength after exposure to temperatures above 500 °C for various durations due to the precipitation of a chromium-rich second phase in the matrix. Heat treatment of PS304 coating after plasma spraying and prior to finish machining is needed to insure dimensional stability and maximum adhesive properties [201]. One example is the development of a self-lubricating PS304 coating on advanced high-temperature nickel-based superalloy foil air bearings to evaluate their performance and durability from 25 °C to 650 °C [202,203]. In order to achieve the PS304 surface smoothening effect that is noted in high-temperature air foil bearings subject to cyclic start/stop operation, thrust-washer tests were also conducted with intermittent, as opposed to continuous, sliding contact [204,205]. The foil surface experiences sliding contact with the shaft during the initial start/stop operation prior to developing a gas film, which may lead to wear and failure due to inadequate load capacity, material capabilities, or rotordynamic performance. These tested bearings with PS304 coatings provided lives well in excess of 30,000 cycles, particularly some of them even exceeding 100,000 cycles, and are well suited for advanced high-temperature oil-free turbomachinery applications. Another example involves the development of self-lubricating steam turbine lift rods, which are designed to work in a frictional contact mode against a stack of seal rings at elevated temperatures and face challenging needs for surface protection. Wang et al. [206] reported a high-temperature self-lubricating composite coating deposited by plasma spraying to overcome the wear and galling damage of steam turbine governor valve lift rods of Waspaloy, a nickel-based alloy (AMS 5604), subjected to metal-metal interaction at 540 °C. A PS304 coating applied on the lift rods was intact even after 8500h of operation at 540 °C. Field operation after 3 years up to the date indicated that PS304 coatings have functioned effectively. A lubricious glaze layer containing Cr_2O_3, Ag, and CaF_2/BaF_2 eutectic was formed on the surface of coated lift rods to effectively protect them from high-temperature wear and galling damage. PS400 was a plasma-sprayed nickel-molybdenum-aluminum matrix containing chromium oxide as a binder, while the silver acted as a solid lubricant at a relatively lower temperature range of room temperature to approximately 450 °C, and BaF_2-CaF_2 eutectic offers effective lubricating above 400 °C, respectively. Therefore, PS400 coating was excellent for high-temperature wear applications due to the formation of a self-lubricating glaze layer, and it was used for microturbine engine foil gas bearing applications at temperatures above 760 °C [207]. The PS400 coating was tested as a shaft coating operating against a hot section foil bearing in a Capstone oil-free 30 kW microturbine engine, and interestingly, the shaft

diameter measurements show almost no wear due to the development of lubricious surface glazes after 2200 start-up and shut-down cycles conducted over 8000 h of operation at 96,000 rpm and approximate 540 °C. These coatings developed by NASA Glenn Research Center were effective at elevated temperatures but typically had friction coefficients above 0.2 at room temperature. In addition, the plasma spray technique intrinsically produces very thick (typically hundreds of microns) coatings, limiting their utility in application to precision components.

Plasma-sprayed ZrO_2-CaF_2 coatings incorporated with and without silver addition exhibited attractive tribological properties in sliding against superalloys [1]. Both coating combinations had fairly high wear rates at room temperature, but wear rates were much lower for the ZrO_2-CaF_2 coating at 650 °C. The effect of different lubricants on the high-temperature friction and wear characteristics of low-pressure plasma-sprayed $ZrO_2(Y_2O_3)$-based ceramic coatings was investigated [15,16,208]. Low friction and wear at temperatures of 600–700 °C were achieved for the low-pressure plasma-sprayed ZrO_2-CaF_2 coating when sliding against an alumina ball [16]. The incorporation of CaF_2/Ag_2O lubricants into the self-lubricating $ZrO_2(Y_2O_3)$ matrix composite coating provided low friction and wear against an alumina ball at temperatures of 300 °C to 700 °C [208]. However, high friction and wear of coatings were observed due to excessive plastic deformation and material transfer at 800 °C. Low-pressure plasma sprayed $ZrO_2(Y_2O_3)$ matrix coating incorporated with 50 vol.% $BaCrO_4$ ternary oxide effectively reduced friction and wear at temperatures of 400 °C to 800 °C on reciprocating ball-on-flat tribometer due to the formation of easy-to-shear $BaCrO_4$-rich tribolayers [15]. The incorporation of CaF_2, BaF_2, and Cr_2O_3 into a plasma-sprayed composite coating also achieved friction coefficients of 0.20–0.30 from 300 °C to 900 °C, which was due to the coexistence of CaF_2 and $BaCrO_4$ induced by the tribo-chemical reaction on the sliding surfaces. Chromium oxide coatings are widely used for tribological applications requiring high wear resistance and lubricity at elevated temperatures [17]. The incorporation of $BaCrO_4$ into chromium oxide coatings was developed to further improve its tribological properties as a high-temperature solid lubricant up to 700 °C. The adaptive formation of lubricious chromate films on worn surfaces of plasma-sprayed Cr_2O_3-$BaCrO_4$ coatings plays a vital role in reducing friction and wear at elevated temperatures [209].

Spray-formed and powder metallurgy materials are usually of high porosity. As one of the secondary processing techniques, hot rolling or forging is used to densify the products and improve their properties [210]. The Al-Si-graphite self-lubricating composite was synthesized by the spray forming process and then densified by warm rolling. Tribological tests were performed in the pin-on-disk method with high-carbon EN 31 steels as the counter surface at room temperature. Finally, the friction coefficient and wear rate were reduced from 0.49 to 0.38 and 2.25×10^{-3} mm^3/(Nm) to 1.25×10^{-3} mm^3/(Nm), respectively, with the thickness reduction of the composite by warm rolling [210].

5.3. Self-Lubricating Composites by Powder Metallurgy

Generally, wear-resistant components with flat surfaces and outside diameter surfaces are readily accessible for a plasma spraying process. However, the inside surfaces of relatively small components such as small cylindrical bearings, bushings, and valve guides are difficult or impossible to deposit coatings from a plasma spray gun. Powder metallurgy processes are appropriate for these types of components. During sintering, various mass transfer processes contribute to the densification of raw powders consisting of matrix materials and solid lubricants. Figure 11 shows the typical microstructure and worn surfaces of a spark-plasma-sintered $ZrO_2(Y_2O_3)$-30CaF$_2$-30Au composite. The obtained self-lubricating materials usually exhibit uniformly distributed grains due to the growth inhibition effect of different constituents [102]. The hot-pressed alumina matrix composite incorporated with Ag and CaF_2 provided low friction and wear at temperatures of 300–750 °C [211–213]. The appropriate number of solid lubricants and sintering aid

appears to improve the formation of a complete, well-adhering self-lubricating film, which seems to be responsible for the reduction of friction and wear at 650 °C.
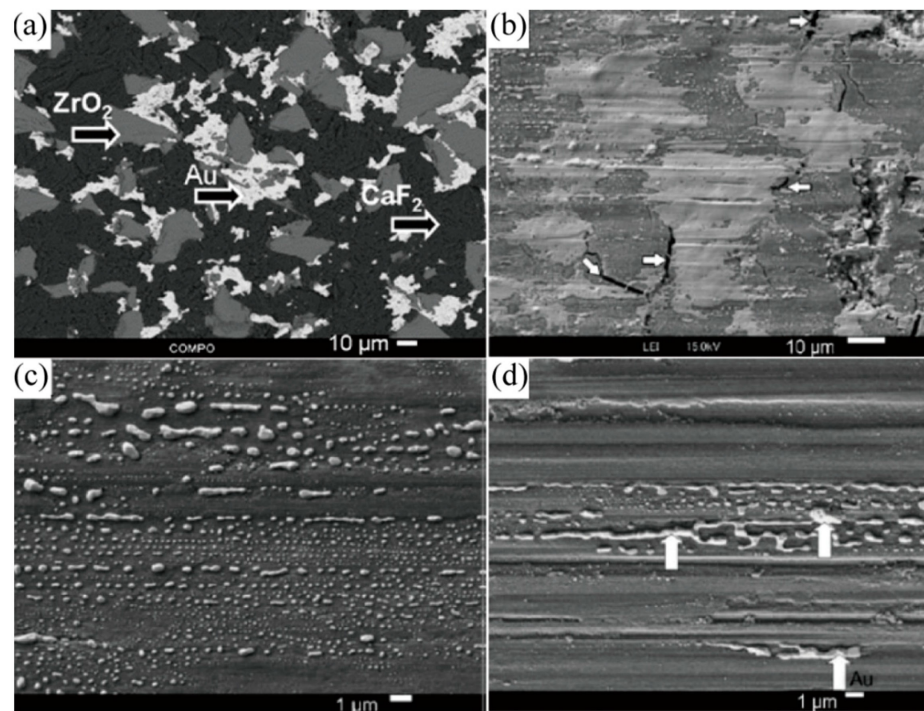

Figure 11. Microstructure and worn surfaces of a $ZrO_2(Y_2O_3)$-30CaF$_2$-30Au composite fabricated by spark plasma sintering: (**a**) Morphology and phase distribution of different constituents, (**b**) worn surface after room temperature wear test, (**c**) worn surface after 400 °C wear test, (**d**) worn surface after 800 °C wear test. Reproduced with permission from Reference [102], Copyright © Elsevier B.V. 2004.

$ZrO_2(Y_2O_3)$-50BaCrO$_4$ composites were spark plasma sintered by optimizing the composition and sintering parameters, and high-temperature friction and wear tester was used to evaluate their friction and wear properties in dry sliding against an alumina ball. The sintered samples exhibit a density of 4.99 g/cm^3 and a Vickers hardness of 426 HV$_1$ and have coefficients of friction from 0.38 to 0.55 and wear rates from 1.44×10^{-5} to 5.35×10^{-5} mm^3/(Nm) from room temperature to 800 °C [143]. A well-covered BaCrO$_4$ fine-grain layer is observed on the sliding surfaces at elevated temperatures due to considerable plastic deformation and smearing of BaCrO$_4$. The synergistic effects of CaF$_2$ and Au lubricants on the friction and wear properties of $ZrO_2(Y_2O_3)$ matrix composites were evaluated with a high-temperature friction and wear tester. The $ZrO_2(Y_2O_3)$-CaF$_2$-Au composite has a density of 5.53 g/cm^3 and a Vickers hardness of 396 HV$_1$ and exhibits a friction coefficient from 0.36 to 0.50 and a wear rate from 1.67×10^{-6} to 3.55×10^{-6} mm^3/Nm over the entire temperature range up to 800 °C [102]. Soft metallic lubricants of gold are observed to diffuse and migrate from the subsurface layer to the sliding surface and finally form a discontinuous lubrication film, which lubricates the oxide matrix synergistically with CaF$_2$. From an engineering standpoint, most machinery runs at low temperatures only during start-up periods; therefore, low friction (<0.30) at high operating temperatures, especially above 300 °C, for a gas turbine seal, for example, is of significant value.

Hot pressing has been used to fabricate NiCr-BaCr$_2$O$_4$ self-lubricating composites in a vacuum sintering furnace for tribological evaluation in sliding against an alumina ball. At 800 °C, a friction coefficient of 0.27 and a wear rate of 4.5×10^{-6} mm^3/(Nm) are achieved for the NiCr-20BaCr$_2$O$_4$ composite, however, for a comparative study, the unmodified NiCr alloy exhibits a friction coefficient of 0.41 and a wear rate of 9.2×10^{-5} mm^3/(Nm) [151]. A dense oxide glaze layer is formed on the sliding surface of the NiCr-20BaCr$_2$O$_4$ composite

to effectively reduce friction and wear at elevated temperatures, and the tribo-oxidation reaction of $BaCr_2O_4$ is responsible for the formation of the glaze layer containing lubricious hexavalent-Cr^{6+} $BaCrO_4$ during high-temperature wear tests.

Self-lubricating $ZrO_2(Y_2O_3)$-Al_2O_3-$Ba_xSr_{1-x}SO_4$ (x = 0.25, 0.5, 0.75) composites were fabricated by spark plasma sintering. The composites containing $Ba_xSr_{1-x}SO_4$ have significant improvements in effectively reducing friction and wear in sliding against an alumina ball as compared to unmodified $ZrO_2(Y_2O_3)$-Al_2O_3 ceramics. Interestingly, the composites have low friction coefficients of less than 0.15 and wear rates in the order of 10^{-6} mm^3/(Nm) at 760 °C. For example, $ZrO_2(Y_2O_3)$-Al_2O_3-$50Ba_{0.5}Sr_{0.5}SO_4$ composite has a density of 4.2 g/cm^3 and a hardness of 3.48 GPa, exhibits friction coefficients and wear rates of 0.2 and 4.8×10^{-5} mm^3/(Nm) at room temperature, and 0.11 and 3.15×10^{-6} mm^3/(Nm) at 760 °C, respectively. While $ZrO_2(Y_2O_3)$-Al_2O_3-$50Ba_{0.75}Sr_{0.25}SO_4$ composite has a density of 4.45 g/cm^3 and a hardness of 3.48 GPa, exhibits friction coefficients and wear rates of 0.24 and 2.06×10^{-5} mm^3/(Nm) at room temperature, and 0.12 and 5.76×10^{-6} mm^3/(Nm) at 760 °C, respectively. The formation and effective spread of the lubricious $Ba_xSr_{1-x}SO_4$ layer is of great significance in lowering friction and wear [157]. Fe_3Al matrix composites containing $Ba_{0.25}Sr_{0.75}SO_4$ fabricated by hot pressing also exhibit a very low friction coefficient from 0.19 to 0.29 and wear rate on the order of 10^{-5} mm^3/(Nm) at temperatures of 600–800 °C, which is lower than unmodified Fe_3Al alloy [158].

For a comparative study, a variety of self-lubricating $ZrO_2(Y_2O_3)$ matrix composites are spark plasma sintered by tailoring the chemical compositions and sintering parameters. Selected lubricants of BaF_2, CaF_2, Ag, Ag_2O, Cu_2O, $BaCrO_4$, $BaSO_4$, $SrSO_4$, and $CaSiO_3$ were added to the oxide ceramic matrix to evaluate their self-lubricity over a wide temperature range up to 800 °C by using a ball-on-block friction and wear tester in sliding against alumina ball [101]. Figure 12 shows the frictional behavior of $ZrO_2(Y_2O_3)$-Al_2O_3 ceramics as a function of wear cycles at different temperatures [101]. Figure 13 shows the frictional behavior of $ZrO_2(Y_2O_3)$-Al_2O_3-$50SrSO_4$ composites as a function of the wear cycle at different temperatures [101]. The incorporation of graphite or MoS_2 into $ZrO_2(Y_2O_3)$ matrix composites was also evaluated for comparison under identical test conditions. The $ZrO_2(Y_2O_3)$-Al_2O_3 ceramics have a hardness of 14.8 GPa at room temperature and 7.8 GPa at 700 °C, and exhibit friction coefficients and wear rates of 0.48 and 2.31×10^{-6} mm^3/(Nm) at room temperature, and 1.15 and 4.77×10^{-4} mm^3/(Nm) at 800 °C, respectively. While, the $ZrO_2(Y_2O_3)$-Al_2O_3-$50SrSO_4$ composites have a density of 4.05 g/cm^3 and a hardness of 455 HV$_1$, and exhibit friction coefficients and wear rates of 0.11 and 1.05×10^{-6} mm^3/(Nm) at room temperature, and 0.19 and 2.28×10^{-6} mm^3/(Nm) at 800 °C, respectively. The dominating wear mechanism of unmodified $ZrO_2(Y_2O_3)$-Al_2O_3 ceramics depends mainly upon surface fatigue and brittle fracture at 800 °C. However, for self-lubricating composites, the most important factor for reducing friction and wear at elevated temperatures is attributed to the formation, plastic deformation, and effective spread of sulfate lubricating films on the sliding surface [101].

Figure 14 shows the frictional behavior of $ZrO_2(Y_2O_3)$ matrix composites incorporated with and without various additives as a function of temperature in sliding against an alumina ball. Figure 15 shows the wear rates of $ZrO_2(Y_2O_3)$ matrix composites incorporated with and without solid lubricants at room temperature and 800 °C [101]. Clearly, the incorporation of $SrSO_4$-$CaSiO_3$ solid lubricants into $ZrO_2(Y_2O_3)$ matrix composites contributes to friction coefficients of 0.2–0.4 and wear rates of 10^{-5}–10^{-6} mm^3/(Nm) from room temperature to 800 °C [101].

The synergistic effects of $SrSO_4$ and Ag on the self-lubricity of alumina matrix composites are evaluated by sliding against an alumina ball over a wide temperature range. The Al_2O_3-$50SrSO_4$-10Ag composites with a density of 3.69 g/cm^3 have a hardness of 129 HV$_1$, and exhibit friction coefficients and wear rates of 0.12 and 1.1×10^{-8} mm^3/(Nm) at room temperature, and 0.22 and 4.89×10^{-8} mm^3/(Nm) at 760 °C, respectively. While Al_2O_3-$50SrSO_4$-20 Ag composites with a density of 4.15 g/cm^3 have a hardness of 319 HV$_1$, and exhibit friction coefficients and wear rates of 0.08 and 1.06×10^{-8} mm^3/(Nm) at room

temperature, and 0.20 and 3.57×10^{-8} mm^3/(Nm) at 760 °C, respectively. The synergistic incorporation of SrSO$_4$ and Ag into the alumina matrix not only greatly improves friction and wear properties at low temperatures, but also provides excellent lubrication properties at elevated temperatures. From the friction and wear point of view, the incorporation of SrSO$_4$ and Ag into the alumina matrix creates a bright future for lubricating ceramic components in sliding or rolling contact over a broad temperature range up to 800 °C. The strontium sulfate lubricants become softened at high temperatures, and further spread out onto the sliding surface as well as the soft Ag clusters extrude and migrate from the subsurface layer due to tribological stressing, forming a lubricious mechanically mixed layer of SrSO$_4$ and Ag [163]. In previous work, the oxometallate-containing coatings were also fabricated by various powder metallurgy processes, such as Al$_2$O$_3$-BaCrO$_4$ coatings by hot pressing and SrSO$_4$–Sr$_2$SiO$_4$ coatings by spark plasma sintering on the surfaces of oxide ceramic components to improve the tribological properties.
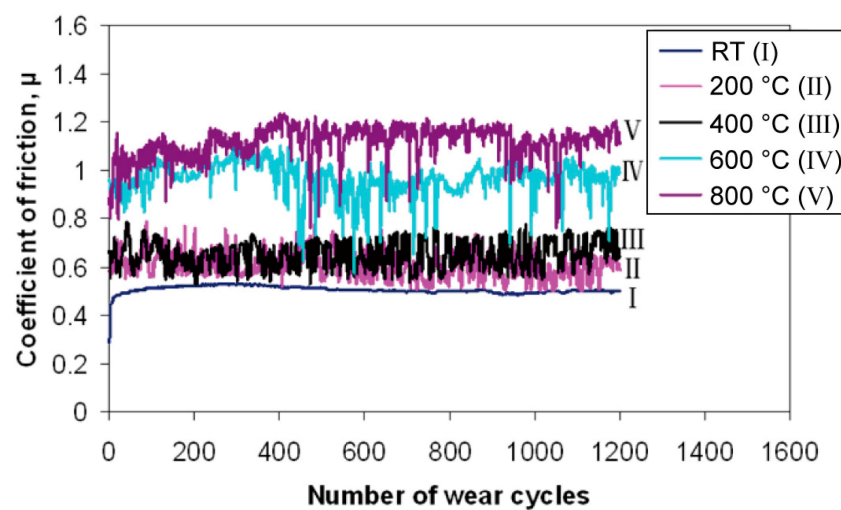

Figure 12. Frictional behavior of ZrO$_2$(Y$_2$O$_3$)-Al$_2$O$_3$ ceramics as a function of wear cycles at different temperatures. Reproduced with permission from Reference [101], Copyright © Elsevier B.V. 2009.

Figure 13. Frictional behavior of ZrO$_2$(Y$_2$O$_3$)-Al$_2$O$_3$-50SrSO$_4$ composites as a function of wear cycle at different temperatures. Reproduced with permission from Reference [101], Copyright © Elsevier B.V. 2009.
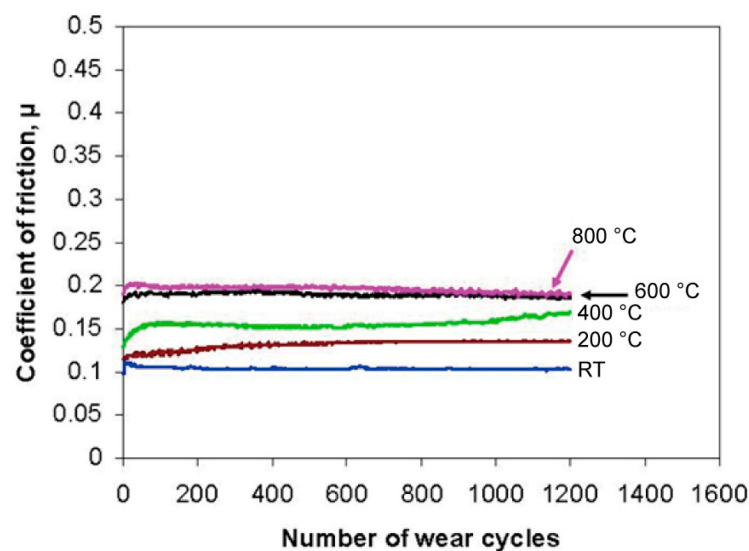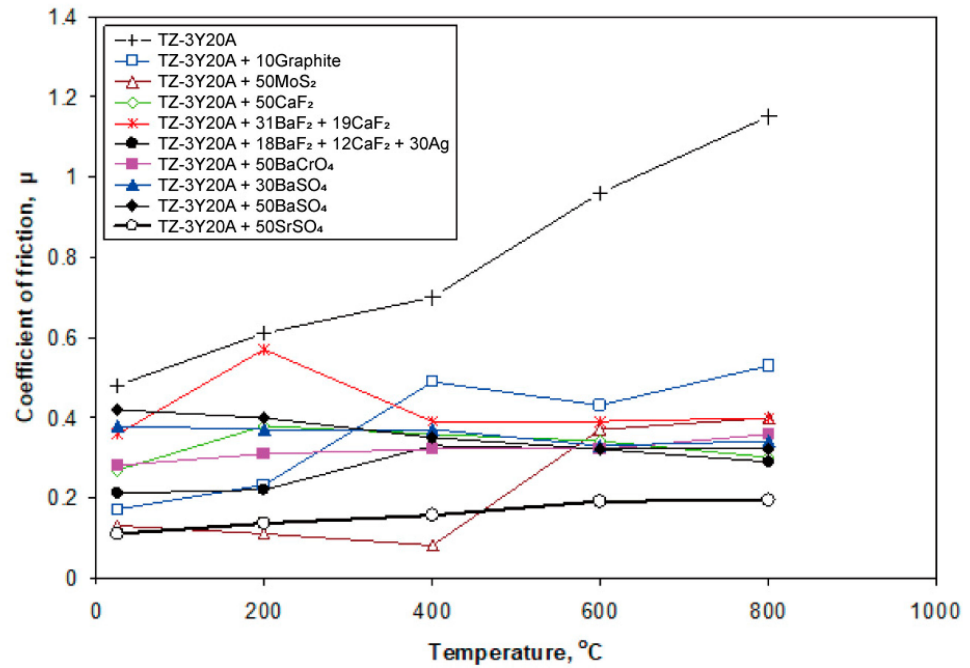
Figure 14. Frictional behavior of $ZrO_2(Y_2O_3)$ matrix composites incorporated with and without various additives as a function of temperature in sliding against an alumina ball. Reproduced with permission from Reference [101], Copyright © Elsevier B.V. 2009.
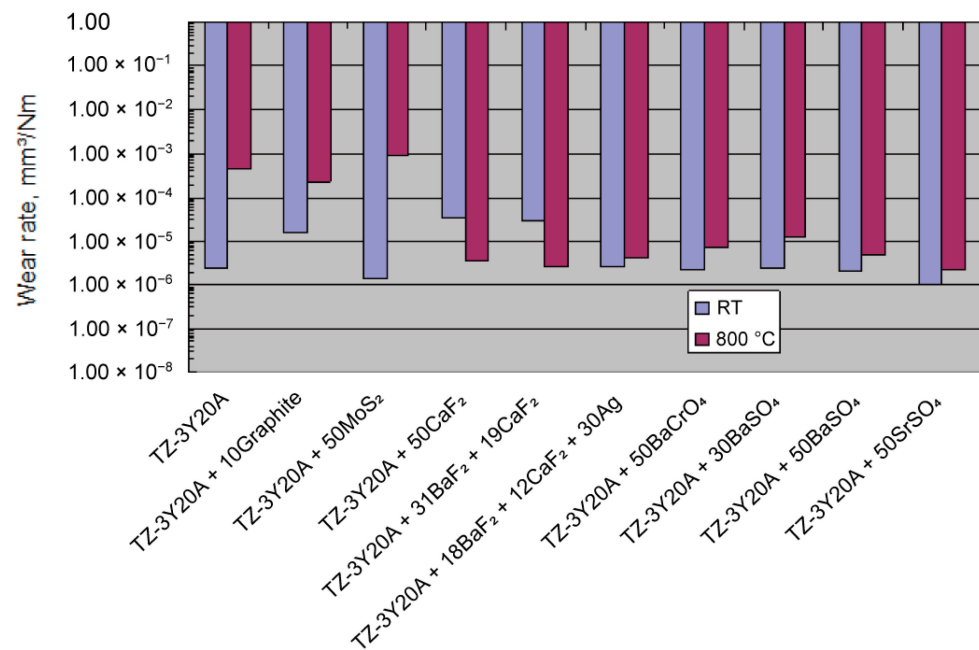
Figure 15. Wear rates of $ZrO_2(Y_2O_3)$ matrix composites incorporated with and without solid lubricants at room temperature and 800 °C. Reproduced with permission from Reference [101], Copyright © Elsevier B.V. 2009.

Spark plasma sintering has also been used in the preparation of self-lubricating composites containing graphene. Hybrid Al-matrix composites containing nano-Al_2O_3 and graphene nanoplatelets were prepared in an argon atmosphere at 500 °C. The friction coefficient decreased from 0.36 to 0.24 against chromium-plated the chrome steel counter body by increasing the content of graphene nanoplatelets from 0.5 wt.% to 5 wt.% [214].

The NiAl matrix composites with 1.5 wt.% graphene nanoplatelets were fabricated at 1150 °C and then the tribological tests were performed by sliding against a Si_3N_4 ball. The friction coefficient reaches 0.36 at 200 °C. On the other hand, the wear rate increases rapidly with temperature, reaching 3.39×10^{-4} mm^3/(Nm) at 400 °C, which may be attributed to surface layer delamination due to the stress-inducing crack propagation parallel to the sliding direction [215]. Moreover, the synergetic effects of multilayer graphene and Ti_3SiC_2 have been studied in TiAl and Ni_3Al matrix composites. Tribological evaluation at various temperatures shows that multilayer graphene enriched on the worn surface can effectively reduce friction and wear below 350–400 °C but lose effect at higher temperatures. Nevertheless, Ti_3SiC_2 will partially decompose and form a lubricating film on a worn surface at 400–800 °C, which contributes to the outstanding high-temperature tribological performance [216,217]. Friction stir processing was also used to obtain an aluminum-graphene composite. The friction tests were performed using the block-on-ring method against AISI 1020 steel. Composites exhibited a low friction coefficient of 0.38, which was distinctly lower than that of 0.57 for the unmodified aluminum alloy [218].

5.4. Self-Lubricating Coatings by Electrodeposition

Electrochemical deposition (also known as electrolytic deposition, electrodeposition, or electroplating, electro-spark deposition) is the widely used and convenient technology of applying metallic coatings with relatively high melting points. Coatings with a thickness of sub-micro to tens of microns can be applied to a metallic surface (e.g., Ni, Co, Cu, Pb, Cr) and, with suitable preparation, to plastics and many other nonconducting substrates at room temperature or slightly higher temperatures of less than 100 °C. Codeposition of two or more metals is possible under suitable conditions of electric potential and polarization. A wide range of composite coatings containing insoluble particles in a metallic matrix can be fabricated by codepositing particles from suspension in agitated electrolytic solutions. The evergrowing demands of industrial surface engineering, such as wear- or corrosion-resistant surface layers, provide a driving force for rapid development of electrodeposition over the decades [219].

Electrodeposition of nickel-matrix composites containing dispersions of second-phase particles has attracted significant importance for potential applications. Incorporation of hard oxides (Al_2O_3, Cr_2O_3, TiO_2) or carbides (SiC, WC, Cr_3C_2), or diamond particles into metallic matrix improves significantly mechanical properties such as hardness and wear resistance. Ni-, NiCo- or Cu-based coatings incorporated with soft solid particles such as PTFE [220], MoS_2 [221], WS_2 [222], graphite [223], *h*-BN [224], single-wall carbon nanotube (SWCNT) [225], graphene nanoplatelet [226], Ti_3C_2 MXenes [227], $SrSO_4$ [159], and $BaCr_2O_4$ [150] can act as excellent self-lubricant layers, especially in precise mechanical parts and in slide bearings. The Cu-Sn, Cu-Sn-TiO_2, Cu-Sn-PTFE, and Cu-Sn-PTFE-TiO_2 coatings were electrodeposited in a pyrophosphate electrolyte with PTFE emulsion and TiO_2 sol, which led to a low friction coefficient of 0.1 and high wear resistance [228]. Sufficient solid lubricants embedded in the metallic-based coatings enable a significantly reduced friction coefficient by the formation of a self-lubricating tribofilm. As compared with plasma nitriding and sputtering deposition of thin, precious metals on superalloys, the electrodeposition process is a simple and economical method. Recently, with the emergence of compositionally- and hydrodynamically modulated layer coatings, the possibility of slow-release coatings for semi-continuous lubrication and modification of diffusion coatings by heat treatment have received considerable interest in composite coatings and surface functionality technologies [219].

As mentioned in Section 5.3, some oxometallates such as alkaline earth sulfates and chromates were developed as effective solid lubricants for sliding and rolling contact components. However, oxometallate-containing composites/coatings produced with the above-mentioned methods are generally associated with powder metallurgy processes such as spark plasma sintering and hot pressing, which may result in a possible chemical reaction between oxometallates and oxide ceramics or decomposition of oxometallates at elevated

temperatures. Thus, it is quite noteworthy to find new low-temperature routes, such as electrodeposition, to fabricate oxometallate-containing composite coatings, not only for cost reduction. Electrodeposition has been employed to produce Ni-SrSO$_4$ composite coatings on superalloy Inconel 718 from a Watts electrolyte containing a SrSO$_4$ suspension. Figure 16 shows the friction coefficients of the Inconel 718 substrate, pure nickel coating, and Ni-SrSO$_4$ composite coatings in sliding against a SAE52100 steel ball. As compared with the pure nickel coating and the substrate, the composite coating incorporated 6.83 vol.% SrSO$_4$ exhibits the enhanced microhardness of 450 HV$_{0.1}$, a low friction coefficient of 0.31, and a small wear rate of 5.3 × 10^{-4} mm^3/(Nm) in sliding against bearing steel ball. The improvement in tribological properties of composite coatings results from the enhanced hardness and the resistance to plastic deformation and scuffing wear. Therefore, electrodeposited Ni-SrSO$_4$ composite coating is a potential self-lubricating material to improve the friction and wear properties of superalloys from room temperature to high operating temperatures for applications in aircraft gas engines, space mechanisms, petrochemical equipment, and offshore industries [159].
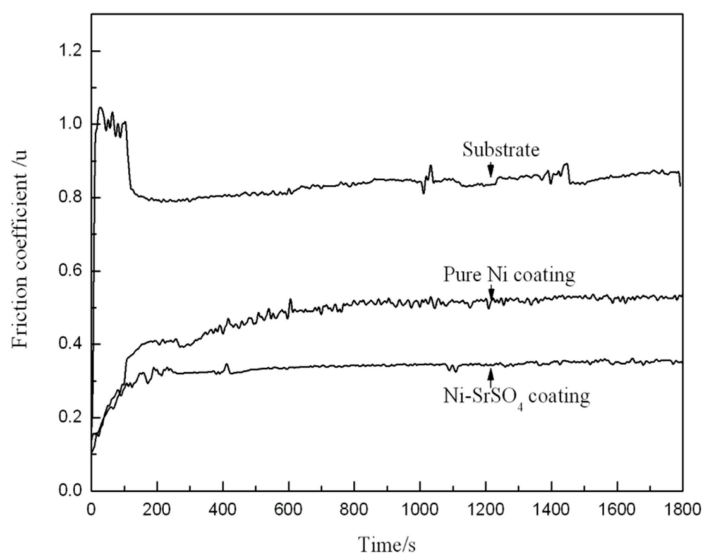

Figure 16. Friction coefficients of Inconel 718 substrate, pure nickel coating and Ni-SrSO$_4$ composite coatings in sliding against SAE52100 steel ball. Reproduced with permission from Reference [159], Copyright © Elsevier B.V. 2009.

In our previous work, electrodeposition was also employed to produce Ni-based chromate-containing composite coatings on Inconel 718 superalloy to improve friction and wear properties [150]. One challenge to depositing these coatings is that BaCrO$_4$ is soluble in an acid electrolyte solution, and a low concentration of Cr^{6+} in the electrolyte significantly decreases the current efficiency of the deposition process, where only a little electrode current density can be assigned to the reduction of Ni^{2+}. In this case, the reduction reaction from Ni^{2+} to metallic Ni at the cathode is very hard to push forward, and then the Ni-BaCrO$_4$ composite coating is difficult to achieve by electrodeposition. However, acid-insoluble BaCr$_2$O$_4$ particles instead of BaCrO$_4$ introduced into the nickel matrix are able to form a Ni-BaCr$_2$O$_4$ composite coating on Inconel 718 superalloy from a Watts electrolyte containing a BaCr$_2$O$_4$ suspension. Figure 17 shows the friction coefficients of the Inconel 718 substrate, pure nickel coating, and Ni-BaCr$_2$O$_4$ composite coatings incorporated with different volume fractions of BaCr$_2$O$_4$ in sliding against an Al$_2$O$_3$ ball. The Ni-16.6 vol.% BaCr$_2$O$_4$ composite coating exhibits a distinctly low friction coefficient of 0.31 and a small wear rate of 2.79 × 10^{-6} mm^3/(Nm) as a comparative study with pure nickel coating and the substrate. The wear resistance of the electrodeposited Ni-BaCr$_2$O$_4$ composite coating was further improved by increasing the BaCr$_2$O$_4$ content. The improvements in tribological properties of Ni-BaCr$_2$O$_4$ composite coatings are attributed to both the

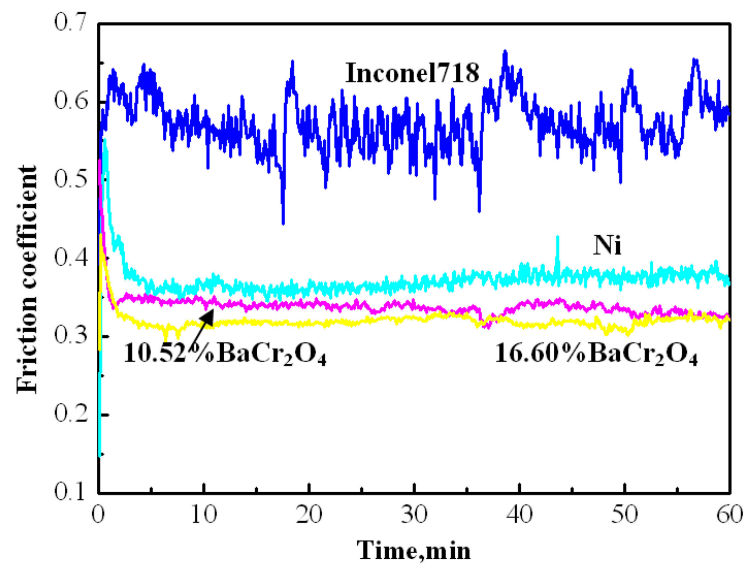enhanced microhardness and self-lubricity of chromate-containing films formed on the sliding surface [150].

Figure 17. Friction coefficients of Inconel 718 substrate, pure nickel coating and Ni-BaCr$_2$O$_4$ composite coatings incorporated with different volume fractions of BaCr$_2$O$_4$ in sliding against Al$_2$O$_3$ ball. Reproduced with permission from Reference [150], Copyright © Elsevier B.V. 2011.

Electrodeposition was employed to produce the composites comprising MoS$_2$ on vertically aligned carbon nanotubes (CNTs) films, and a low friction coefficient of 0.03 and a wear rate of 10^{-13} mm^3/(Nm) were achieved even at 300 °C, which were about 2 orders of magnitude better than those of MoS$_2$-based nanoparticulate coatings [229].

6. Challenges Highlighted in High Temperature Solid Lubrication Applications

Industrial applications for high-temperature lubrication include not only the aerospace (sliding and rolling contact bearings, seals, and gears in the propulsion system of reusable launch vehicles, and precision satellite and spacecraft components), and aviation industries (bearing, abradable seals), but also other industries (hot metal forming process, high-speed dry machining process, side dams for the thin-strip steel casting process, pantograph contact strip for electric railways, cylinder wall/piston ring in diesel engines and automotives, as well as various furnace components) [2,8].

6.1. Bearings for Advanced Propulsion Systems

High-temperature bearings that must be self-lubricated include bearings of the shuttle, air foil bearings, rolling bearings of a gas turbine engine, rudder bearings of supersonic aircraft, bearings of adiabatic diesel engines, etc. The classic failure mode of rolling-bearing, which accommodates relative motion primarily by the action of rolling with a small slip (sliding) enabling it to carry high contact stresses, is fatigue spalling under cyclic contact stressing. However, when the rolling surface contains substantial sliding, severe adhesive wear, commonly called scuffing or smearing, worsens the surface damage. For bearings that operate at high temperatures (up to 1200 °C) and/or at high speeds with high precision, refractory materials and compounds such as alumina, yttria-stabilized zirconia, and silicon nitride are considered. Therefore, adaptive hard and soft multilayered coatings must be considered for long-lifetime rolling-element bearings at elevated temperatures.

One example is the lubrication application for advanced engines in hypersonic vehicles, which requires the lubricity and reliability of solid lubricants from ambient temperature to above 1000 °C during high-Mach-number (larger than 5) flights [3]. Air foil bearings in high Mach engines are designed to operate under heavy loads in the air at 900 °C or even higher.

The lubrication demands are challenging at different contact stages, such as start-up at room temperature, acceleration, or deceleration during operation, and shutdown at elevated temperatures, which may be well-suited for developing thermally stable oxide lubrication.

6.2. Seals Components for Advanced Propulsion Systems

Sliding of the seal surface occurs in a direction normal to the leakage flow under even no lubrication condition (e.g., in gas-path components such as a turbine or compressor blade tip). Seal components are subjected to adhesive wear, abrasive wear, corrosive wear, fatigue wear, and blistering during operation. Abradable (rub-tolerant) seals are used at the rotor-stator interface in the compressor and turbine sections of gas turbine engines to maintain the close tolerance without catastrophic failure. Plasma-sprayed Ni-Cr-bonded chrome carbide and tungsten carbide coatings are usually applied as abradable coatings in sliding against rub-tolerant plasma-sprayed chrome oxide coatings to compressor and turbine castings [19].

New technologies and approaches are urgently needed to explore high-temperature sealing materials and technologies for next-generation advanced propulsion systems, particularly in hypersonic vehicles, to prevent damage from both hot engine combustion gases and the friction heat of the atmosphere. In this case, sliding seal components will need to operate and resist environmental damage from an extreme temperature higher than 1000 °C, water vapor, oxidation, or reduction. Previous work on both alumina-boria-silica and complex carbide-oxide fiber materials demonstrated their potential use as high-temperature seal materials, although their sliding durability was still limited due to the reactive nature of boria and the oxidation/abrasion mechanism of carbide constituents, especially at elevated temperatures [12].

6.3. Hot Metal Forming Process

Components used in the hot metal forming industry such as molds, rolls, tools, and dies usually operate under conditions of extremely high temperature (strip/pipe/profile temperature up to 1100 °C for rolling, up to 1200 °C in hot extrusion) and mechanical (more than 1.0 GPa) dynamic loads and high velocity (10 m/s for rolling), which results in severe plastic deformation wear and fatigue [176]. Different processes, such as sheet forming, hydroforming, warm forming, superplastic forming, deep drawing, hot stamping, and forging, are used to produce aluminum parts for the automotive industry. However, in order to prevent direct metallic contact, seizure, and galling by lowering the friction stresses, all these processes require proper lubrication [230]. Reducing the friction coefficient is very important in a metal-forming process in order to prolong the lifetime of the tool, enhance the formability of the material, and improve the quality of the finished product.

Layered graphite has been widely used for the cold and hot forming of aluminum; however, dark stains remaining on the surface of the formed parts usually lead to additional grinding or polishing. h-BN has not only essentially the same lubricating mechanism as graphite but also high thermal stability, low thermal expansion, and good thermal shock resistance, although its lubricity is inferior to graphite and MoS_2. Therefore, when lubrication at elevated temperatures or cleanliness of working environments is of critical concern, a clean h-BN solid lubricant is capable of successfully replacing dirty graphite or MoS_2 to lubricate the surface of the formed parts during metalworking processes [60]. The stability of the lubrication film and the resulting surface quality depend mainly upon the particle size and concentration of h-BN powders [69]. Besides h-BN, a variety of high-temperature lubricants of inorganic additives such as borate-, silicate-, and polyphosphate salts exhibit suitable lubrication properties, which helps to reduce material loss and energy consumption and finally ensure the quality control and dimensional stability of the hot-formed components [176].

6.4. High-Speed Dry Machining

Machining technology is closely related to the development of high-temperature cutting tool materials with hard and wear-resistant surfaces such as nitride-, carbide-, or carbonitride-based monolithic and multilayered hard coatings. In consideration of environmental protection requirements and the elimination of coasts for coolant media recirculation and utilization, cutting and milling operations gradually shift to high-speed dry machining without any oil-based coolant used. Surface functionality design in nanostructure and chemistry is urgently needed for a modern intelligent machining operation, which endows hard coatings with synergistic self-adaptation to lubricate up to 1000 °C and assure surface chemical and structural reversibility during thermo-mechanical cycling to maintain high cutting performance [30].

High-quality precision components can be rapidly produced by high-speed dry machining at the tip of the cutting edge. The material removal rate depends mainly upon allowable feeding rates, tool speeds, and cutting temperatures. Face or crater wear from chip motion and flank wear from the rubbing action are the main failure modes for a cutting tool, which is significantly influenced by a built-up edge generated from highly strained and hardened fragments. Therefore, the resistance to tool wear depends mainly upon the hot hardness, strength, fracture toughness, chemical stability, and reactivity of tool materials [19].

Cemented carbide or carbonitride tool materials are composed of granular graded transition metallic carbide or carbonitride particles of tungsten, titanium, tantalum, niobium, and other refractory metals bonded with cobalt, nickel, and molybdenum, and are produced by powder metallurgy processes. Various single or multilayered hard coatings of ceramic materials such as TiN, Al_2O_3, TiC_xN_y, $TiVO_xN_y$, TiAlCrSiN, doped DLC, or diamond are deposited on cemented-carbide substrates to increase tool life by ion plating, magnetron sputtering, or chemical vapor deposition. The properties of these hard nitride coatings are generally modified with various elements, such as aluminum, silicon, chromium, and vanadium, to provide additional properties such as thermal stability, low adhesion, and even easy-to-shear [231]. Mo-N- and W-N-based coatings are designed for induced oxidation during dry machining operations and create wear-resistant and lubricious oxide phases such as molybdates and tungstates upon heating [232]. Multi-arc ion plating was employed to deposit VAlCN-Ag nanocomposite and VAlCN/VN-Ag multilayered coatings on Inconel 718 alloy, and the synergistic lubrication effect of both $AgVO_3$ and V_2O_5 Magneli phases was evaluated to verify their contributions to the lowest friction coefficient of about 0.18 for VAlCN-Ag coating at 600 °C [233]. A self-lubricating $WC-Co-Cu-BaF_2/CaF_2$ wear-resistant coating with a friction coefficient of only 0.02 was fabricated for the application of machining tools [195]. CaF_2 is filled into the micro-texture of the rake face of the tool to form a self-lubricating film to improve the high-temperature machining performance, especially at elevated temperatures above 450 °C [234]. A self-lubricating Ti(C,N) cermet material modified with a multilayer core-shell microstructure exhibited enhanced wear-resistance and cutting performance [235]. In order to improve cutting performance, the benefits of $Al(OH)_3$ shell on CaF_2 solid lubricant were validated on hot-pressed $Al_2O_3/Ti(C,N)$ ceramic tools by incorporating with ZrO_2 whiskers-reinforced $CaF_2@Al(OH)_3$ [236]. Nowadays, hard nanocomposite or multilayered nitride coatings with adaptive surface texturing lubrication will be developed as next-generation cutting tool coating materials.

6.5. Electric Contacts for Electric Railways and Transmission in Space

The coupling action between frictional and electric contact must be taken into account when sliding and rolling electrical contacts are involved, such as pantograph contact strips for electric railways and slip-roll rings for electric transmission in space. In machines that utilize a commutator, electrical brushes must be able to realize the commutation function when the load current is transferred to the external circuit. In the case of a pantograph contact strip, the selected materials must be able to operate at a rated current of 1000 A, a rated voltage of 25 kV, a sliding speed of 300 km/h and an applied load of 70 N with

an allowable wear loss of only 1 mm/10,000 km) [4]. Arc discharge attack and high-temperature mechanical wear are the key factors influencing the high-power and long-lifetime performance of current collectors. Electric brush wear is generally due to adhesion and particle transfer, and in some circumstances, fatigue and fracture are caused by the mechanical impact. Most electric brushes are comprised of graphite-based materials such as electrographite, carbon-graphite, and metal-graphite due to their low friction and wear and high electrical conductivity, which are fabricated either by conventional powder metallurgy process or by infiltration of porous graphite with molten metals (e.g., Ag, Cu) and other additives [19]. The metallized MAX phase or carbon contact strip is designed for electric railways, and the noble metal-containing slip-roll ring is employed for electric transmission in space mechanisms. Graphene-reinforced copper matrix composites exhibit an enhanced tensile strength of 253 MPa, a low friction coefficient, and a small wear rate due to excellent comprehensive properties such as self-lubricity, mechanical reliability, and chemical and thermal stability of graphene. Examples of graphene-reinforced copper matrix composites exhibit a service lifetime of electrical contact performance of 10 times longer than that of commercially available pure copper and are almost comparable to the CuAg20 contacts used in electrical engineering systems [237].

6.6. Refractory Side Dams for Thin-Strip Steel Casting Process

With the development of the thin-strip steel casting process, more requirements for two fixed refractory side dams are put forward associated with extreme circumstances such as mechanical stress (pressed against the water-cooled rollers), high-temperature corrosion, and thermal shock (due to contact with liquid steel), and wear (due to contact with nickel-coated copper rollers and steel strip) [71–73]. The sides of the rollers must be sealed to block the overflow of molten steel by high-performance side dams [53,70]. BN-based materials incorporated with m-ZrO_2 and SiC are employed as the best side-dam materials for twin roll strip steel casting and as a break ring for horizontal continuous casting, as contrasted with other candidate materials such as sialon-BN, Si_3N_4-Al_2O_3-BN, TiN-MgO-BN, AlN-BN, mullite-AlN-BN, Si_3N_4-AlN-BN, AlON-BN, and C_f-SiO_2-BN [53,73].

7. Conclusions

Understanding the friction and wear behavior of various solid lubricants and self-lubricating composites under extreme environments is of significant importance for different industrial applications, such as advanced propulsion systems in aerospace and aviation, nuclear power engines, automotive, metal processing (cutting, forming, forging), metallurgy, electric railways, etc. A survey has been made of various compounds which could be considered environmentally compatible solid lubricant materials. The main groups of solid lubricants are polymers, soft metals, laminar solids, chemically stable fluorides, binary or ternary oxides, chromates, sulfates, and combinations of various solid lubricants.

(1) The noble metals such as Ag and Au offer good lubricity due to enhanced ductility and plastic deformation over a wide temperature range. The polymer composites containing PTFE or polyimides provide lubrication with the lowest temperature capacity, up from 300 to 350 °C.

(2) MoS_2/WS_2 are able to form a transfer film and generate excellent lubrication in a vacuum and dry N_2, while a graphite-like transfer film from graphite and DLC provides lubrication in moist air. Layer-lattice solid lubricants such as graphite, MoS_2, and graphite fluoride generate structural degradation such as oxidation or dissociation at certain temperatures, as well as the complex chalcogenides of Cs_2MoOS_3, Cs_2WOS_3, and $ZnMoOS_3$.

(3) CaF_2 and BaF_2/CaF_2 eutectic are chemically stable non-layered inorganic compounds under oxidizing environments, which exhibit low shear strength and easy film-forming ability to provide good lubricity from 500 to 900 °C.

(4)   Alkaline earth chromates of $BaCrO_4$ and $BaCr_2O_4$, and sulfates of $BaSO_4$ and $SrSO_4$ and their solid solutions show very good thermal stability and exceptional promise for lubricity over a wide temperature range.

(5)   For extreme temperature circumstances, oxide lubrication is the focus of future studies. A new approach to solving low-temperature brittleness in oxide lubrication is to reduce their grain size to a few nanometers. In this case, plastic deformation in large part results from grain boundary sliding or grain rotating and only a minor contribution is associated with dislocation activity in ultrafine grains.

(6)   Self-lubricating composites/coatings have been developed by a variety of material preparation techniques, which include powder metallurgy, physical/chemical vapor depositions, thermal spraying, electrodeposition, laser cladding, and additive manufacturing.

(7)   Synergistic effects of different solid lubricants are widely explored for humidity-, temperature-, vacuum- or load-adaptive tribological applications. The underlying adaptive mechanisms are associated with environmental-assisted oxidation or interfacial tribo-reaction to form easy-to-shear and low-melting-point binary and ternary compounds, temperature-activated diffusion or melting of soft metals, and thermomechanically induced softening or surface self-glazing.

(8)   The challenge associated with wide-range solid lubrication is the reversibility of the humidity-, temperature-, vacuum-, or load-adaptive tribological surfaces over multiple thermal cycles occurring in various engineering applications. Various approaches are postulated for adaptive multilayered coatings and surface multifunctional design, such as bionic compositing, tunable surface texturing, and tribo-reaction of oriented lubricants. Temperature-adaptive composites/coatings exhibiting diffusion-, melting-, oxidation-, or triboreaction-limiting lubrication are developed over multiple thermal cycles through microlaminate architectures to activate the functionality of various solid lubricants.

(9)   Adaptive solid lubrication design that can operate on earth and in space from room temperature to 1000 °C or even higher would be considered a breakthrough, which would increase air and space vehicle lifetime and performance. The challenges in high-temperature solid lubrication applications such as sliding and rolling contact bearings, seal components in advanced propulsion systems, hot-metal forming, high-speed dry machining, pantograph contact strips for electric railways, and side dams for thin-strip steel casting are highlighted. Microstructurally engineered combinations of solid lubricants will be of significant importance for the development of advanced lubrication systems under extreme environments of low/high temperature, high pressure, high chemical reactivity, and ultrahigh vacuum.

Author Contributions: Conceptualization, J.-H.O.; methodology, J.-H.O.; software, Y.-Z.Z.; validation, Y.-F.L. and Y.-Z.Z.; formal analysis, Y.-M.W.; investigation, Y.-F.L. and J.-H.O.; resources, Y.-J.W.; data curation, Y.-Z.Z.; writing—original draft preparation, J.-H.O. and Y.-Z.Z.; writing—review and editing, J.-H.O.; supervision, J.-H.O.; project administration, J.-H.O.; funding acquisition, J.-H.O. and Y.-J.W. All authors have read and agreed to the published version of the manuscript.

References

1.   Sliney, H.E. Solid lubricant materials for high-temperatures: A review. *Tribol. Int.* **1982**, *15*, 303–315. [CrossRef]
2.   Torres, H.; Ripoll, M.R.; Prakash, B. Tribological behavior of self-lubricating materials at high temperatures. *Int. Mater. Rev.* **2018**, *63*, 309–340. [CrossRef]
3.   Muratore, C.; Voevodin, A.A. Chameleon coatings: Adaptive surfaces to reduce friction and wear in extreme environments. *Ann. Rev. Mater. Res.* **2009**, *39*, 297–324. [CrossRef]
4.   Zhu, S.; Cheng, J.; Qiao, Z.; Yang, J. High temperature solid-lubricating materials: A review. *Tribol. Int.* **2019**, *133*, 206–223. [CrossRef]

5.   John, M.; Menezes, P.L. Self-lubricating materials for extreme condition applications. *Materials* **2021**, *14*, 5588. [CrossRef]

6.   Rosado, L.; Forster, N.H.; Trivedi, H.K.; King, J.P. Solid lubrication of silicon nitride with cesium-based compounds: Part I rolling contact endurance, friction and wear. *Tribol. Trans.* **2000**, *43*, 489–497. [CrossRef]

7.   Dellacorte, C.; Fellenstein, J.A.; Benoy, P.A. Evaluation of advanced solid lubricant coatings for foil air bearings operating at 25 °C and 500 °C. *Tribol. Trans.* **1999**, *42*, 338–342. [CrossRef]

8.   Aouadi, S.M.; Luster, B.; Kohli, P.; Muratore, C.; Voevodin, A.A. Progress in the development of adaptive nitride-based coatings for high temperature tribological application. *Surf. Coat. Technol.* **2009**, *204*, 962–968. [CrossRef]

9.   Skopp, A.; Woydt, M. Ceramic and ceramic composite materials with improved friction and wear properties. *Tribol. Trans.* **1995**, *38*, 233–242. [CrossRef]

10. Erdemir, A. A crystal-chemical approach to lubrication by sloid oxides. *Tribol. Lett.* **2000**, *8*, 97–102. [CrossRef]

11. Allam, I.M. Solid lubricants for applications at elevated temperatures. *J. Mater. Sci.* **1991**, *26*, 3977–3984. [CrossRef]

12. Dellacorte, C.; Steinetz, B. Tribological evaluation of an Al_2O_3-SiO_2 ceramic fiber candidate for high temperature sliding seals. *Tribol. Trans.* **1994**, *37*, 369–377. [CrossRef]

13. Wang, Y.; Liu, X.B.; Liu, Y.F.; Luo, Y.S.; Meng, Y. Microstructure and tribological performance of Ni60-based composite coatings on Ti6Al4V alloy with different Ti_3SiC_2 ceramic additions by laser cladding. *Ceram. Int.* **2020**, *46*, 28996–29010. [CrossRef]

14. Chen, J.F.; Zhao, W.J. Simple method for preparing nanometer thick Ti_3C_2TX sheets towards highly efficient lubrication and wear resistance. *Tribol. Trans.* **2021**, *153*, 106598. [CrossRef]

15. Ouyang, J.H.; Sasaki, S.; Umeda, K. The friction and wear characteristics of plasma-sprayed ZrO_2-$BaCrO_4$ coating at elevated temperatures. *Surf. Coat. Technol.* **2002**, *154*, 131–139. [CrossRef]

16. Ouyang, J.H.; Sasaki, S.; Umeda, K. Low-pressure plasma-sprayed ZrO_2-CaF_2 composite coating for high temperature tribological applications. *Surf. Coat. Technol.* **2001**, *137*, 21–30. [CrossRef]

17. Ouyang, J.H.; Sasaki, S.; Umeda, K. Effects of different additives on microstructure and high temperature tribological properties of plasma-sprayed Cr_2O_3 ceramic coatings. *Wear* **2001**, *249*, 56–66. [CrossRef]

18. Ouyang, J.H.; Sasaki, S.; Umeda, K. The friction and wear characteristics of plasma-sprayed ZrO_2-Cr_2O_3-CaF_2 from room temperature to 800 °C. *J. Mater. Sci.* **2001**, *36*, 547–555. [CrossRef]

19. Bhushan, B. *Principles and Applications of Tribology*; John Wiley & Sons, Ltd.: New York, NY, USA, 2013.

20. Kumar, R.; Hussainova, I.; Rahmani, R.; Antonov, M. Solid lubrication at high-temperature—A review. *Materials* **2022**, *15*, 1695. [CrossRef]

21. Stachowiak, G.W.; Batchelor, A.W. *Engineering Tribology*, 3rd ed.; Elsevier Butterworth-Heinemann: Amsterdam, The Netherlands, 2001.

22. Ouyang, J.H.; Murakami, T.; Sasaki, S. High-temperature tribological properties of a cathodic arc ion-plated (V,Ti)N coating. *Wear* **2007**, *263*, 1347–1353. [CrossRef]

23. Erdemir, A. A crystal chemical approach to the formulation of self-lubricating nanocomposite coatings. *Surf. Coat. Technol.* **2005**, *200*, 1792–1796. [CrossRef]

24. Gulbinski, W.; Suszko, T. Thin films of Mo_2N/Ag nanocomposite- the structure, mechanical and tribological properties. *Surf. Coat. Technol.* **2006**, *201*, 1469–1476. [CrossRef]

25. Aouadi, S.M.; Paudel, Y.; Voevodin, A.A. Adaptive Mo_2N/MoS_2/Ag tribological nanocomposite coatings for aerospace applications. *Tribol. Lett.* **2008**, *29*, 95–103. [CrossRef]

26. Ouyang, J.H.; Liang, X.S. High-temperature solid lubricating materials. In *Encyclopedia of Tribology*; Wang, Q.J., Chung, Y.W., Eds.; Springer: New York, NY, USA, 2013; pp. 1671–1681.

27. Stone, D.; Liu, J.; Singh, D.P.; Muratore, C.; Voevodin, A.A.; Mishra, S.; Rebholz, C.; Ge, Q.; Aouadi, S.M. Layered atomic structures of double oxides for low shear strength at high temperatures. *Scr. Mater.* **2010**, *62*, 735–738. [CrossRef]

28. Ageh, V.; Mohseni, H.; Scharf, T.W. Lubricious zinc titanate coatings for high temperature applications. *Surf. Coat. Technol.* **2013**, *237*, 241–247. [CrossRef]

29. Mohseni, H.; Scharf, T.W. Atomic layer deposition of ZnO/Al_2O_3/ZrO_2 nanolaminates for improved thermal and wear resistance in carbon-carbon composites. *J. Vac. Sci. Technol. A* **2012**, *30*, 01A149. [CrossRef]

30. Voevodin, A.A.; Muratore, C.; Aouadi, S.M. Hard coatings with high temperature adaptive lubrication and contact thermal management: A review. *Surf. Coat. Technol.* **2014**, *257*, 247–265. [CrossRef]

31. Franz, R.; Mitterer, C. Vanadium containing self-adaptive low-friction hard coatings for high-temperature applications: A review. *Surf. Coat. Technol.* **2013**, *228*, 1–13. [CrossRef]

32. Glieter, H. Nanocrystalline Materials. *Prog. Mater. Sci.* **1989**, *33*, 223–315. [CrossRef]

33. Karch, J.; Birringer, R.; Glieter, H. Ceramics ductile at low temperature. *Nature* **1987**, *330*, 556–558. [CrossRef]

34. Kumar, K.N.P.; Keizer, K.; Burggraaf, A.J.; Okubo, T.; Nagamoto, H.; Morooka, S. Densification of nanostructured titania assisted by a phase transformation. *Nature* **1992**, *358*, 48–51. [CrossRef]

35. Yin, M.H.; Zhang, Y.C.; Zhou, R.M.; Zhai, Z.Y.; Wang, J.L.; Cui, Y.H.; Li, D.S. Friction mechanism and application of PTFE coating in finger seals. *Tribol. Trans.* **2022**, *65*, 260–269. [CrossRef]

36. Khedkar, J.; Negulescu, I.; Meletis, E.I. Sliding wear behavior of PTFE composites. *Wear* **2002**, *252*, 361–369. [CrossRef]

37. Sliney, H.E. Evaluation of two polyimides and of an improved liner retention design for self-lubricating bushings. In Proceedings of the Joint Lubrication Conference; San Diego, CA, USA, 22 October 1984. Available online: https://ntrs.nasa.gov/citations/19840019818 (accessed on 30 April 2022).

38. Guo, Y.; Xu, J.; Yan, C.; Chen, Y.; Zhang, X.; Jia, X.; Liu, Y.; Wang, X.; Zhou, F. Direct ink writing of high performance architectured polyimides with low dimensional shrinkage. *Adv. Eng. Mater.* **2019**, *21*, 1801314. [CrossRef]

39. Yao, X.; Liu, S.; Ji, Z.; Guo, R.; Sun, C.; Guo, Y.; Wang, X.; Wang, Q. 3D printing of PTFE-filled polyimide for programmable lubricating in the region where lubrication is needed. *Tribol. Int.* **2022**, *167*, 107405. [CrossRef]

40. Guleryuz, C.G.; Krzanowski, J.E.; Veldhuis, S.C.; Fox-Rabinovich, G.S. Machining performance of TiN coatings incorporating indium as a solid lubricant. *Surf. Coat. Technol.* **2009**, *203*, 3370–3376. [CrossRef]

41. Chen, J.; Zhao, X.; Zhou, H.; Chen, J.; An, Y.; Yan, F. HVOF-sprayed adaptive low friction NiMoAl-Ag coating for tribological application from 20 to 800 °C. *Tribol. Lett.* **2014**, *56*, 55–66. [CrossRef]

42. Zhong, H.; Feng, X.; Jia, J.; Yi, G. Tribological characteristics and wear mechanisms of NiMoAl composite coatings in reversible temperature cycles from RT to 900 °C. *Tribol. Int.* **2017**, *114*, 48–56. [CrossRef]

43. Baker, C.C.; Hu, J.J.; Voevodin, A.A. Preparation of Al_2O_3/DLC/Au/MoS_2 chameleon coatings for space and ambient environments. *Surf. Coat. Technol.* **2006**, *201*, 4224–4229. [CrossRef]

44. Li, J.; Zhang, X.; Wang, J.; Li, H.; Huang, J.; Xiong, D. Frictional properties of silver overcoated on surface textured tantalum interlayer at elevated temperatures. *Surf. Coat. Technol.* **2019**, *365*, 189–199. [CrossRef]

45. Wang, Y.J.; Liu, Z.M.; Wang, S.R.; Yang, L.Y. Fabrication and tribological properties of HSS-based self-lubrication composites with an interpenetrating network. *Lubr. Sci.* **2010**, *22*, 453–463. [CrossRef]

46. Spalvins, T.; Sliney, H.E. Frictional behavior and adhesion of Ag and Au films applied to aluminum-oxide by oxygen-ion assisted screen cage ion plating. *Surf. Coat. Technol.* **1994**, *68*, 482–488. [CrossRef]

47. Liu, Z. Elevated temperature diffusion self-lubricating mechanisms of a novel cermet sinter with orderly micro-pores. *Wear* **2007**, *262*, 600–606. [CrossRef]

48. Baker, C.C.; Chromik, R.R.; Wahl, K.J.; Hu, J.J.; Voevodin, A.A. Preparation of chameleon coatings for space and ambient environments. *Thin Solid Film.* **2007**, *515*, 6737–6743. [CrossRef]

49. Hu, J.J.; Muratore, C.; Voevodin, A.A. Silver diffusion and high-temperature lubrication mechanisms of YSZ-Ag-Mo based nanocomposite coatings. *Compos. Sci. Technol.* **2007**, *67*, 336–347. [CrossRef]

50. Rosenkranz, A.; Costa, H.L.; Baykara, M.Z.; Martini, A. Synergetic effects of surface texturing and solid lubricants to tailor friction and wear: A review. *Tribo. Inter.* **2021**, *155*, 106792. [CrossRef]

51. Basnyat, R.; Luster, B.; Muratore, C.; Voevodin, A.; Haasch, R.; Zakeri, R. Surface texturing for adaptive solid lubrication. *Surf. Coat. Technol.* **2008**, *203*, 73–79. [CrossRef]

52. Huai, W.; Zhang, C.; Wen, S. Graphite-based solid lubricant for high-temperature lubrication. *Friction* **2021**, *9*, 1660–1672. [CrossRef]

53. Eichler, J.; Lesniak, C. Boron nitride (BN) and BN composites for high-temperature applications. *J. Eur. Ceram. Soc.* **2008**, *28*, 1105–1109. [CrossRef]

54. Marian, M.; Berman, D.; Rota, A.; Jackson, R.L.; Rosenkranz, A. Layered 2D Nanomaterials to tailor friction and wear in machine elements—A review. *Adv. Mater. Interfaces* **2021**, *9*, 2101622. [CrossRef]

55. Martin, J.M.; Le Mogne, T.; Chassagnette, C.; Gardos, M.N. Friction of hexagonal boron nitride in various environments. *Tribol. Trans.* **1992**, *35*, 462–472. [CrossRef]

56. Cao, Y.; Du, L.; Huang, C.; Liu, W.; Zhang, W. Wear behavior of sintered hexagonal boron nirtride under atmosphere and water vapor ambiences. *Appl. Surf. Sci.* **2011**, *257*, 10195–10200. [CrossRef]

57. Pawlak, Z.; Pai, R.; Bayraktar, E.; Kaldonski, T.; Oloyede, A. Lamellar lubrication in vivo and vitro: Friction testing of hexagonal boron nitride. *Biosystems* **2008**, *94*, 202–208. [CrossRef]

58. Pawlak, Z.; Kaldonski, T.; Pai, R.; Bayraktar, E.; Oloyede, A. A comparative study on the tribological behavior of hexagonal boron nitride (*h*-BN) as lubricating micro-particles-an additive in porous sliding bearing for a car clutch. *Wear* **2009**, *267*, 1198–1202. [CrossRef]

59. Chen, B.; Bi, Q.; Yang, J.; Xia, Y.; Hao, J. Tribological properties of solid lubricants (graphite, *h*-BN) for Cu-based P/M friction composites. *Tribol. Int.* **2008**, *41*, 1145–1152. [CrossRef]

60. Kimura, Y.; Wakabayashi, T.; Okada, K.; Wada, T.; Nishikawa, H. Born nitride as a lubricant additive. *Wear* **1999**, *232*, 199–206. [CrossRef]

61. Cho, D.H.; Kim, J.S.; Kwon, S.H.; Lee, C.; Lee, Y.Z. Evaluation of hexagonal boron nitride nano-sheets as a lubricant additive in water. *Wear* **2013**, *302*, 981–986. [CrossRef]

62. Li, X.; Gao, Y.; Wei, S.; Yang, Q. Tribological behavior of B_4C-hBN ceramic composites used as pins or discs coupled with B_4C ceramic under dry sliding condition. *Ceram. Int.* **2017**, *43*, 1578–1583. [CrossRef]

63. Du, L.; Huang, C.; Zhang, W.; Li, T.; Liu, W. Preparation and wear performance of NiCr/Cr_3C_2-NiCr/hBN plasma sprayed composite coating. *Surf. Coat. Technol.* **2011**, *205*, 3722–3728. [CrossRef]

64. Leon, O.A.; Staia, M.H.; Hintermann, H.E. Wear mechanism of Ni–P–BN(h) composite autocatalytic coatings. *Surf. Coat. Technol.* **2005**, *200*, 1825–1829. [CrossRef]

65. Tyagi, R.; Xiong, D.S.; Li, J.; Dai, J. Elevated temperature tribological behavior of Ni based composites containing nano-silver and hBN. *Wear* **2010**, *269*, 884–890. [CrossRef]

66. Skopp, A.; Woydt, M.; Habig, K.H. Tribological behavior of silicon nitride materials under unlubricated sliding between 22 °C and 1000 °C. *Wear* **1995**, *181–183*, 571–580.

67. Guo, X.; Zhu, Z.; Ekevad, M.; Bao, X.; Cao, P. The cutting performance of Al_2O_3 and Si_3N_4 ceramic cutting tools in the milling plywood. *Adv. Appl. Ceram.* **2018**, *117*, 16–22. [CrossRef]

68. Akhtar, S.S. A critical review on self-lubricating ceramic-composite cutting tools. *Ceram. Int.* **2021**, *47*, 20745–20767. [CrossRef]

69. Podgornik, B.; Kosec, T.; Kocijan, A.; Donik, C. Tribological behavior and lubrication performance of hexagonal boron nitride (*h*-BN) as a replacement for graphite in aluminum forming. *Tribol. Int.* **2015**, *81*, 267–275. [CrossRef]

70. Fournier, P.; Platon, F. Wear of refractory ceramics against nickel. *Wear* **2000**, *244*, 118–125. [CrossRef]

71. Chen, L.; Wang, Y.; Yao, M.; Ouyang, J.H.; Zhou, Y.; Guo, Y. Corrosion kinetics and corrosion mechanisms of BN-ZrO$_2$-SiC composites in molten steel. *Corrosion Sci.* **2014**, *89*, 93–100. [CrossRef]

72. Chen, L.; Zhen, L.; Wang, Y.; Duan, X.; Ouyang, J.H.; Zhou, Y. Corrosion behavior and microstructural evolution of BN-ZrO$_2$-SiC composites in molten steel. *Int. J. Appl. Ceram. Technol.* **2017**, *14*, 665–674. [CrossRef]

73. Chen, L.; Wang, Y.; Ouyang, J.H.; Duan, X.; Zhou, Y. Low-temperature sintering nehavior and mechanical properties of BN-ZrO$_2$-SiC composites. *Mater. Sci. Eng. A-Struct.* **2017**, *681*, 50–55. [CrossRef]

74. Duan, X.; Yang, Z.; Chen, L.; Tian, Z.; Cai, D.; Wang, Y.; Jia, D.; Zhou, Y. Review on the properties of hexagonal boron nitride matrix composite ceramics. *J. Eur. Ceram. Soc.* **2016**, *36*, 3725–3737. [CrossRef]

75. Niu, Z.B.; Chen, F.; Xiao, P.; Li, Z.; Pang, L.; Li, Y. Effect of *h*-BN addition on friction and wear properties of C/C-SiC composites fabricated by LSI. *Int. J. Appl. Ceram. Technol.* **2022**, *19*, 108–118. [CrossRef]

76. Yuan, S.; Toury, B.; Benayoun, S. Novel chemical process for preparing *h*-BN solid lubricant coatings on titanium-based substrates for high temperature tibological applications. *Surf. Coat. Technol.* **2015**, *272*, 366–372. [CrossRef]

77. Yuan, S.; Benayoun, S.; Briouse, A.; Dezellus, O.; Beaugiraud, B.; Toury, B.J. New potential for preparation of performing *h*-BN coatings via polymer pyrolysis in RTA furnace. *Eur. Ceram. Soc.* **2013**, *33*, 393–402. [CrossRef]

78. Miyoshi, K.; Buckley, D.H.; Pouch, J.J.; Alterovitz, S.A.; Sliney, H.E. Mechanical strength and tribological behavior of ion-beam deposited boron-nitride films on non-metallic substrates. *Surf. Coat. Technol.* **1987**, *33*, 221–233. [CrossRef]

79. Spear, J.C.; Ewers, B.W.; Batteas, J.D. 2D-nanomaterials for controlling friction and wear at interfaces. *Nano Today* **2015**, *10*, 301–314. [CrossRef]

80. Vazirisereshk, M.R.; Martini, A.; Strubbe, D.A.; Baykara, M.Z. Solid lubrication with MoS$_2$: A review. *Lubricants* **2019**, *7*, 57. [CrossRef]

81. Martin, J.M.; Donnet, C.; Lemogne, T.; Epicier, T. Superlubricity of molybdenum disulfide. *Phys. Rev. B* **1993**, *48*, 10583–10586. [CrossRef]

82. Zhu, J.; Zeng, Q.; Wang, Y.; Yan, C.; He, W. Nano-crystallization-driven high temperature self-lubricating properties of magnetron-sputtered WS$_2$ coatings. *Tribol. Lett.* **2020**, *68*, 1–11. [CrossRef]

83. Rapoport, L.; Fleischer, N.; Tenne, R. Fullerene-like WS$_2$ nanoparticles: Superior lubricants for harsh conditions. *Adv. Mater.* **2003**, *15*, 651–655. [CrossRef]

84. Sun, X. Solid lubricants for space mechanisms. In *Encyclopedia of Tribology*; Wang, Q.J., Chung, Y.W., Eds.; Springer: Boston, MA, USA, 2013.

85. Roberts, E.W. Space tribology: Its role in spacecraft mechanisms. *J. Phys. D Appl. Phys.* **2012**, *45*, 503001. [CrossRef]

86. Miyoshi, K. Aerospace mechanisms and tribology technology: Case study. *Tribol. Int.* **1999**, *32*, 673–685. [CrossRef]

87. Lince, J.R. Effective application of solid lubricants in spacecraft mechanisms. *Lubricants* **2020**, *8*, 74. [CrossRef]

88. Davis, D.; Marappan, G.; Sivalingam, Y.; Panigrahi, B.B.; Singh, S. Tribological behavior of NiMoAl-based self-lubricating composites. *ACS Omega* **2020**, *5*, 14669–14678. [CrossRef] [PubMed]

89. Gupta, S.; Filimonov, D.; Palanisamy, T.; El-Raghy, T.; Barsoum, M.W. Ta$_2$AlC and Cr$_2$AlC Ag-based composites—New solid lubricant materials for use over a wide temperature range against Ni-based superalloys and alumina. *Wear* **2007**, *262*, 1479–1489. [CrossRef]

90. Barsoum, M.W. The M$_{n+1}$AX$_n$ phases: A new class of solids thermodynamically stable nanolaminates. *Prog. Solid State Chem.* **2000**, *28*, 201–208. [CrossRef]

91. Gupta, S.; Filimonov, D.; Zaitsev, V.; Palanisamy, T.; Barsoum, M.W. Ambient and 550 °C tribological behavior of select MAX phases against Ni-based superalloys. *Wear* **2008**, *264*, 270–278. [CrossRef]

92. Zhang, R.; Zhang, H.M.; Liu, F.Y. Microstructure and tribological properties of spark plasma sintered Ti$_3$SiC$_2$-Pb-Ag composites at elevated temperatures. *Materials* **2022**, *15*, 1437. [CrossRef]

93. Sliney, H.E.; DellaCorte, C.; Lukaszewicz, V. The tribology of PS212 coatings and PM212 composites for the lubrication of titanium 6Al-4V components of a stirling engine space power-system. *Tribol. Trans.* **1995**, *38*, 497–506. [CrossRef]

94. DellaCorte, C.; Laskowski, J.A. Tribological evaluation of PS300: A new chrome oxide-based solid lubricant coating sliding against Al$_2$O$_3$ from 25° to 650 °C. *Tribol. Trans.* **1997**, *40*, 163–167. [CrossRef]

95. Bemis, K.; Bogdanski, M.S.; DellaCorte, C.; Sliney, E. The effect of prolonged exposure to 750 °C air on the tribological performance of PM212 self-lubricating composite material. *Tribol. Trans.* **1995**, *38*, 745–756. [CrossRef]

96. Mazumder, S.; Metsalaar, H.S.C.; Sukiman, N.L.; Zulkifli, N.W.M. An overview of fluoride-based solid lubricants in sliding contacts. *J. Eur. Ceram. Soc.* **2020**, *40*, 4974–4996. [CrossRef]

97. Ding, C.H.; Li, P.L.; Ran, G.; Tian, Y.W.; Zhou, J.N. Tribological property of self-lubricating PM304 composite. *Wear* **2007**, *262*, 575–581. [CrossRef]

98. Zhu, S.Y.; Bi, Q.L.; Yang, J.; Liu, W.M.; Xue, Q.J. Ni$_3$Al matrix high temperature self-lubricating composites. *Tribol. Int.* **2011**, *44*, 445–453. [CrossRef]

99. Zhu, S.Y.; Bi, Q.L.; Yang, J.; Liu, W.M.; Xue, Q.J. Effect of particle size on tribological behavior of Ni$_3$Al matrix high temperature self-lubricating composites. *Tribol. Int.* **2011**, *44*, 1800–1809. [CrossRef]

100. Zhu, S.Y.; Bi, Q.L.; Kong, L.Q.; Yang, J.; Liu, W.M. Influence of Cr content on tribological properties of Ni$_3$Al matrix high temperature self-lubricating composites. *Tribol. Int.* **2011**, *44*, 1182–1187. [CrossRef]

101. Ouyang, J.H.; Li, Y.F.; Wang, Y.M.; Zhou, Y.; Murakami, T.; Sasaki, S. Microstructure and tribological properties of $ZrO_2(Y_2O_3)$ matrix composites doped with different solid lubricants from room temperature to 800 °C. *Wear* **2009**, *267*, 1353–1360. [CrossRef]

102. Ouyang, J.H.; Sasaki, S.; Murakami, T.; Umeda, K. The synergistic effects of CaF_2 and Au lubricants on tribological properties of spark-plasma-sintered $ZrO_2(Y_2O_3)$ matrix composites. *Mater. Sci. Eng. A Struct.* **2004**, *386*, 234–243. [CrossRef]

103. Ouyang, J.H.; Sasaki, S.; Murakami, T.; Umeda, K. Tribological properties of spark plasma sintered (SPS) ZrO_2-CaF_2-Ag composites at elevated temperatures. *Wear* **2005**, *258*, 1444–1454. [CrossRef]

104. Gong, H.; Yu, C.; Zhang, L.; Xie, G.; Guo, D.; Luo, J. Intelligent lubricating materials: A review. *Compos. Pt. B* **2020**, *202*, 108450. [CrossRef]

105. Dimitrov, V.; Komatsu, T. Classification of simple oxides: A polarizability approach. *J. Solid State Chem.* **2002**, *163*, 100–112. [CrossRef]

106. Prakash, B.; Celis, J.P. The lubricity of oxides revised based on a polarizability approach. *Tribol. Lett.* **2007**, *27*, 105–112. [CrossRef]

107. Reeswinkel, T.; Music, D.; Schneider, J.M. Coulomb-potential-dependent decohesion of Magneli phases. *J. Phys. Condens. Matter* **2010**, *22*, 292203–292207. [CrossRef] [PubMed]

108. Berger, L.M.; Stahr, C.C.; Saaro, S.; Thiele, S.; Woydt, M.; Kelling, N. Dry sliding up to 7.5 m/s and 800 °C of thermally sprayed coatings of the TiO_2-Cr_2O_3 system and (Ti,Mo)(C,N)-Ni(Co). *Wear* **2009**, *267*, 954–964. [CrossRef]

109. Gulbinski, W.; Suszko, T.; Sienicki, W.; Warcholinski, B. Tribological properties of silver- and copper-doped transition metal oxide coatings. *Wear* **2003**, *254*, 129–135. [CrossRef]

110. Fateh, N.; Fontalvo, G.A.; Mitterer, C. Tribological properties of reactive magnetron sputtered V_2O_5 and VN-V_2O_5 coatings. *Tribol. Lett.* **2008**, *30*, 21–26. [CrossRef]

111. Heo, S.J.; Kim, K.H.; Kang, M.C.; Suh, J.H.; Park, C.G. Synthesis and mechanical properties of Mo-S-N coatings by a hybrid coating system. *Surf. Coat. Technol.* **2006**, *201*, 4180–4184. [CrossRef]

112. Cavaleiro, A.; Trindade, B.; Vieira, M.T. Influence of Ti addition on the properties of W-Ti-C/N sputtered films. *Surf. Coat. Technol.* **2003**, *174*, 68–75. [CrossRef]

113. Ding, Q.D.; Li, C.S.; Dong, L.R.; Wang, M.L.; Peng, Y.; Yan, X.H. Preparation and properties of $YBa_2Cu_3O_{7\text{-delta}}$/Ag self-lubricating composites. *Wear* **2008**, *265*, 1136–1141. [CrossRef]

114. Zhou, Z.; Rainforth, W.M.; Luo, Q.; Hovsepian, P.E.; Ojeda, J.J.; Romero-Gonzalez, M.E. Wear and Friction of TiAlN/VN Coatings Against Al_2O_3 in Air at Room and Elevated Temperatures. *Acta Mater.* **2010**, *58*, 2912–2925. [CrossRef]

115. Fateh, N.; Fontalvo, G.A.; Gassner, G.; Mitterer, C. The beneficial effect of high-temperature oxidation on the tribological behavior of V and VN coatings. *Tribol. Lett.* **2007**, *28*, 1–7. [CrossRef]

116. Peterson, M.B.; Li, S.Z.; Murray, S.F. Wear-Resisting Oxide Films for 900 °C. *Mater. Sci. Technol.* **1997**, *13*, 99–106. Available online: https://www.jmst.org/EN/Y1997/V13/I2/99 (accessed on 30 April 2022).

117. Zabinski, J.S.; Day, A.E.; Donley, M.S.; DellaCorte, C.; McDevitt, N.T. Synthesis and characterization of a high-temperature oxide lubricant. *J. Mater. Sci.* **1994**, *29*, 5875–5879. [CrossRef]

118. Ouyang, J.H.; Shi, C.C.; Liu, Z.G.; Wang, Y.M.; Wang., Y.J. Fabrication and high-temperature tribological properties of self-lubricating NiCr-$BaMoO_4$ composites. *Wear* **2015**, *330–331*, 272–279. [CrossRef]

119. Aouadi, S.M.; Paudel, Y.; Simonson, W.J.; Ge, Q.; Kohli, P.; Muratore, C.; Voevodin, A.A. Tribological investigation of adaptive Mo_2N/MoS_2/Ag coatings with high sulfur content. *Surf. Coat. Technol.* **2009**, *203*, 1304–1309. [CrossRef]

120. Lei, M.; Ye, C.X.; Ding, S.S.; Bi, K.; Xiao, H.; Sun, Z.B.; Fan, D.Y.; Yang, H.J.; Wang, Y.G. Controllable route to barium molybdate crystal and their photoluminescence. *J. Alloy. Compd.* **2015**, *639*, 102–105. [CrossRef]

121. Aouadi, S.M.; Singh, D.P.; Stone, D.S.; Polychronopoulou, K.; Nahif, F.; Rebholz, C.; Muratore, C.; Voevodin, A.A. Adaptive VN/Ag Nanocomposite Coatings with Lubricious Behavior from 25 to 1000 °C. *Acta Mater.* **2010**, *58*, 5326–5331. [CrossRef]

122. Hao, E.; An, Y.; Chen, J.; Zhao, X.; Hou, G.; Chen, J.M.; Gao, M.; Yan, F. In-situ formation of layer-like Ag_2MoO_4 induced by high-temperature oxidation and its effect on the self-lubricating properties of NiCoCrAlYTa/Ag/Mo coatings. *J. Mater. Sci. Technol.* **2021**, *75*, 164–173. [CrossRef]

123. Chen, J.; An, Y.L.; Yang, J.; Zhao, X.Q.; Yan, F.Y.; Zhou, H.D.; Chen, J.M. Tribological properties of adaptive NiCrAlY-Ag-Mo coatings prepared by atmospheric plasma spraying. *Surf. Coat. Technol.* **2013**, *235*, 521–528. [CrossRef]

124. Zhu, S.; Li, F.; Ma, J.; Cheng, J.; Yin, B.; Yang, J.; Qiao, Z.; Liu, W. Tribological properties of Ni_3Al matrix composites with addition of silver and barium salt. *Tribol. Int.* **2015**, *84*, 118–123. [CrossRef]

125. Wenda, E. High temperature reactions in the MoO_3-Ag_2O system. *J. Therm. Anal. Calorim.* **1998**, *53*, 861–870. [CrossRef]

126. John, P.J.; Prasad, S.V.; Voevodin, A.A.; Zabinski, J.S. Calcium sulfate as a high temperature solid lubricant. *Wear* **1998**, *219*, 155–161. [CrossRef]

127. Prasad, S.; McDevitt, N.; Zabinski, J. Tribology of tungsten disulfide-nanocrystalline zinc oxide adaptive lubricant films from ambient to 500 °C. *Wear* **2000**, *237*, 186–196. [CrossRef]

128. Zhu, S.; Bi, Q.; Yang, J.; Liu, W.M. Ni_3Al matrix composite with lubricious tungstate at high temperatures. *Tribol. Lett.* **2012**, *45*, 251–255. [CrossRef]

129. Xie, B.; Wu, Y.; Jiang, Y.; Li, F.; Wu, J.; Yuan, S.; Yu, W.; Qian, Y.T. Shape-controlled synthesis of $BaWO_4$ crystals under different surfactants. *J. Cryst. Growth* **2002**, *235*, 283–286. [CrossRef]

130. Shi, H.T.; Qi, L.M.; Ma, J.M.; Cheng, H.M. Polymer-directed synthesis of penniform $BaWO_4$ nanostructures in reverse micelles. *J. Am. Chem. Soc.* **2003**, *125*, 3450–3451. [CrossRef]

131. Shi, H.T.; Wang, X.H.; Zhao, N.; Qi, L.M.; Ma, J.M. Growth mechanism of penniform BaWO$_4$ nanostructures in catanionic reverse micelles involving polymers. *J. Phys. Chem. B* **2006**, *110*, 748–753. [CrossRef]

132. Guo, H.J.; Han, M.M.; Chen, W.Y.; Lu, C.; Li, B.; Wang, W.Z.; Jia, J.H. Microstructure and properties of VN/Ag composite films with various silver content. *Vacuum* **2017**, *137*, 97–103. [CrossRef]

133. Xin, B.B.; Yu, Y.J.; Zhou, J.S.; Wang, L.Q.; Ren, S.F.; Zhen, L. Effect of silver vanadate on the lubricating proeprties of NiCrAlY laser cladding coating at elevated temperatures. *Surf. Coat. Technol.* **2016**, *307*, 136–145. [CrossRef]

134. Song, J.M.; Lin, Y.Z.; Yao, H.B.; Fan, F.J.; Li, X.G.; Yu, S.H. Superlong beta-AgVO$_3$ nanoribbons: High-yield synthesis by a pyridine-assisted solution approach, their stability, electrical and electrochemical properties. *ACS Nano* **2009**, *3*, 653–660. [CrossRef]

135. Wang, G.; Ren, Y.; Zhou, G.J.; Wang, J.P.; Cheng, H.F.; Wang, Z.Y. Synthesis of highly efficient visible light Ag@Ag$_3$VO$_4$ plasmonic photocatalysts. *Surf. Coat. Technol.* **2013**, *228*, S283–S286. [CrossRef]

136. Su, Y.; Hu, L.; Fan, H.; Song, J.; Zhang, Y. Surface engineering design of alumina/molybdenum fibrous monolithic ceramic to achieve continuous lubrication from room temperature to 800 °C. *Tribol. Lett.* **2017**, *65*, 47. [CrossRef]

137. Stone, D.S.; Harbin, S.; Mohseni, H.; Mogonye, J.E.; Scharf, T.W.; Muratore, C.; Voevodin, A.A.; Martini, A.; Aouadi, S.M. Lubricious silver tantalate films for extreme temperature applications. *Surf. Coat. Technol.* **2013**, *217*, 140–146. [CrossRef]

138. Valant, M.; Axelsson, A.K.; Zou, B.; Alford, N. Oxygen transport during formation and decomposition of AgNbO$_3$ and AgTaO$_3$. *J. Mater. Res.* **2007**, *22*, 1650–1655. [CrossRef]

139. Gao, H.; Stone, D.S.; Mohseni, H.; Aouadi, S.M.; Scharf, T.W.; Martini, A. Mechanistic studies of high temperature friction reduction in silver tantalate. *Appl. Phys. Lett.* **2013**, *102*, 121603–121605. [CrossRef]

140. Gao, H.; Otero-de-la-Roza, A.; Gu, J.; Stone, D.; Aouadi, S.M.; Johnson, E.R.; Martini, A. (Ag,Cu)-Ta-O ternaries as high-temperature solid-lubricant coatings. *ACS Appl. Mater. Interfaces* **2015**, *7*, 15422–15429. [CrossRef] [PubMed]

141. Gao, H.; Otero-de-la-Roza, A.; Aouadi, S.M.; Johnson, E.R.; Martini, A. An empirical model for silver tantalite. *Model. Simul. Mater. Sci. Eng.* **2013**, *21*, 055002. [CrossRef]

142. Liang, X.S.; Ouyang, J.H.; Liu, Z.G.; Yang, Z.L. Friction and wear characteristics of BaCr$_2$O$_4$ ceramics at elevated temperature in sliding against sintered alumina ball. *Tribol. Lett.* **2012**, *47*, 203–209. [CrossRef]

143. Ouyang, J.H.; Sasaki, S.; Murakami, T.; Umeda, K. Spark-plasma-sintered ZrO$_2$(Y$_2$O$_3$)-BaCrO$_4$ self-lubricating composites for high temperature tribological applications. *Ceram. Int.* **2005**, *31*, 543–553. [CrossRef]

144. Murakami, T.; Ouyang, J.; Korenaga, A.; Umeda, K.; Sasaki, S.; Yoneyama, Y. High temperature tribological properties of Al$_2$O$_3$-X (X: BaCrO$_4$, BaSO$_4$ and CaSO$_4$) spark-plasma-sintered composites containing sintering additives. *Mater. Trans.* **2004**, *45*, 2614–2617. [CrossRef]

145. Liang, X.S.; Ouyang, J.H.; Liu, Z.G. Preparation of BaCrO$_4$ particles in the presence of EDTA from aqueous solutions. *J. Coord. Chem.* **2012**, *65*, 2432–2441. [CrossRef]

146. Muller-Buschbaum, H.K. The crystal chemistry of AM$_2$O$_4$ oxometallates. *J. Alloy. Compd.* **2003**, *349*, 49–104. [CrossRef]

147. Liang, X.S.; Ouyang, J.H.; Liu, Z.G. Influences of temperature and atmosphere on thermal stability of BaCrO$_4$. *J. Therm. Anal. Calorim.* **2013**, *111*, 371–375. [CrossRef]

148. Gontarz, Z. Analysis of the steps of thermal decomposition of oxo-compounds of the dsp block elements. *J. Therm. Anal. Calorim.* **1995**, *43*, 57–68. [CrossRef]

149. Azad, A.M.; Sudha, R.; Sreedharan, O.M. The standard Gibbs energies of formation of ACrO$_4$ (A = Ca, Sr or Ba) from EMF measurements. *Thermochim. Acta* **1992**, *194*, 129–136. [CrossRef]

150. Ouyang, J.H.; Liang, X.S.; Wen, J.; Liu, Z.G.; Yang, Z.L. Electrodeposition and tribological properties of self-lubricating Ni-BaCr$_2$O$_4$ composite coatings. *Wear* **2011**, *271*, 2037–2045. [CrossRef]

151. Ouyang, J.H.; Liang, X.S.; Liu, Z.G.; Yang, Z.L.; Wang, Y.J. Friction and wear properties of hot-pressed NiCr-BaCr$_2$O$_4$ high temperature self-lubricating composites. *Wear* **2013**, *301*, 820–827. [CrossRef]

152. Li, Y.F.; Ouyang, J.H.; Zhou, Y.; Liang, X.S.; Zhong, J.Y. Facile fabrication of SrSO$_4$ nanocrystals with different crystallographic morphologies via a simple surfactant-free aqueous solution route. *Mater. Lett.* **2008**, *62*, 4417–4420. [CrossRef]

153. Li, Y.F.; Ouyang, J.H.; Zhou, Y. Novel fabrication of monodispersed peanut-type celestine particles using Sr-EDTA chelating precursors. *Mater. Chem. Phys.* **2008**, *111*, 508–512. [CrossRef]

154. Li, Y.F.; Ouyang, J.H.; Zhou, Y.; Liang, X.S.; Murakami, T.; Sasaki, S. Room temperature template-free synthesis of dumbbell-like SrSO$_4$ nanostructures with a hierarchical architecture. *J. Cryst. Growth.* **2010**, *312*, 1886–1890. [CrossRef]

155. Li, Y.F.; Ouyang, J.H.; Zhou, Y.; Liang, X.S.; Zhong, J.Y. Synthesis and characterization of nano-sized Ba$_x$Sr$_{1-x}$SO$_4$ ($0 \leq x \leq 1$) solid solution by a simple surfactant-free aqueous solution route. *Bull. Mat. Sci.* **2009**, *32*, 149–153. [CrossRef]

156. Murakami, T.; Ouyang, J.H.; Sasaki, S.; Umeda, K.; Yoneyama, Y. High temperature tribological properties of spark-plasma-sintered Al$_2$O$_3$ composites containing barite-type structure sulfates. *Tribol. Int.* **2007**, *40*, 246–253. [CrossRef]

157. Li, Y.F.; Ouyang, J.H.; Sasaki, S. Tribological properties of spark plasma sintered ZrO$_2$(Y$_2$O$_3$)-Al$_2$O$_3$-Ba$_x$Sr$_{1-x}$SO$_4$ (x = 0.25, 0.5, 0.75) composites at elevated temperature. *Tribol. Lett.* **2012**, *45*, 291–300. [CrossRef]

158. Zhang, X.; Cheng, J.; Niu, M.; Tan, H.; Liu, W.; Yang, J. Microstructure and high temperature tribological behavior of Fe$_3$Al-Ba$_{0.25}$Sr$_{0.75}$SO$_4$ self-lubricating composites. *Tribol. Int.* **2016**, *101*, 81–87. [CrossRef]

159. Liang, X.S.; Ouyang, J.H.; Li, Y.F.; Wang, Y.M. Electrodeposition and tribological properties of Ni-SrSO$_4$ composite coatings. *Appl. Surf. Sci.* **2009**, *255*, 4316–4321. [CrossRef]

160. Murakami, T.; Umeda, K.; Sasaki, S.; Ouyang, J.H. High-temperature tribological properties of strontium sulfate films formed on zirconia-alumina, alumina and silicon nitride substrates. *Tribol. Int.* **2006**, *39*, 1576–1583. [CrossRef]
161. Borawski, A. Conventional and unconventional materials used in the production of brake pads—Review. *Sci. Eng. Compos. Mater.* **2020**, *27*, 374–396. [CrossRef]
162. Menapace, C.; Leonardi, M.; Matejka, V.; Gialanella, S.; Straffelini, G. Dry sliding behavior and frictional layer formation in copper-free barite containing friction materials. *Wear* **2018**, *398–399*, 191–200. [CrossRef]
163. Li, Y.F.; Ouyang, J.H.; Zhou, Y.; Wang, Y.M.; Murakami, T.; Sasaki, S. High temperature tribological properties of spark plasma sintered Al_2O_3-$SrSO_4$ self-lubricating nanocomposites incorporated with and without Ag addition. *Int. J. Mod. Phys. B* **2009**, *23*, 1425–1431. [CrossRef]
164. Murakami, T.; Ouyang, J.H.; Umeda, K.; Sasaki, S. High-temperature friction properties of $BaSO_4$ and $SrSO_4$ powder films formed on Al_2O_3 and stainless steel substrates. *Mat. Sci. Eng. A Struct.* **2006**, *432*, 52–58. [CrossRef]
165. Carter, C.B.; Norton, M.G. *Ceramic Materials: Science and Engineering*; Springer: New York, NY, USA, 2007.
166. Calas, G.; Henderson, G.S.; Stebbins, J.F. Glasses and melts: Linking geochemistry and materials science. *Elements* **2006**, *2*, 265–268. [CrossRef]
167. Yue, W.; Wang, C.B.; Liu, Y.D.; Huang, H.P.; Wen, Q.F.; Liu, J.J. Study of the regenerated layer on the worn surface of a cylinder liner lubricated by a novel silicate additive in lubricating oil. *Tribol. Trans.* **2010**, *53*, 288–295. [CrossRef]
168. Nan, F.; Xu, Y.; Xu, B.S.; Gao, F.; Wu, Y.X.; Li, Z.G. Tribological behaviors and wear mechanisms of ultrafine magnesium aluminum silicate powders as lubricant additive. *Tribol. Int.* **2015**, *81*, 199–208. [CrossRef]
169. Zhang, J.; Tian, B.; Wang, C.B. Long-term surface restoration effect introduced by advanced silicate based lubricant additive. *Tribol. Int.* **2013**, *57*, 31–37. [CrossRef]
170. Wang, L.; Tieu, A.K.; Cui, S.; Deng, G.; Wang, P.; Zhu, H.; Yang, J. Lubrication mechanism of sodium metasilicate at elevated temperatures through tribo-interface observation. *Tribol. Int.* **2020**, *142*, 105972. [CrossRef]
171. Wang, B.; Gao, K.; Chang, Q.; Berman, D.; Tian, Y. Magnesium silicate hydroxide-MoS_2-Sb_2O_3 coating nanomaterials for high-temperature superlubricity. *ACS Appl. Nano. Mater.* **2021**, *4*, 7097–7106. [CrossRef]
172. Gao, K.; Wang, B.; Shirani, A.; Chang, Q.; Berman, D. Macroscale superlubricity accomplished by Sb_2O_3-MSH/C under high-temperature. *Front. Chem.* **2021**, *9*, 226. [CrossRef]
173. Strong, K.L.; Zabinski, J.S. Characterization of annealed pulsed laser deposited (PLD) thin films of cesium oxythiomolybdate (Cs_2MoOS_3). *Thin Solid Films* **2002**, *406*, 164–173. [CrossRef]
174. Strong, K.L.; Zabinski, J.S. Tribology of pulsed laser deposited thin films of cesium oxythiomolybdate (Cs_2MoOS_3). *Thin Solid Films* **2002**, *406*, 174–184. [CrossRef]
175. Rosado, L.; Forster, N.H.; Whittberg, T.N. Solid lubrication of silicon nitride with cesium-based compounds: Part II-Surface analysis. *Tribol. Trans.* **2000**, *43*, 521–527. [CrossRef]
176. Wan, S.; Tieu, A.K.; Xia, Y.; Zhu, H.; Tran, B.H.; Cui, S. An overview of inorganic polymer as potential lubricant additive for high temperature tribology. *Tribol. Int.* **2016**, *102*, 620–635. [CrossRef]
177. Zabinski, J.S.; Sanders, J.H.; Nainaparampil, J.; Prasad, S.V. Lubrication using a microstructurally engineered oxide: Performance and mechanisms. *Tribol. Lett.* **2000**, *8*, 103–116. [CrossRef]
178. Zabinski, J.S.; Donley, M.S.; Dyhouse, V.J.; McDevitt, N.T. Chemical and tribological characterization of PbO-MoS_2 films grown by pulsed laser deposition. *Thin Solid Films* **1992**, *214*, 156–163. [CrossRef]
179. Muratore, C.; Voevodin, A.A. Molybdenum disulfide as a lubricant and catalyst in adaptive nanocomposite coatings. *Surf. Coat. Technol.* **2006**, *201*, 4125–4130. [CrossRef]
180. Gautam, R.K.S.; Rao, U.S.; Tyagi, R. Influence of load on friction and wear behavior of Ni-based self-lubricating coatings deposited by atmospheric plasma spray. *J. Mater. Eng. Perform.* **2019**, *28*, 7398–7406. [CrossRef]
181. Yang, J.F.; Jiang, Y.; Hardell, J.; Prakash, B.; Fang, Q.F. Influence of service temperature on tribological characteristics of self-lubricant coatings: A review. *Front. Mater. Sci.* **2013**, *7*, 28–39. [CrossRef]
182. Aouadi, S.M.; Gao, H.; Martini, A.; Scharf, T.W.; Muratore, C. Lubricious oxide coatings for extreme temperature applications: A review. *Surf. Coat. Technol.* **2014**, *257*, 266–277. [CrossRef]
183. Etsion, I. Improving tribological performance of mechanical components by laser surface texturing. *Tribol. Lett.* **2004**, *17*, 733–737. [CrossRef]
184. Etsion, I. State of the art in laser surface texturing. *J. Tribol. Trans. ASME* **2005**, *127*, 248–253. [CrossRef]
185. Wang, X.L.; Kato, K.; Adachi, K.; Aizawa, K. Loads carrying capacity map for the surface texture design of SiC thrust bearing sliding in water. *Tribol. Int.* **2003**, *36*, 189–197. [CrossRef]
186. Schreck, S.; Zum Gahr, K.H. Laser-assisted structuring of ceramic and steel surfaces for improving tribological properties. *Appl. Surf. Sci.* **2005**, *247*, 616–622. [CrossRef]
187. Moshkovith, A.; Perfiliev, V.; Gindin, D.; Parkansky, N.; Boxman, R.; Rapoport, L. Surface texturing using pulsed air arc treatment. *Wear* **2007**, *163*, 1467–1469. [CrossRef]
188. Voevodin, A.A.; Zabinski, J.S. Laser surface texturing for adaptive solid lubrication. *Wear* **2006**, *261*, 1285–1292. [CrossRef]
189. Mitterer, C.; Lenhart, H.; Mayhofer, P.H.; Kathrein, M. Sputter-deposited Al-Au coatings. *Intermetallics* **2004**, *12*, 579–587. [CrossRef]
190. Wang, Y.; Lee, J.W.; Duh, J.G. Mechanical strengthening in self-lubricating CrAlN/VN multilayer coatings for improved high-temperature tribological characteristics. *Surf. Coat. Technol.* **2016**, *303*, 12–17. [CrossRef]

191. Stone, D.S.; Gao, H.; Chantharangsi, C.; Paksunchai, C.; Bischof, M.; Martini, A.; Aouadi, S.M. Reconstruction mechanisms of tantalum oxide coatings with low concentrations of silver for high temperature tribological applications. *Appl. Phys. Lett.* **2014**, *105*, 4901817. [CrossRef]

192. Velasco, S.C.; Cavaleiro, A.; Carvalho, S. Functional properties of ceramic-Ag nanocomposite coatings produced by magnetron sputtering. *Prog. Mater. Sci.* **2016**, *84*, 158–191. [CrossRef]

193. Tejero-Martin, D.; Rad, M.R.; McDonald, A.; Hussain, T. Beyond traditional coatings: A review on thermal-sprayed functional and smart coatings. *J. Therm. Spray Technol.* **2019**, *28*, 598–644. [CrossRef]

194. DellaCorte, C.; Zaldana, A.R.; Radil, K.C. A systems approach to the solid lubrication of foil air bearings for oil-free turbomachinery. *J. Tribol. Trans. ASME* **2004**, *126*, 200–207. [CrossRef]

195. Yuan, J.H.; Zhu, Y.C.; Ji, H.; Zheng, X.B.; Ruan, Q.C.; Niu, Y.R.; Liu, Z.W.; Zheng, Y. Microstructures and tribological properties of plasma sprayed WC-Co-Cu-BaF$_2$/CaF$_2$ self-lubricating wear resistant coating. *Appl. Surf. Sci.* **2010**, *256*, 4938–4944. [CrossRef]

196. Li, B.; Jia, J.H.; Gao, Y.M.; Han, M.M.; Wang, W.Z. Microstructural and tribological characterization of NiAl matrix self-lubricating composite coatings by atmospheric plasma spraying. *Tribol. Int.* **2017**, *109*, 563–570. [CrossRef]

197. Chen, J.M.; Hou, G.L.; Chen, J.; An, Y.L.; Zhou, H.D.; Zhao, X.Q.; Yang, J. Composition versus friction and wear behavior of plasma sprayed WC-(W,Cr)$_2$C-Ni/Ag/BaF$_2$-CaF$_2$ self-lubricating composite coatings for use up to 600 °C. *Appl. Surf. Sci.* **2012**, *261*, 584–592. [CrossRef]

198. Sliney, E. Sliding contact PM212 bearings for service to 700 °C. *Tribol. Trans.* **1997**, *40*, 579–588. [CrossRef]

199. Dellacorte, C. The evaluation of a modified chrome oxide based high temperature solid lubricant coating for foil gas bearings. *Tribol. Trans.* **2000**, *43*, 257–262. [CrossRef]

200. Dellacorte, C. The effects of substrate material and thermal processing atmosphere on the strength of PS304: A high temperature solid lubricant coating. *Tribol. Trans.* **2003**, *46*, 361–368. [CrossRef]

201. Dellacorte, C.; Edmonds, B.J.; Benoy, P.A. Thermal processing effects on the adhesive strength of PS304 high temperature solid lubricant coatings. *Tribol. Trans.* **2002**, *45*, 499–505. [CrossRef]

202. Dellacorte, C.; Lukaszewicz, V.; Valco, M.J.; Radil, K.C.; Heshmat, H. Performance and durability of high temperature foil air bearings for oil-free turbomachinery. *Tribol. Trans.* **2000**, *43*, 774–780. [CrossRef]

203. Radil, K.C.; Dellacorte, C. The effect of journal roughness and foil coatings on the performance of heavily loaded foil air bearings. *Tribol. Trans.* **2002**, *45*, 199–204. [CrossRef]

204. Blanchet, T.A.; Kim, J.H.; Calabrese, S.J.; Dellacorte, C. Thrust-washer evaluation of self-lubricating PS304 composite coatings in high temperature sliding contact. *Tribol. Trans.* **2002**, *45*, 491–498. [CrossRef]

205. Balic, E.E.; Blanchet, T.A. Thrust-washer tribological evaluation of PS304 coatings against Rene 41. *Wear* **2005**, *259*, 876–881. [CrossRef]

206. Wang, W. Application of a high temperature self-lubricating composite coating on steam turbine components. *Surf. Coat.Technol.* **2004**, *177–178*, 12–17. [CrossRef]

207. Radil, K.; DellaCorte, C. The performance of PS400 subjected to sliding contact at temperatures from 260 to 927 °C. *Tribol. Trans.* **2017**, *60*, 957–964. [CrossRef]

208. Ouyang, J.H.; Sasaki, S.; Umeda, K. Microstructure and tribological properties of low pressure plasma-sprayed ZrO$_2$-CaF$_2$-Ag$_2$O surface composite at elevated temperature. *Wear* **2001**, *249*, 440–451. [CrossRef]

209. Su, W.M.; Niu, S.P.; Huang, Y.C.; Wang, C.; Wen, Y.Y.; Li, X.; Deng, C.M.; Deng, C.G.; Liu, M. Friction and wear properties of plasma-sprayed Cr$_2$O$_3$-BaCrO$_4$ coating at elevated temperatures. *Ceram. Int.* **2022**, *48*, 8696–8705. [CrossRef]

210. Chourasiya, S.K.; Gautam, G.; Singh, D. Mechanical and tribological behavior of warm rolled Al-6Si-3Graphite self lubricating composite synthesized by spray forming process. *Silicon* **2019**, *12*, 831–842. [CrossRef]

211. Jin, Y.; Kato, K.; Umehara, N. Effects of sintering aids and solid lubricants on tribological behaviors of CMC/Al$_2$O$_3$ pair at 650 °C. *Tribol. Lett.* **1999**, *6*, 15–21. [CrossRef]

212. Jin, Y.; Kato, K.; Umehara, N. Tribological properties of self-lubricating CMC/Al$_2$O$_3$ pairs at high temperature in air. *Tribol. Lett.* **1998**, *4*, 243–250. [CrossRef]

213. Jin, Y.; Kato, K.; Umehara, N. Further investigation on the tribological behavior of Al$_2$O$_3$–20Ag20CaF$_2$ composite at 650 °C. *Tribol. Lett.* **1999**, *6*, 225–232. [CrossRef]

214. Charoo, M.S.; Srivyas, P.D. Friction and wear characterization of spark plasma sintered hybrid aluminum composite under different sliding conditions. *J. Tribol.* **2020**, *142*, 121701.

215. Ibrahim, A.M.M.; Shi, X.; Zhang, A.; Yang, K.; Zhai, W. Tribological characteristics of NiAl matrix composites with 1.5 wt% graphene at elevated temperatures: An experimental and theoretical study. *Tribol. Trans.* **2015**, *58*, 1076–1083. [CrossRef]

216. Xu, Z.; Zhang, Q.; Shi, X.; Zhai, W.; Yang, K. Tribological properties of TiAl matrix self-lubricating composites containing multilayer graphene and Ti$_3$SiC$_2$ at high temperatures. *Tribol. Trans.* **2015**, *58*, 1131–1141. [CrossRef]

217. Yan, Z.; Shi, X.; Huang, Y.; Deng, X.; Yang, K.; Liu, X. Tribological performance of Ni$_3$Al matrix self-lubricating composites containing multilayer graphene and Ti$_3$SiC$_2$ at elevated temperatures. *J. Mater. Eng. Perform.* **2017**, *26*, 4605–4614. [CrossRef]

218. Fernandez, J.B.; Macias, E.J.; Muro, J.S.-D.; Caputi, L.; Miriello, D.; De Luca, R.; Roca, A.S.; Fals, H.C. Tribological behavior of AA1050H24-Graphene nanocomposite obtained by friction stir processing. *Metals* **2018**, *8*, 113. [CrossRef]

219. Kerr, C.; Barker, D.; Walsh, F.; Archer, J. The electrodeposition of composite coatings based on metal matrix-included particle deposits. *Trans. Inst. Metal Finish.* **2000**, *78*, 171–178. [CrossRef]

220. Sangeetha, S.; Kalaignan, G.P.; Anthuvan, J.T. Pulse electrodeposition of self-lubricating Ni-W/PTFE nanocomposite coatings on mild steel surface. *Appl. Surf. Sci.* **2015**, *359*, 412–419. [CrossRef]

221. He, Y.; Wang, S.C.; Walsh, F.C.; Chiu, Y.L.; Reed, P.A.S. Self-lubricating Ni-P-MoS$_2$ composite coatings. *Surf. Coat. Technol.* **2016**, *307*, 926–934. [CrossRef]

222. He, Y.; Sun, W.T.; Wang, S.C.; Reed, P.A.S.; Walsh, F.C. An electrodeposited Ni-P-WS$_2$ coating with combined super-hydrophobicity and self-lubricating properties. *Electrochim. Acta* **2017**, *245*, 872–882. [CrossRef]

223. Zhao, H.J.; Liu, L.; Hu, W.B.; Shen, B. Friction and wear behavior of Ni-graphite composites prepared by electroforming. *Mater. Des.* **2007**, *28*, 1374–1378. [CrossRef]

224. Cao, T.K.; Xiao, Z.J. Tribological behaviors of self-lubricating coatings prepared by electrospark deposition. *Tribol. Lett.* **2014**, *56*, 231–237. [CrossRef]

225. Dogan, F.; Duru, E.; Uysal, M.; Akbulut, H.; Aslan, S. Tribology study of pulse electrodeposited Ni-B-SWCNT composite coating. *JOM* **2022**, *74*, 574–583. [CrossRef]

226. Baiocco, G.; Menna, E.; Rubino, G.; Ucciardello, N. Mechanical characterization of functional Cu-GnP composite coatings for lubricant applications. *Surf. Eng.* **2022**, *38*, 72–78. [CrossRef]

227. Mai, Y.J.; Li, Y.G.; Li, S.L.; Zhang, L.Y.; Liu, C.S.; Jie, X.H. Self-lubricating Ti$_3$C$_2$ nanosheets copper composite coatings. *J. Alloy. Compd.* **2019**, *770*, 1–5. [CrossRef]

228. Ying, L.X.; Fu, Z.; Wu, K.; Wu, C.X.; Zhu, T.F.; Xie, Y.; Wang, G.X. Effect of TiO$_2$ sol and PTFE emulsion on properties of Cu-Sn antiwear and friction reduction coatings. *Coatings* **2019**, *9*, 59. [CrossRef]

229. Zhang, X.; Luster, B.; Church, A.; Muratore, C.; Voevodin, A.A.; Kohli, P.; Aouadi, S.; Talapatra, S. Carbon nanotube-MoS$_2$ composites as solid lubricants. *ACS Appl. Mater. Inter.* **2009**, *1*, 735–739. [CrossRef] [PubMed]

230. Caminaga, C.; Neves, F.O.; Gentile, F.C.; Button, S.T. Study of alternative lubricants to the cold extrusion of steel shafts. *J. Mater. Process. Technol.* **2007**, *182*, 432–439. [CrossRef]

231. Mayrhofer, P.H.; Hovsepian, P.E.; Mitterer, C.; Munz, W.D. Calorimetric evidence for friction self-adaptation of TiAlN/VN superlattice coatings. *Surf. Coat. Technol.* **2004**, *177–179*, 341–347. [CrossRef]

232. Gassner, G.; Mayrhofer, P.H.; Kutschej, K.; Mitterer, C.; Katherein, M. Magneli phase formation of PVD Mo-N and W-N coatings. *Surf. Coat. Technol.* **2006**, *201*, 3335–3341. [CrossRef]

233. Cai, Q.; Bai, X.; Pu, J. Adaptive VAlCN-Ag composite and VAlCN/VN-Ag multilayer coatings intended for applications at elevated temperature. *J. Mater. Sci.* **2022**, *57*, 8113–8126. [CrossRef]

234. Song, W.L.; Wang, S.J.; Lu, Y.; Xia, Z.X. Tribological performance of microhole-textured carbide tool filled with CaF$_2$. *Materials* **2018**, *11*, 1643. [CrossRef]

235. Yi, M.; Wang, J.; Li, C.; Bai, X.; Wei, G.; Zhang, J.; Xiao, G.; Chen, Z.; Zhou, T.; Wang, L.; et al. Friction and wear behavior of Ti(C,N) self-lubricating cermet materials with multilayer core-shell microstructure. *Int. J. Refract. Met. Hard Mat.* **2021**, *100*, 105629. [CrossRef]

236. Chen, Z.; Zhang, S.; Guo, R.; Ji, L.; Guo, N.; Li, Q.; Xu, C. Preparation of Al$_2$O$_3$/Ti(C,N)/ZrO$_2$/CaF$_2$@Al(OH)$_3$ ceramic tools and cutting performance in turning. *Materials* **2019**, *12*, 3820. [CrossRef]

237. Shu, S.C.; Zhang, Q.; Ihde, J.; Yuan, Q.L.; Dai, W.; Wu, M.L.; Dai, D.; Yang, K.; Wang, B.; Xue, C.; et al. Surface modification on copper particles toward graphene reinforced copper matrix composites for electrical engineering application. *J. Alloy. Compd.* **2022**, *891*, 162058. [CrossRef]